Electrochemical properties of minerals:
XAS/XRD characterization of mineral analogs used in Li-ion batteries

Gabriele Giuli

Scuola di Scienze e Tecnologie - Divisione Geologia
Universita' di Camerino

1. **The *'early days'* of battery research**

   → Cell chemistries and working principles

2. **The transition to *'host structure'* batteries**

   → The "charge carrier concept"

3. **Classifying *'state-of-the-art'* electrode materials**

   a) Insertion/Intercalation-type electrode materials

   b) Alloying vs. conversion vs. conversion/alloying materials

5. **X-ray Absorption Spectroscopy**

   → information on local structure and oxidation state

6. ***The case of doped $LiFePO_4$, ZnO, SnO_2***

→ The very beginning: Volta develops the voltaic pile…

Note:
Zn can be replaced by, e.g., Sn
Cu can be replaced by, e.g., Ag

working principle

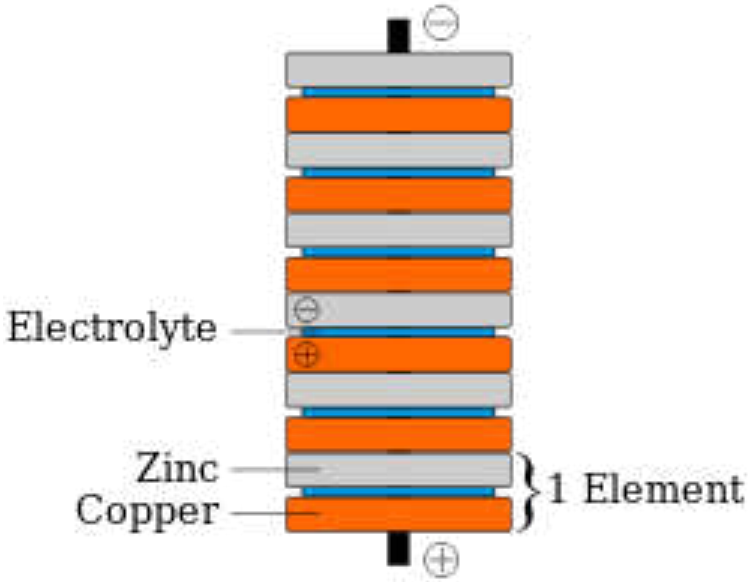

Anode: $Zn^0 \rightarrow Zn^{2+} + 2\ e^-$

Cathode: $Cu^{2+} + 2\ e^- \rightarrow Cu^0$

… see also the Daniell cell
(addition of $CuSO_4$ to the electrolyte)

→ Why does this work?

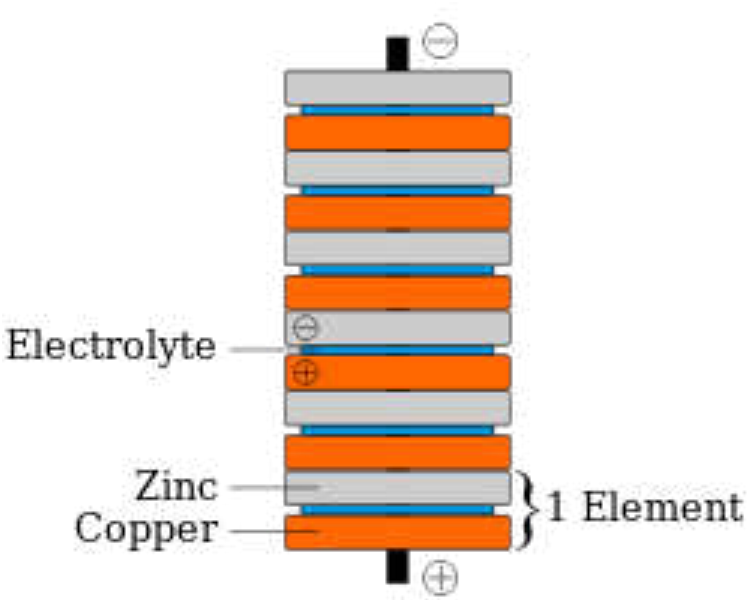

Anode: $Zn^0 \rightarrow Zn^{2+} + 2\ e^-$

Cathode: $Cu^{2+} + 2\ e^- \rightarrow Cu^0$

⇨ **Cu is more noble than Zn, i.e., has a higher redox potential.**

→ What happens to the electrodes?

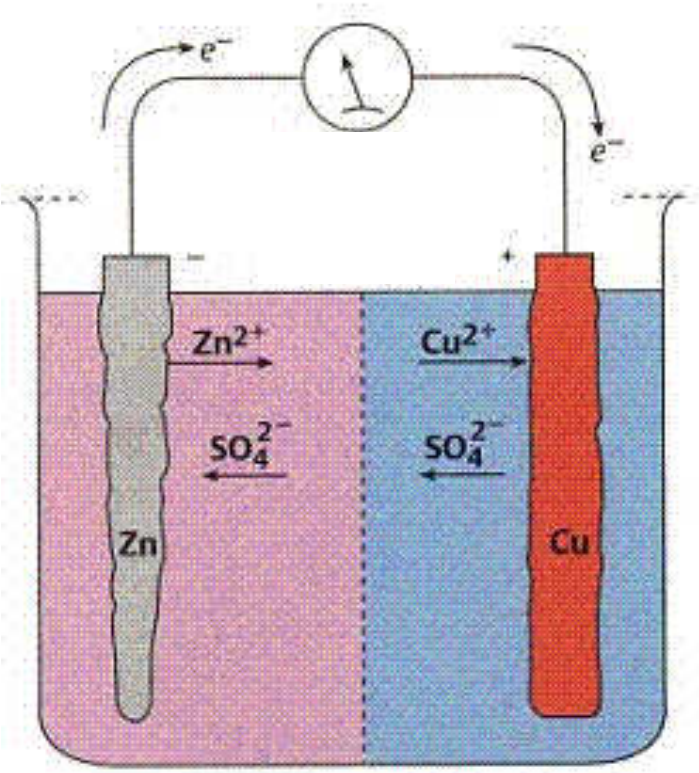

⇨ **Electrodes are "actively" involved and Zn is continuously consumed**

→ The next leap forward: Planté develops the lead-acid battery...

Raymond Louis Gaston Planté
22 April 1834 – 21 May 1889

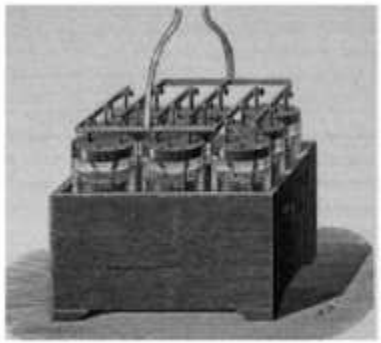

9-cell battery: 26 March 1860

working principle

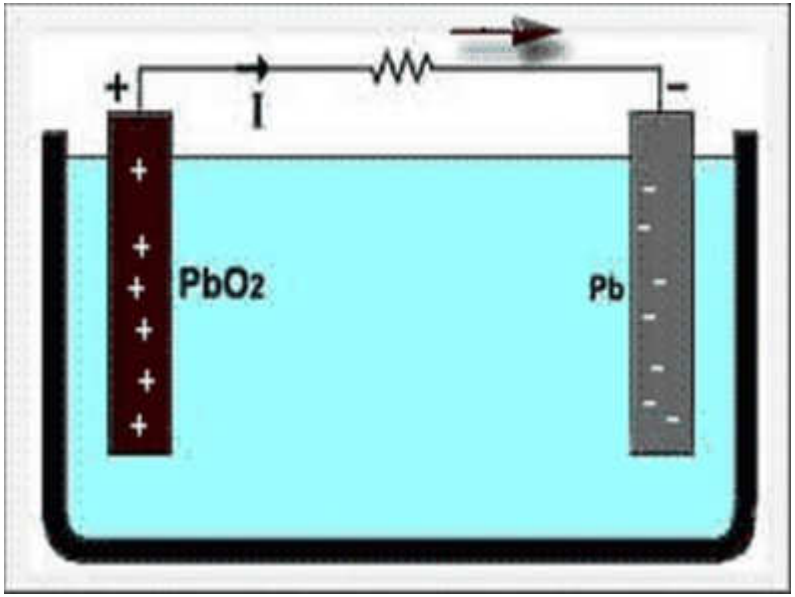

Anode: $Pb^{0} + SO_4^{2-} \rightarrow PbSO_4 + 2\ e^-$

Cathode: $Pb^{+IV}O_2 + SO_4^{2-} + 4\ H_3O^+ + 2\ e^-$

$\downarrow$

$Pb^{+II}SO_4 + 6\ H_2O$

→ Once again… What happens to the electrodes?

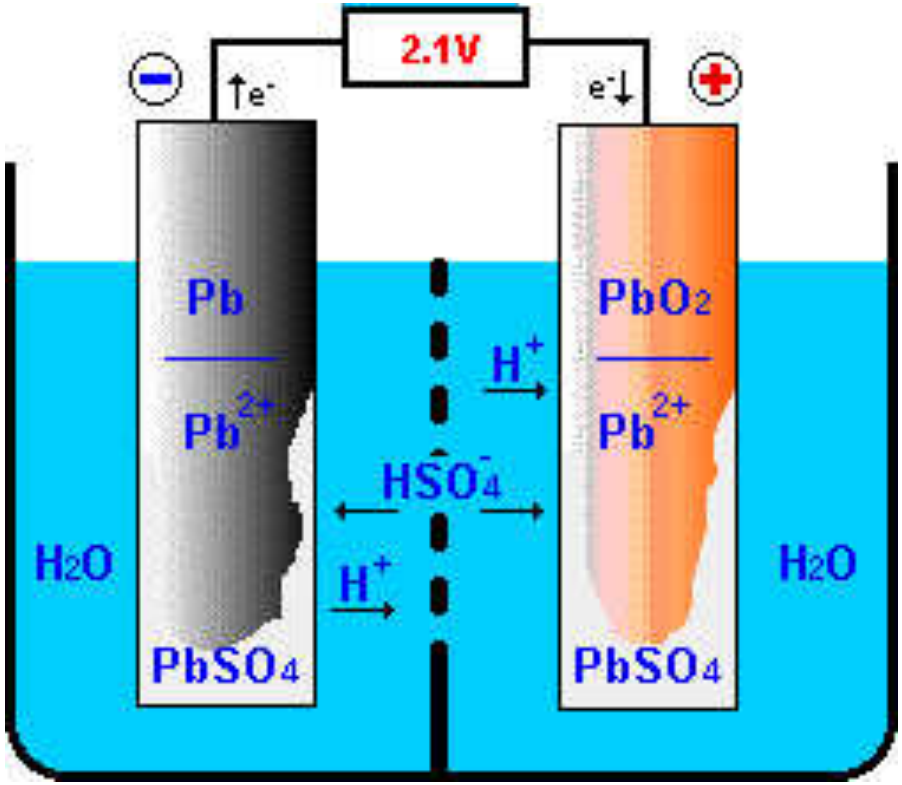

⇨ Electrodes and electrolyte are “actively” involved and in this case both – Pb and PbO_2 – are continuously consumed

→ One more famous battery technology of the *'early days'*…

Leclanché
(1866)

working principle

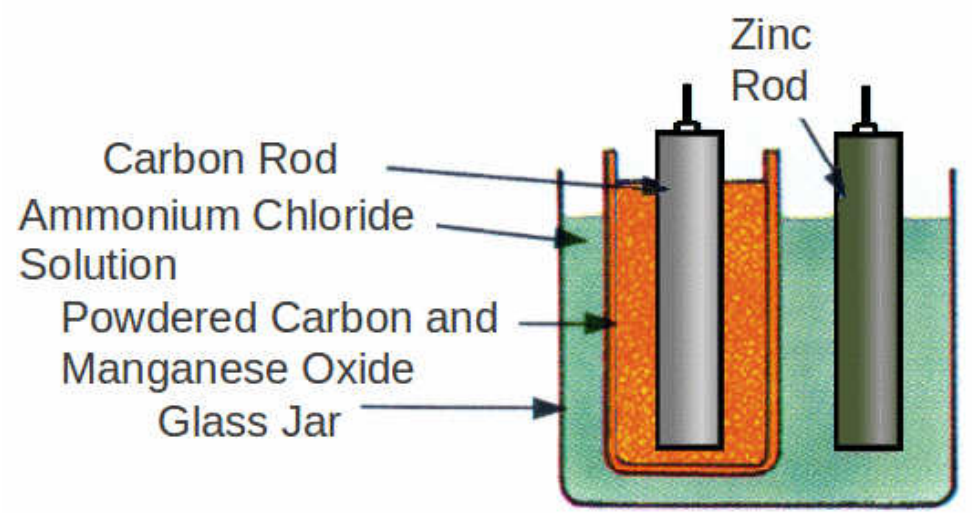

Anode: $Zn^0 \rightarrow Zn^{2+} + 2\ e^-$

Cathode: $2\ MnO_2 + 2\ H^+ + 2\ e^- \rightarrow 2\ MnO(OH)$

⇨ **Also for the Leclanché cell the electrodes (and electrolyte) are "actively" involved and continuously consumed**

→ 1975: The 1st step – nickel-metal hydride batteries...

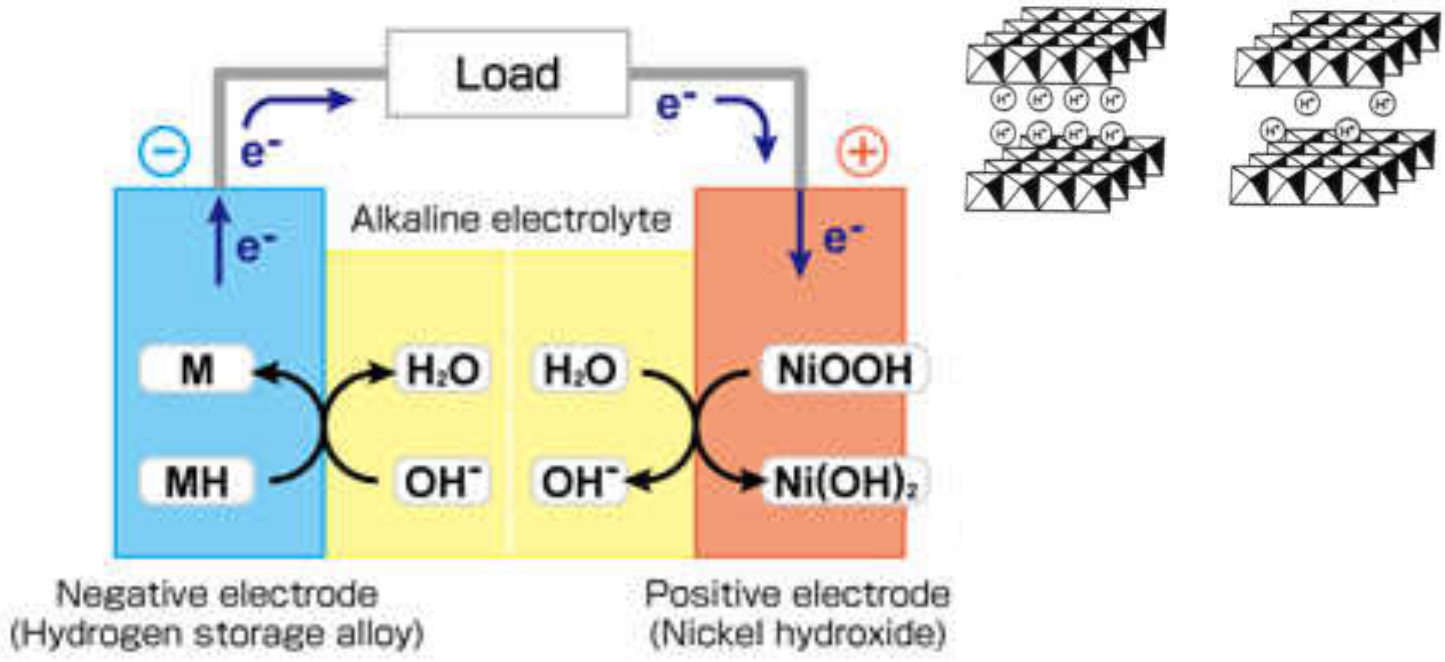

Anode: $M^0 + H_2O + e^- \leftrightarrow M^{+1}H + OH^-$

Cathode: $Ni^{3+}O(OH) + H_2O + e^- \leftrightarrow Ni^{2+}(OH)_2 + OH^-$

⇨ **Net transfer** (i.e., ***'charge carrier'***): H^+

⇨ **Electrodes are "solely" acting as 'host structure' for the charge carrier**

→ 1991: The 2nd step – lithium-ion batteries...

… replacing the H^+ as charge carrier by Li^+:

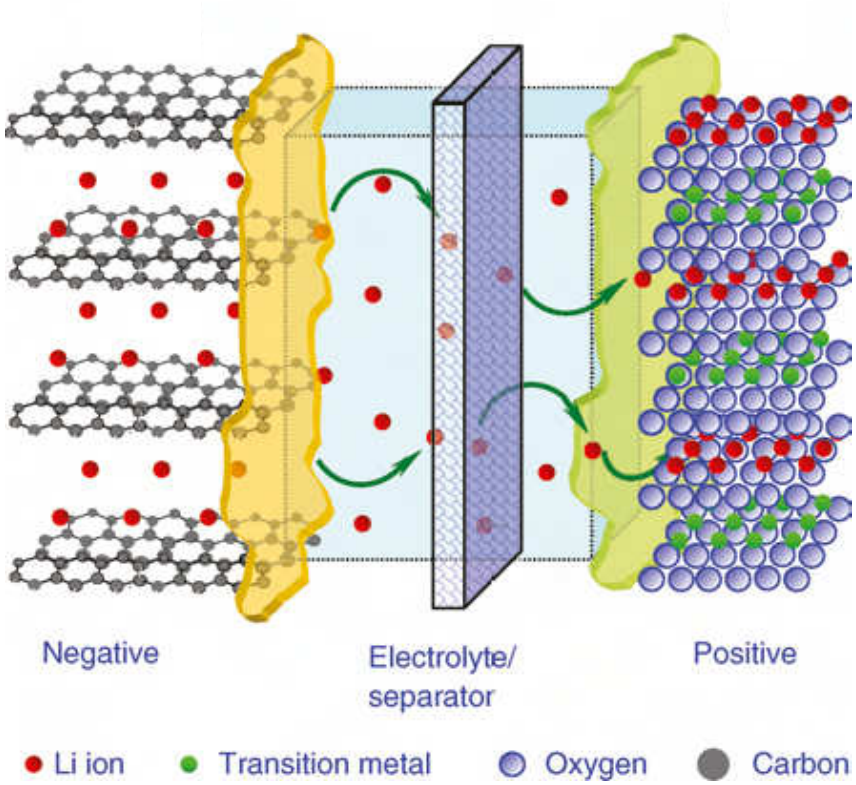

Anode: $C_6 + Li^+ + e^- \leftrightarrow LiC_6$

Cathode: $LiM^{3+}O_2 \leftrightarrow M^{2+}O_2 + Li^+ + e^-$

K. Xu, Encyclopedia of Power Sources

→ 1991: The 2nd step – lithium-ion batteries...

… replacing the H^+ as charge carrier by Li^+:

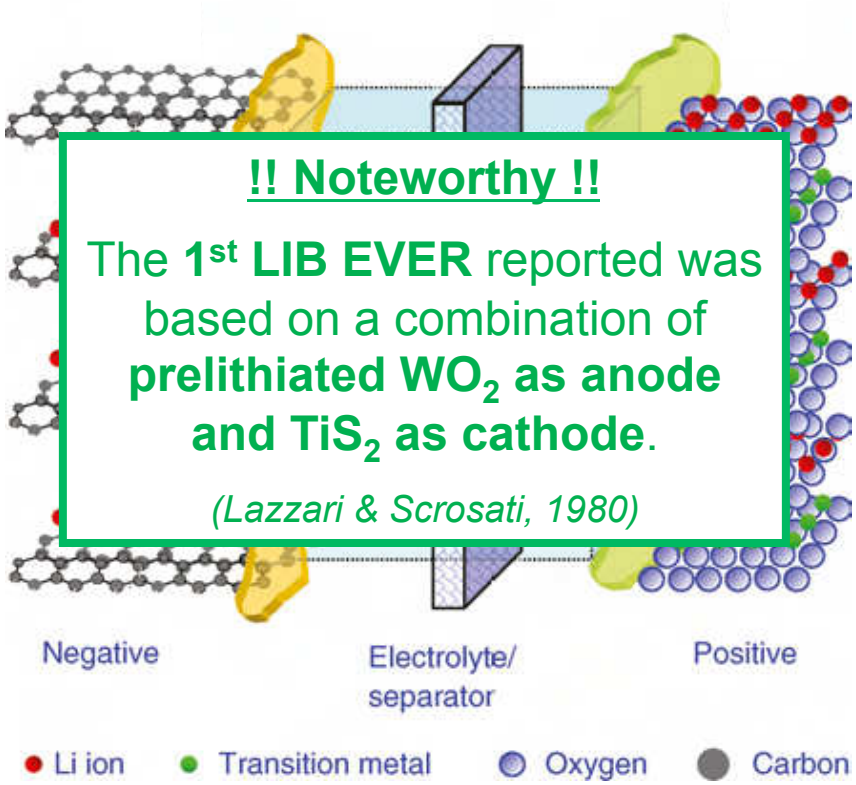

Anode: $C_6 + Li^+ + e^- \leftrightarrow LiC_6$

Cathode: $LiM^{3+}O_2 \leftrightarrow M^{2+}O_2 + Li^+ + e^-$

K. Xu, Encyclopedia of Power Sources

Lithium-Ion Battery

Charge

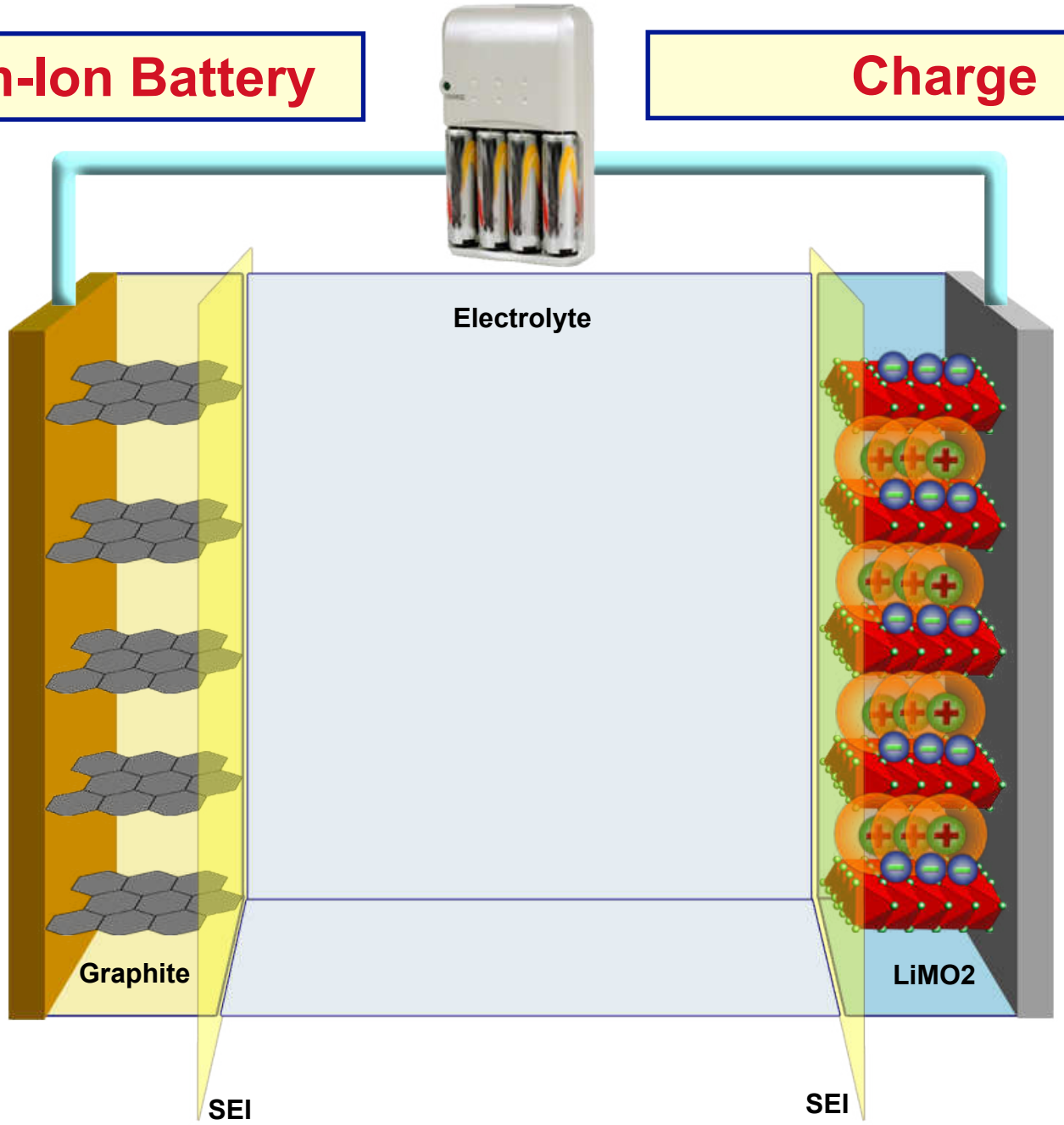

Lithium-Ion Battery

Discharge

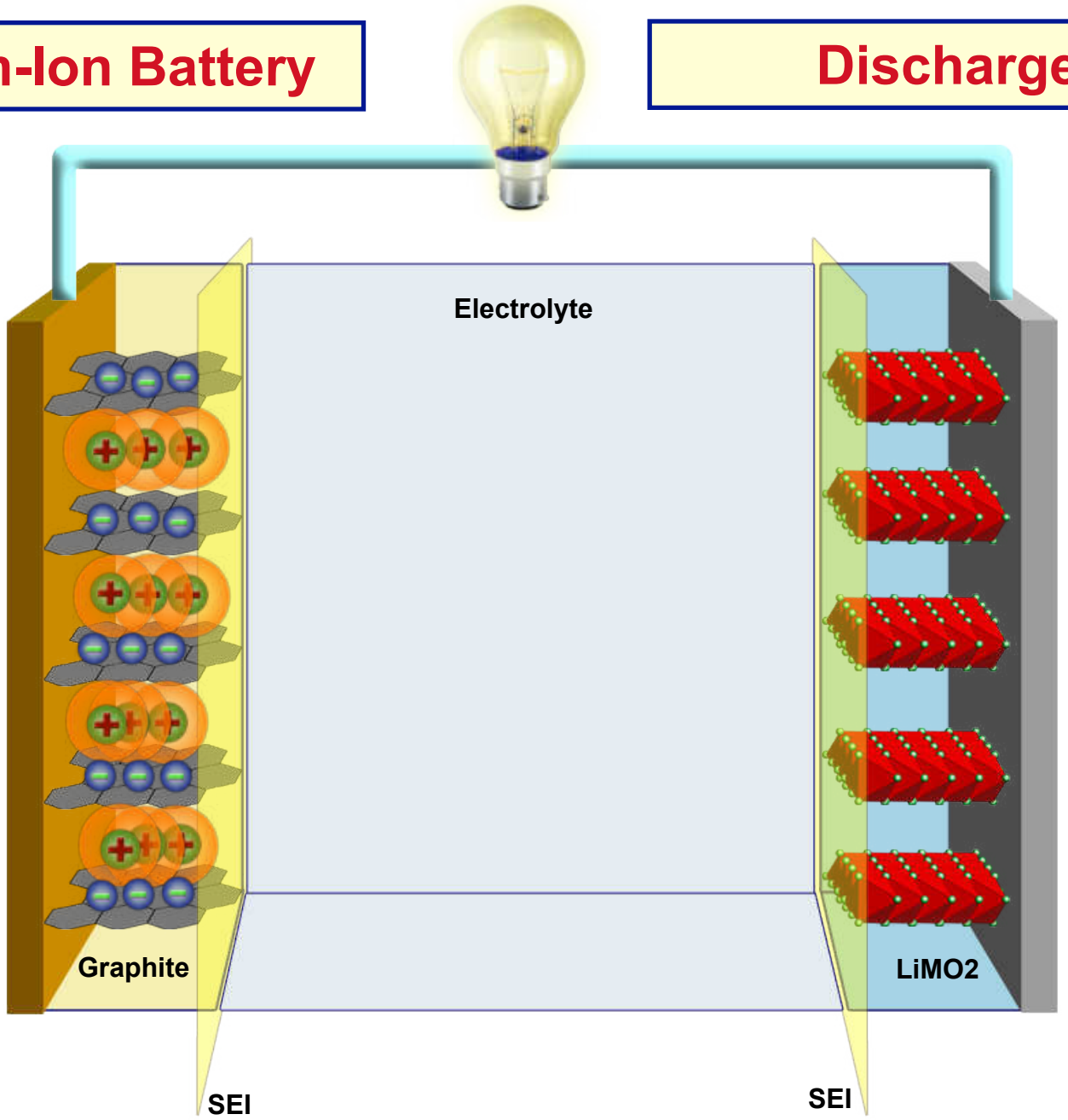

→ 3rd step – replacing Li^+, for instance, by …

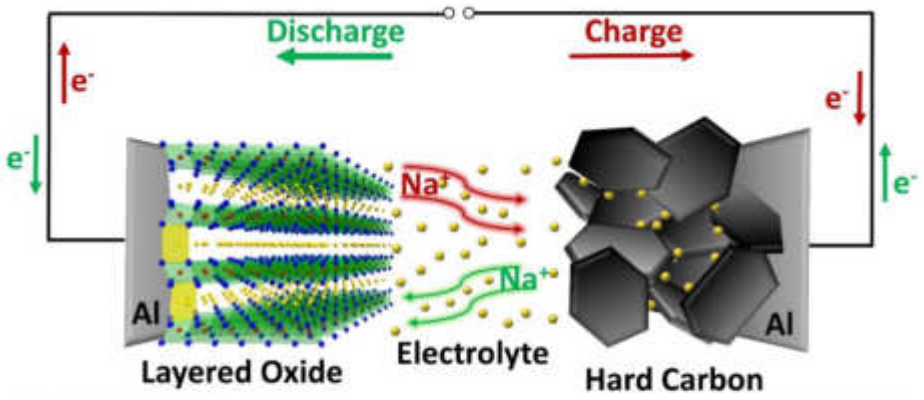

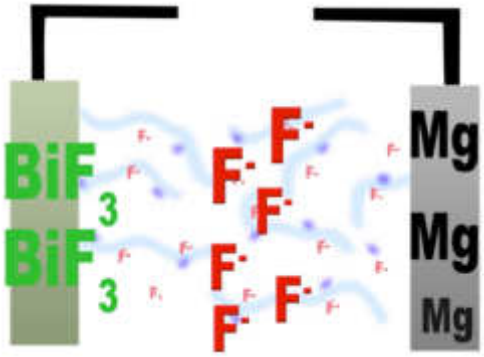

… each of them with its own advantages and challenges.

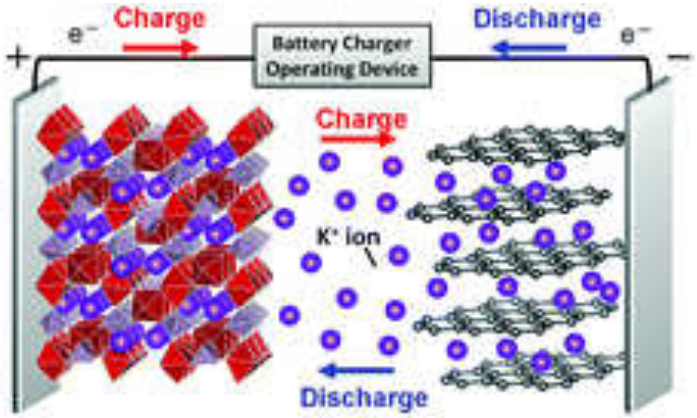

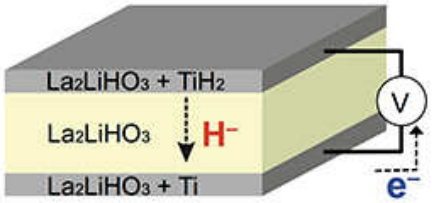

$TiH_2 + xe^- \longrightarrow TiH_{2-x} + xH^-$

$Ti + xH^- \longrightarrow TiH_x + xe^-$

Keller et al., ChemElectroChem 2016 (3) 1124-1132; Chihara et al., Chem. Commun. 2017 (53) 5208-5211; Kobayashi et al., Science 2016 (351) 1314-1317; Gschwind, Habilitation Presentation, Univ. Ulm, Germany, 2017.

→ Three main classes are known today:

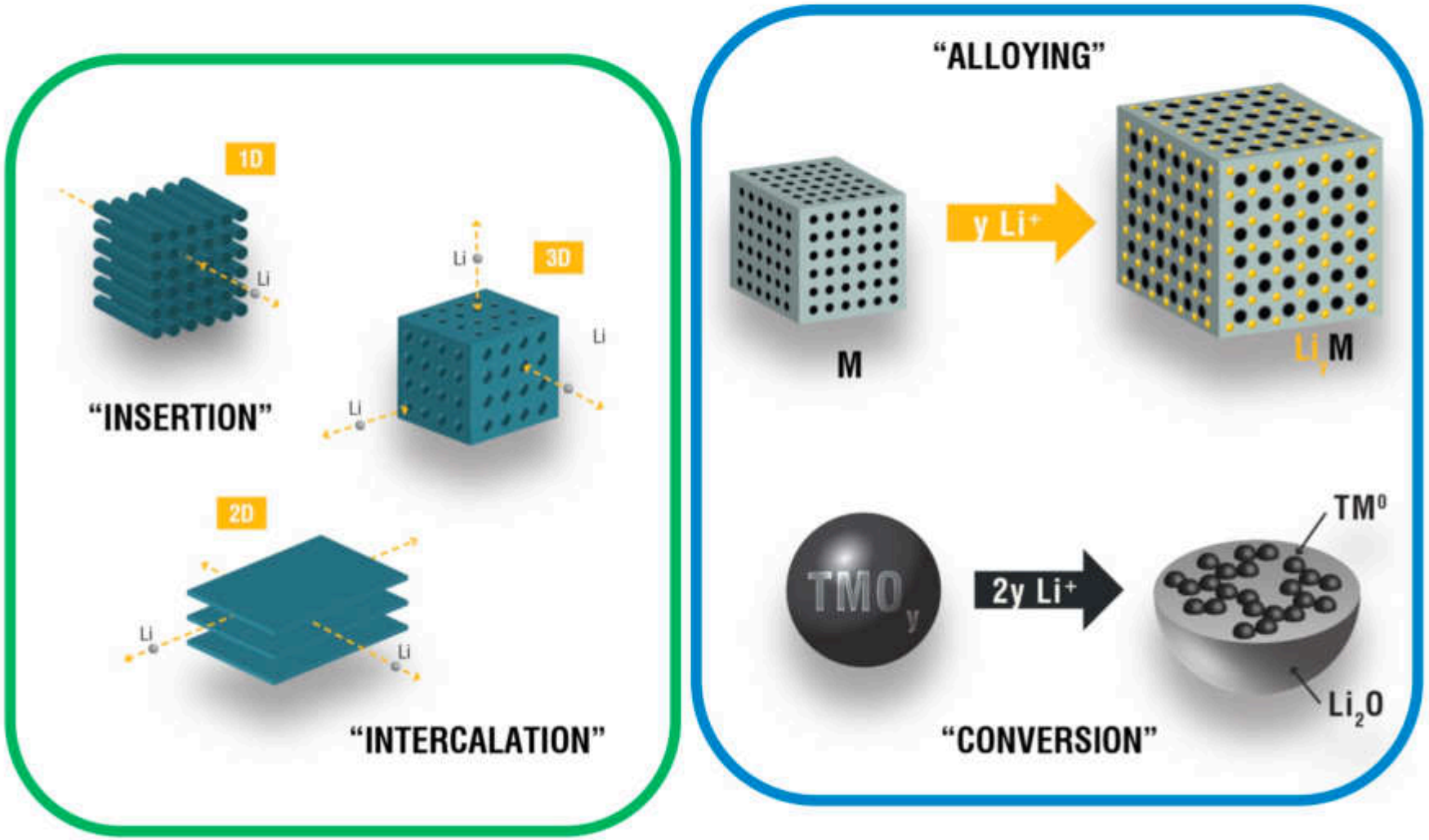

Bresser et al., Energy Environ. Sci. 2016 (9) 3348-3367.

→ Some classic examples for insertion-type materials:

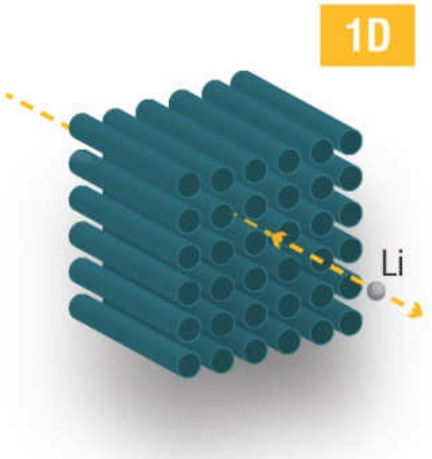

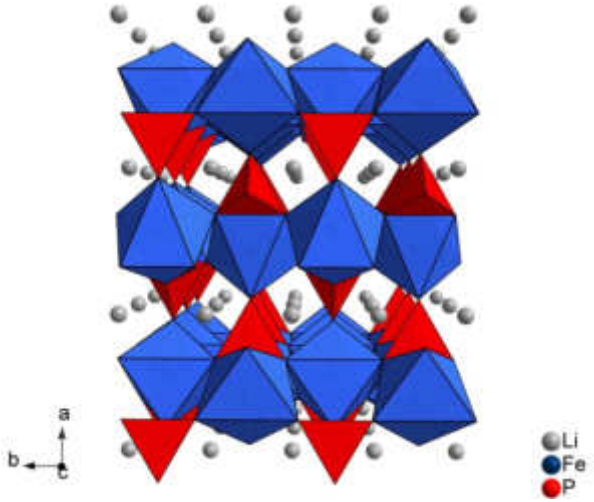

$LiFePO_4$

olivine structure

spec. capacity$_{(theor)}$: 170 mAh g^{-1}

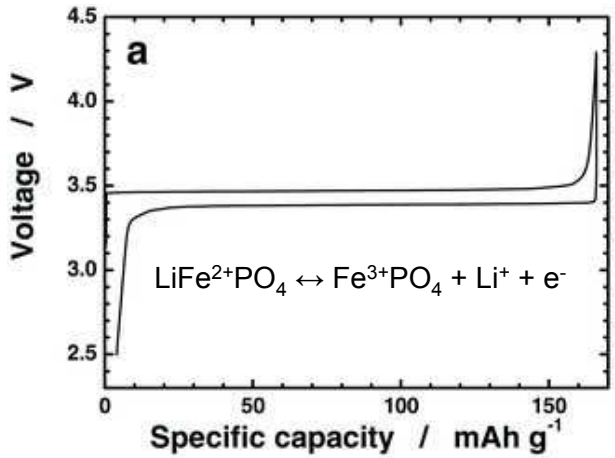

flat dis-/charge plateau at ca. 3.4 V

(2-phase equilibrium; 1st order phase transition)

Bresser et al., Energy Environ. Sci. 2016 (9) 3348-3367; Molenda & Molenda, doi: 10.5772/21635; Oh et al., Adv. Mater. 2010 (22) 4842-4845..

→ Some classic examples for insertion-type materials:

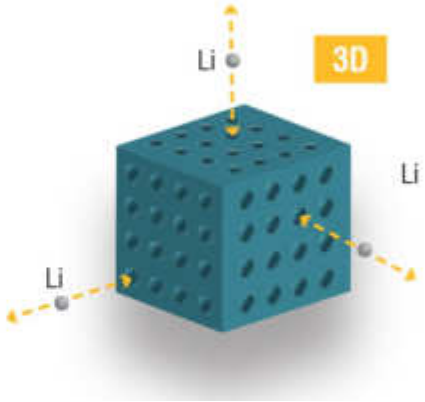

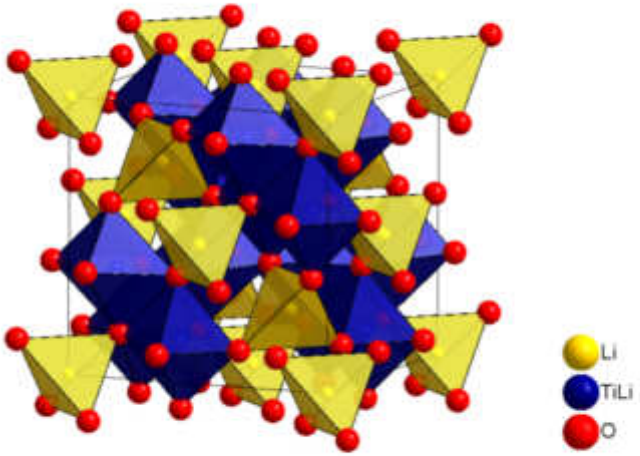

$Li_4Ti_5O_{12}$

spinel structure

spec. capacity$_{(theor)}$: 175 mAh g^{-1}

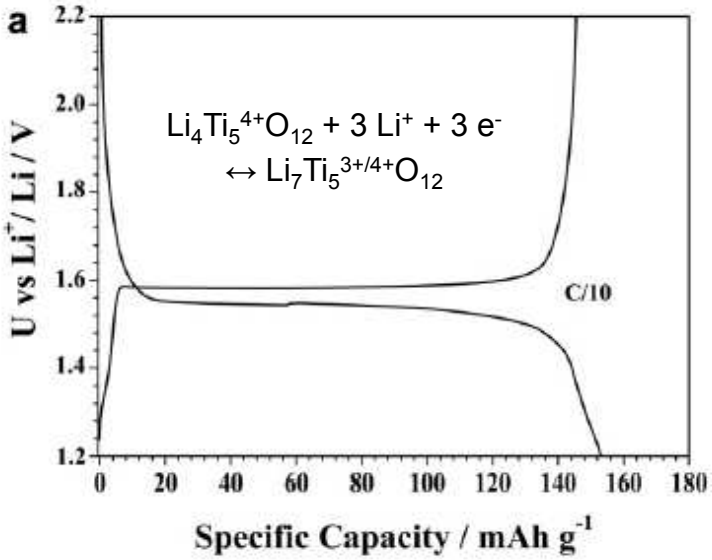

flat dis-/charge plateau at ca. 1.5 V

(2-phase equilibrium;)

Bresser et al., Energy Environ. Sci. 2016 (9) 3348-3367; Bresser et al., J. Power Sources 2012 (219) 217-222.

→ Some classic examples for intercalation-type materials:

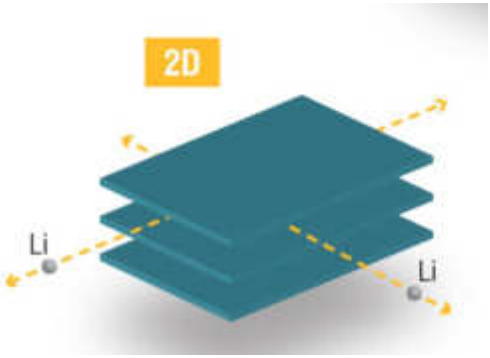

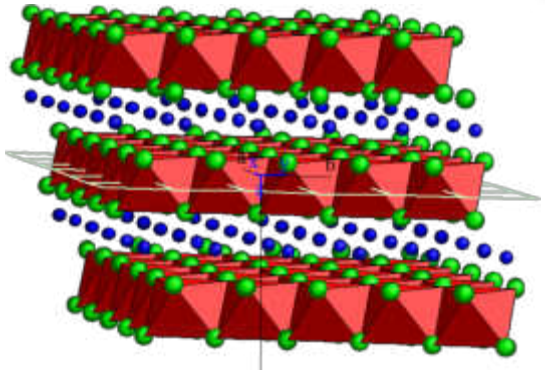

$LiCoO_2$

the 1st LIB cathode material

spec. capacity$_{(theor)}$: 274 mAh g^{-1}

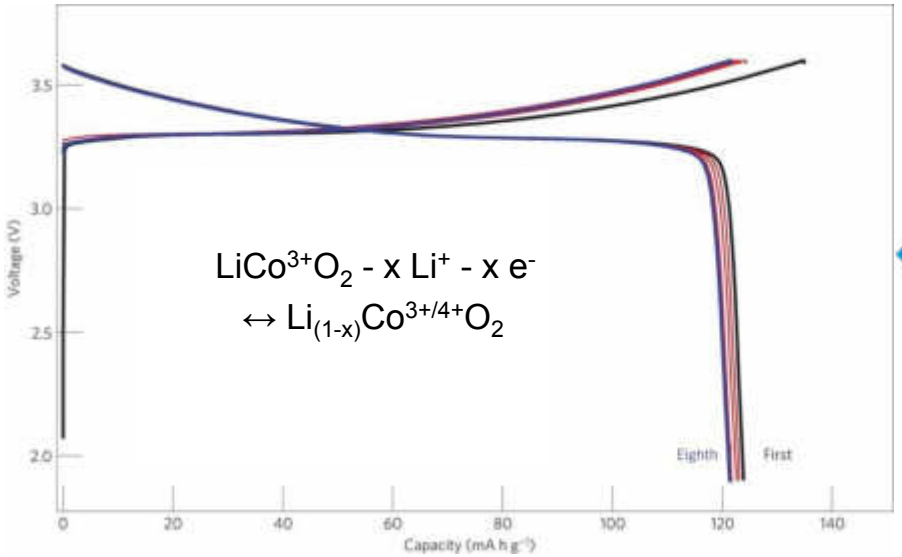

$LiCo^{3+}O_2$ - x Li^+ - x e^-
↔ $Li_{(1-x)}Co^{3+/4+}O_2$

continuously sloped profile

Bresser et al., Energy Environ. Sci. 2016 (9) 3348-3367; Kamya et al., Nature Mater. 2011 (10) 682-686.

→ Some classic examples for intercalation-type materials:

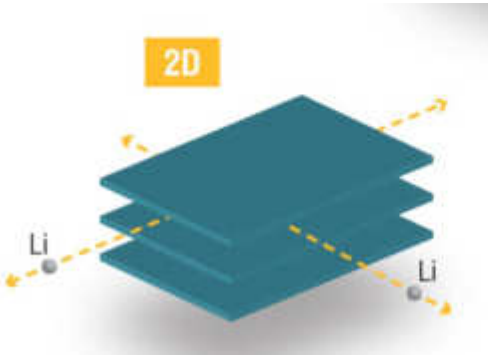

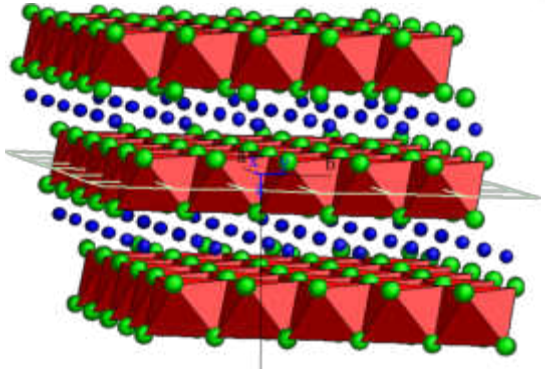

$Li[Ni_{1/3}Mn_{1/3}Co_{1/3}]O_2$

Co partially replaced by Ni and Mn

spec. capacity$_{(theor)}$: 290 mAh g^{-1}

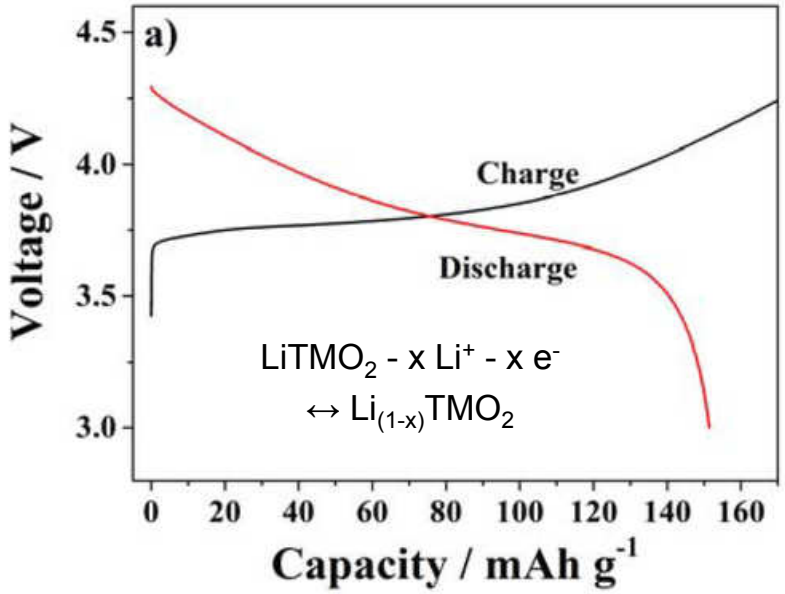

continuously sloped profile

Bresser et al., Energy Environ. Sci. 2016 (9) 3348-3367; Carvalho et al., Membranes 2015 (5) 632-645.

➔ Synergetic combination of the two de-/lithiation mechanisms

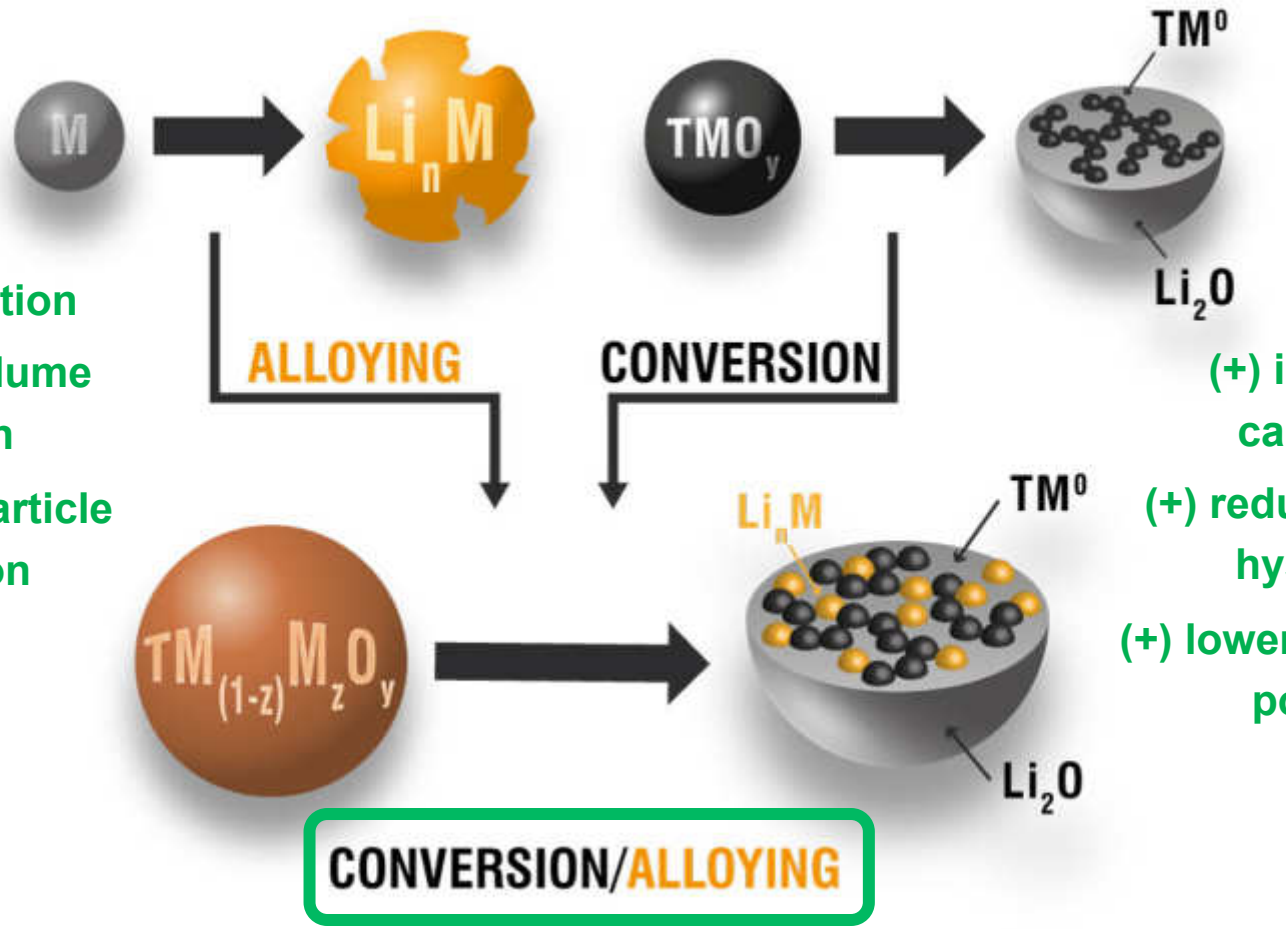

(+) e^- conduction

(+) limited volume expansion

(+) hindered particle aggregation

(+) increased capacities

(+) reduced voltage hysteresis

(+) lower de-/lithiation potential

Bresser et al., Energy Environ. Sci. 2016 (9) 3348.

➔ Confirmation of the general reaction mechanism by means of *in situ* XRD and XAS (ESRF):

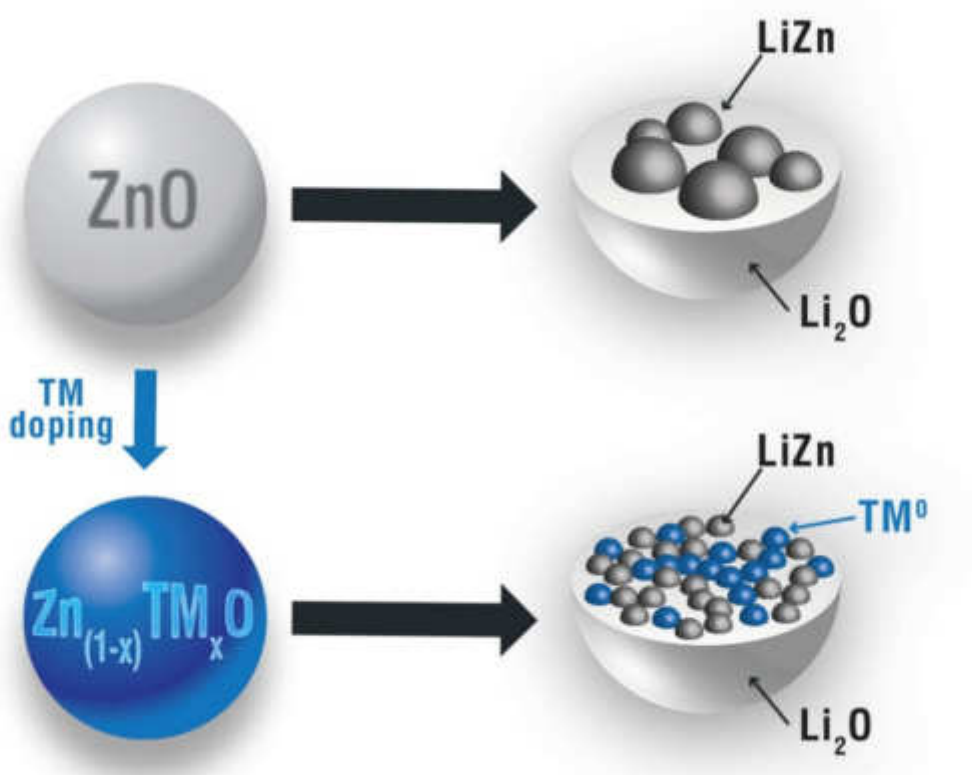

➔ Realization of an e^--conducting network within the single particle

➔ Hindered aggregation of the alloying element nanograins
(kinetics, confinement)

Ma et al., in preparation; Giuli et al., in preparation; Mueller et al., ChemElectroChem 2016 (3) 1311; Bresser et al. Energy Environ. Sci. 2016 (9) 3348.

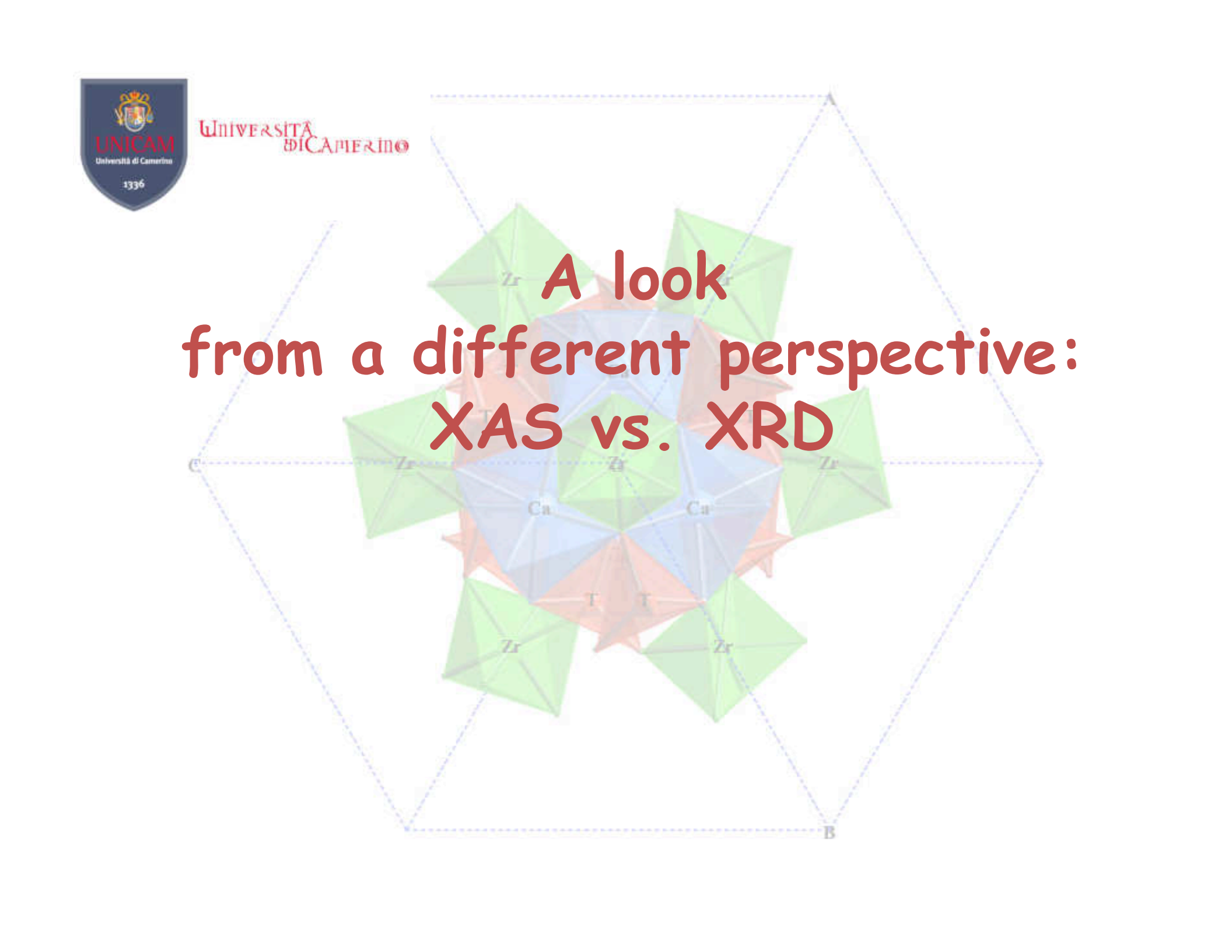

A look from a different perspective: XAS vs. XRD

overview

OXIDATION STATE information from the edge energy

OXIDATION STATE information from the pre-edge peak

LOCAL GEOMETRY theoretical XANES

Local geometry of substituents EXAFS-XANES

Layer silicate and a garnet

STRUCTURAL RELAXATION

AMORPHOUS SAMPLES EXAFS-XANES

peptides

XAS (X-ray Absorption Spectroscopy)

XANES (X-ray Absorption Near Edge Spectroscopy)

EXAFS (Extended X-ray Absorption Fine Structure)

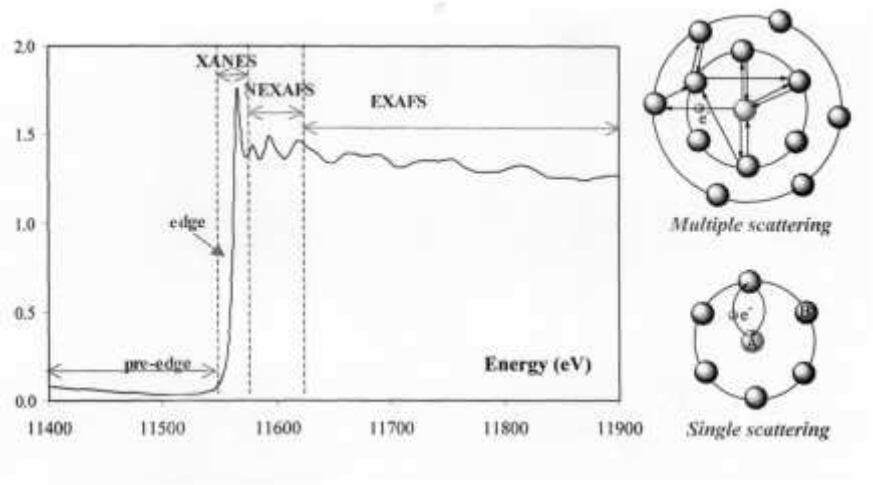

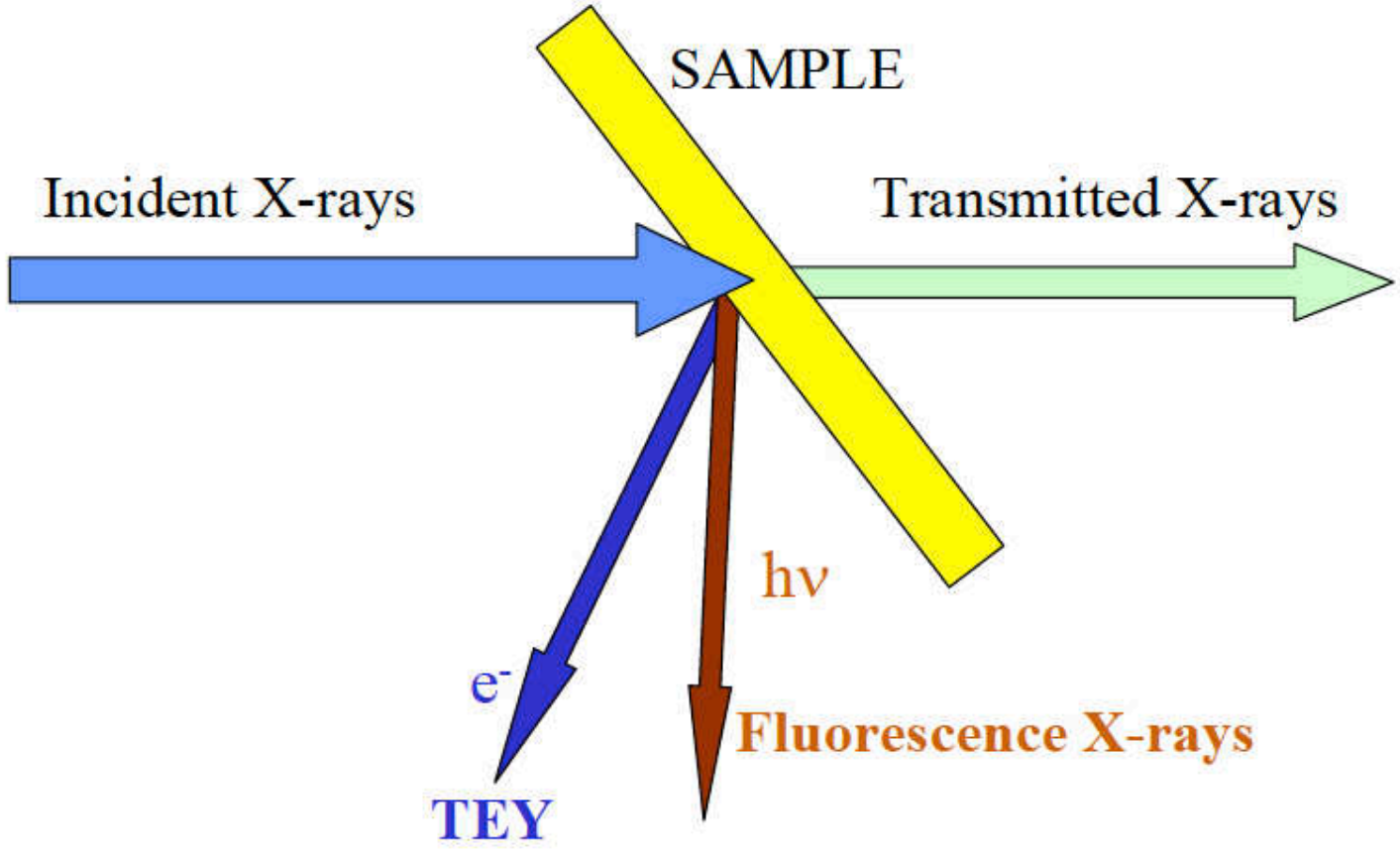
SAMPLE
Incident X-rays
Transmitted X-rays
hν
e-
Fluorescence X-rays
TEY

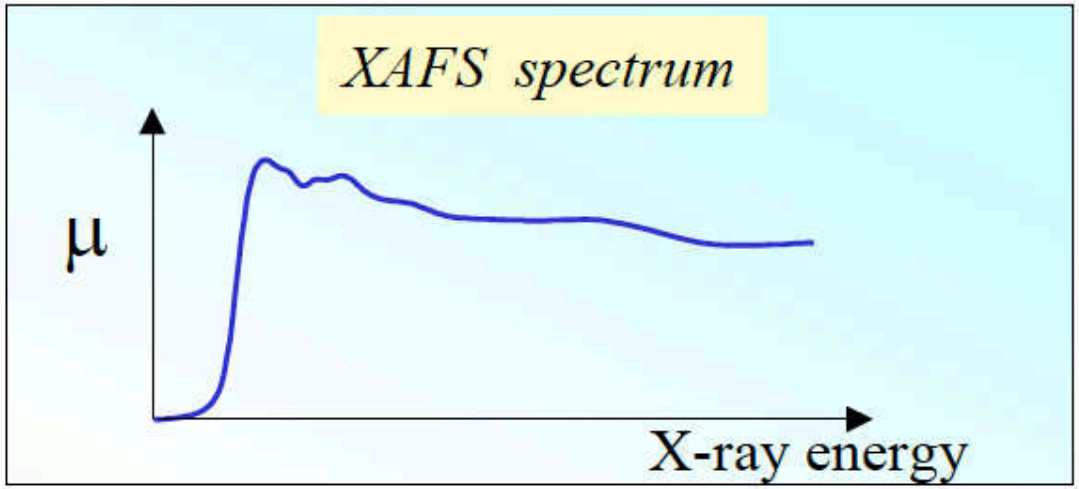
XAFS spectrum
μ
X-ray energy

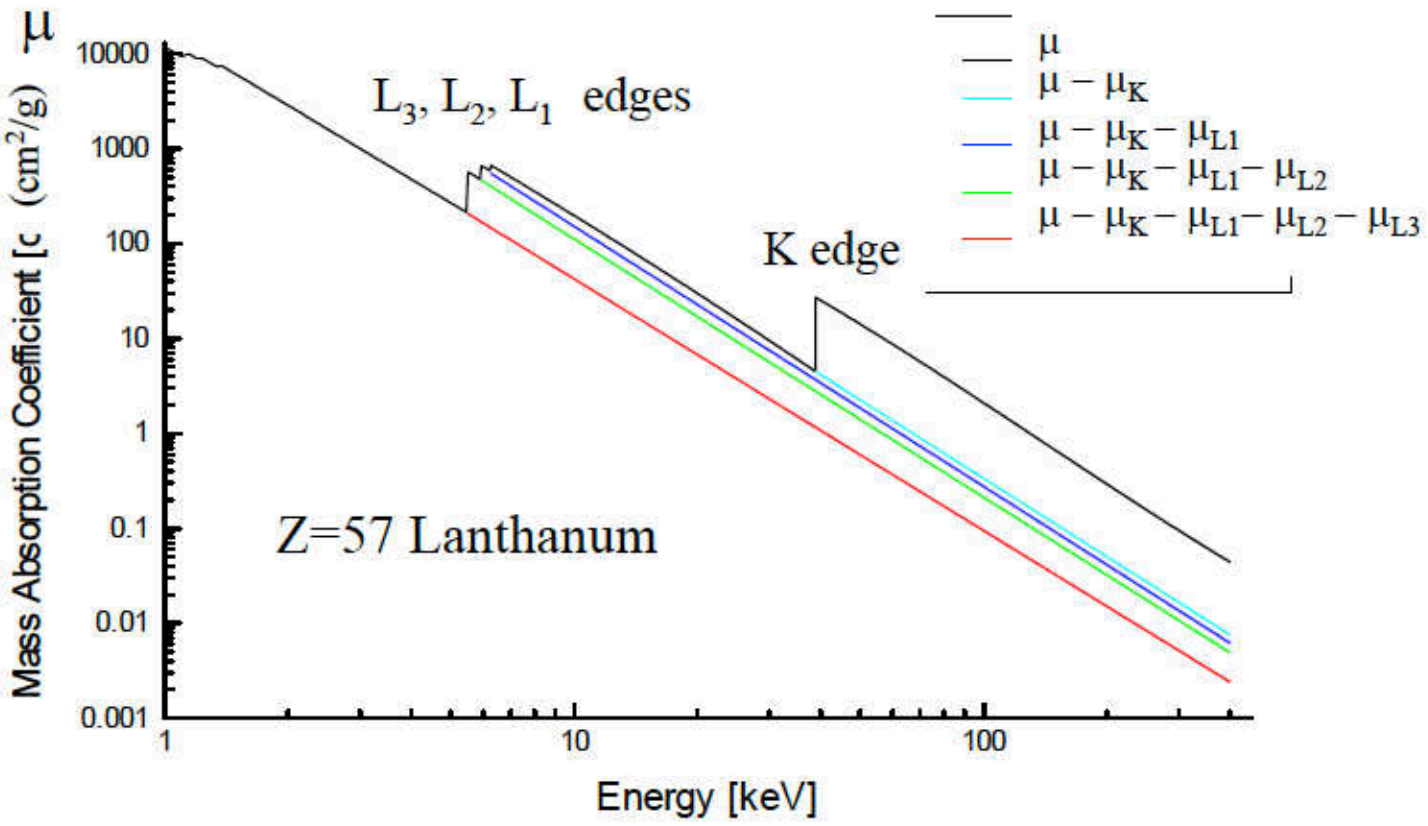

When the photons reach an energy equal to an absorption edge, μ increases abruptly because the photons are suddenly able to remove some more electrons.

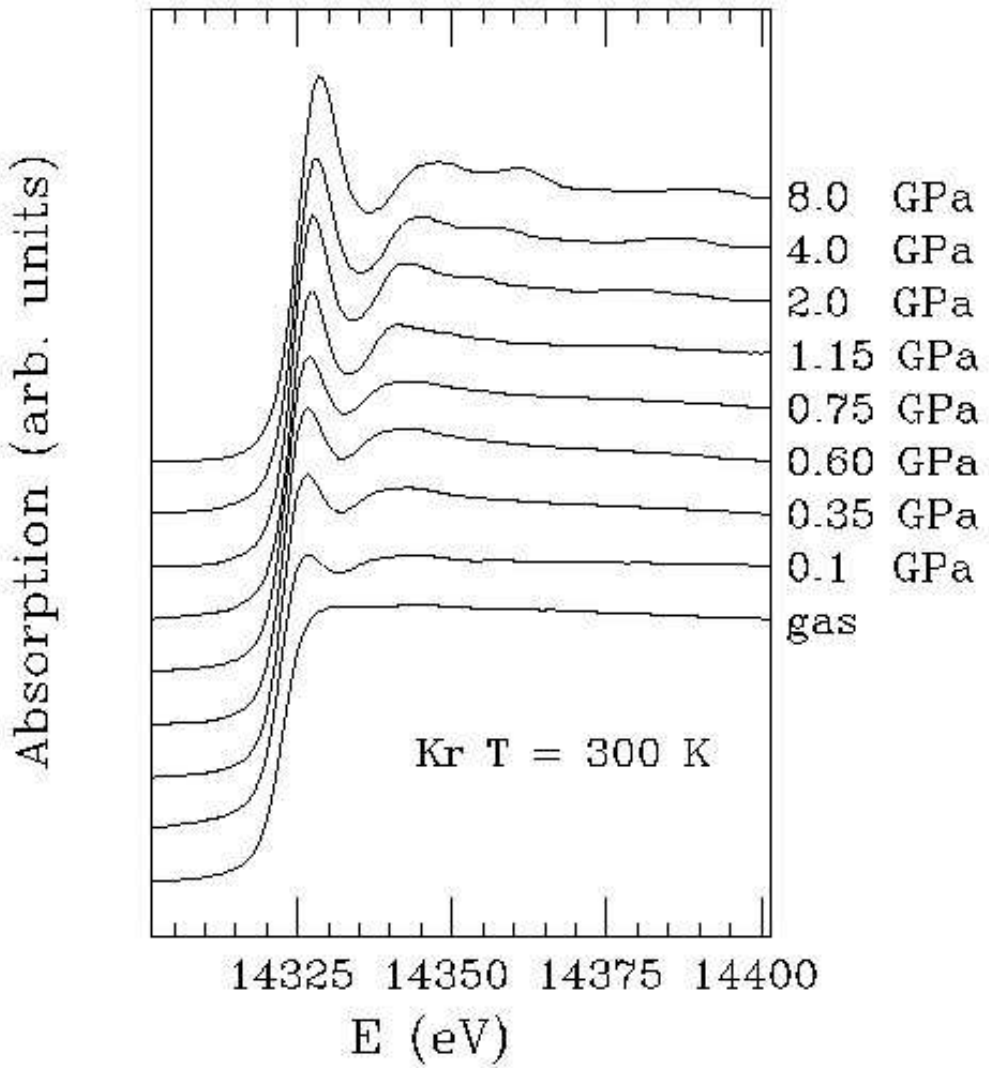
Absorption (arb. units)
8.0 GPa
4.0 GPa
2.0 GPa
1.15 GPa
0.75 GPa
0.60 GPa
0.35 GPa
0.1 GPa
gas
Kr T = 300 K
14325 14350 14375 14400
E (eV)

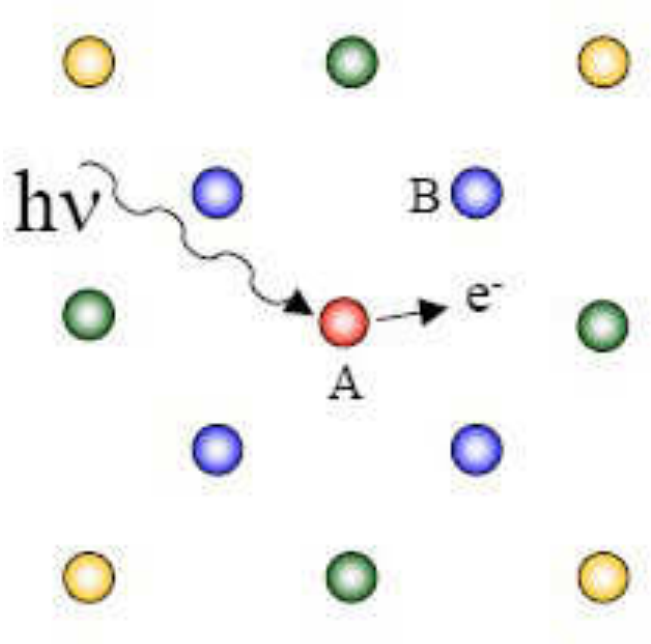
hν
B
e-
A

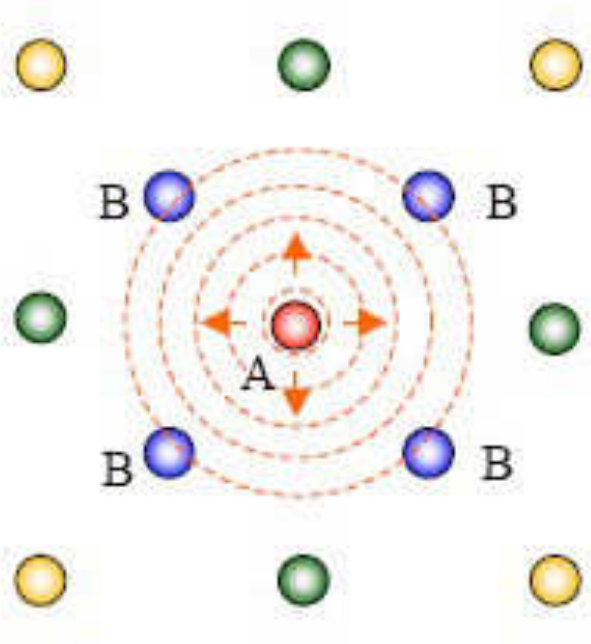
B
B
A
B
B

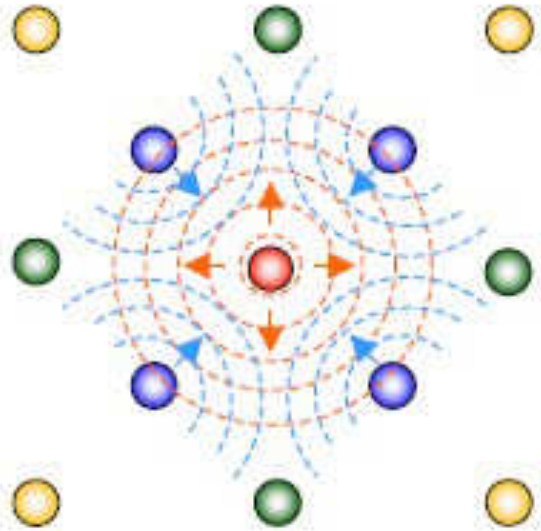

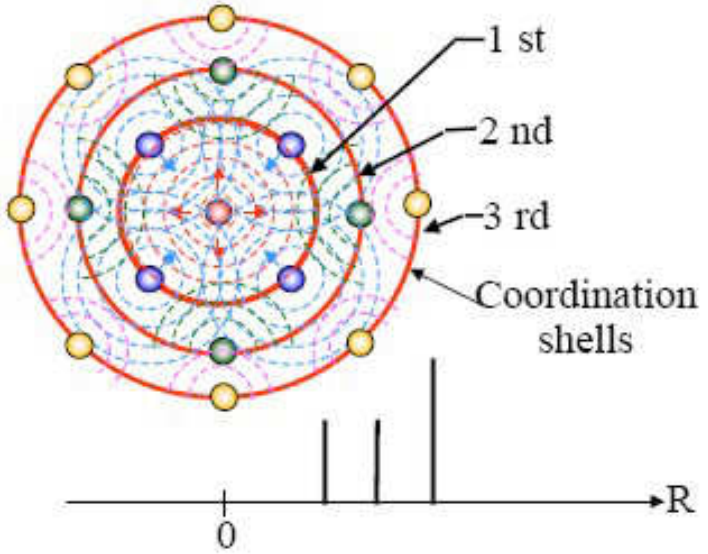
1 st
2 nd
3 rd
Coordination shells
R
0

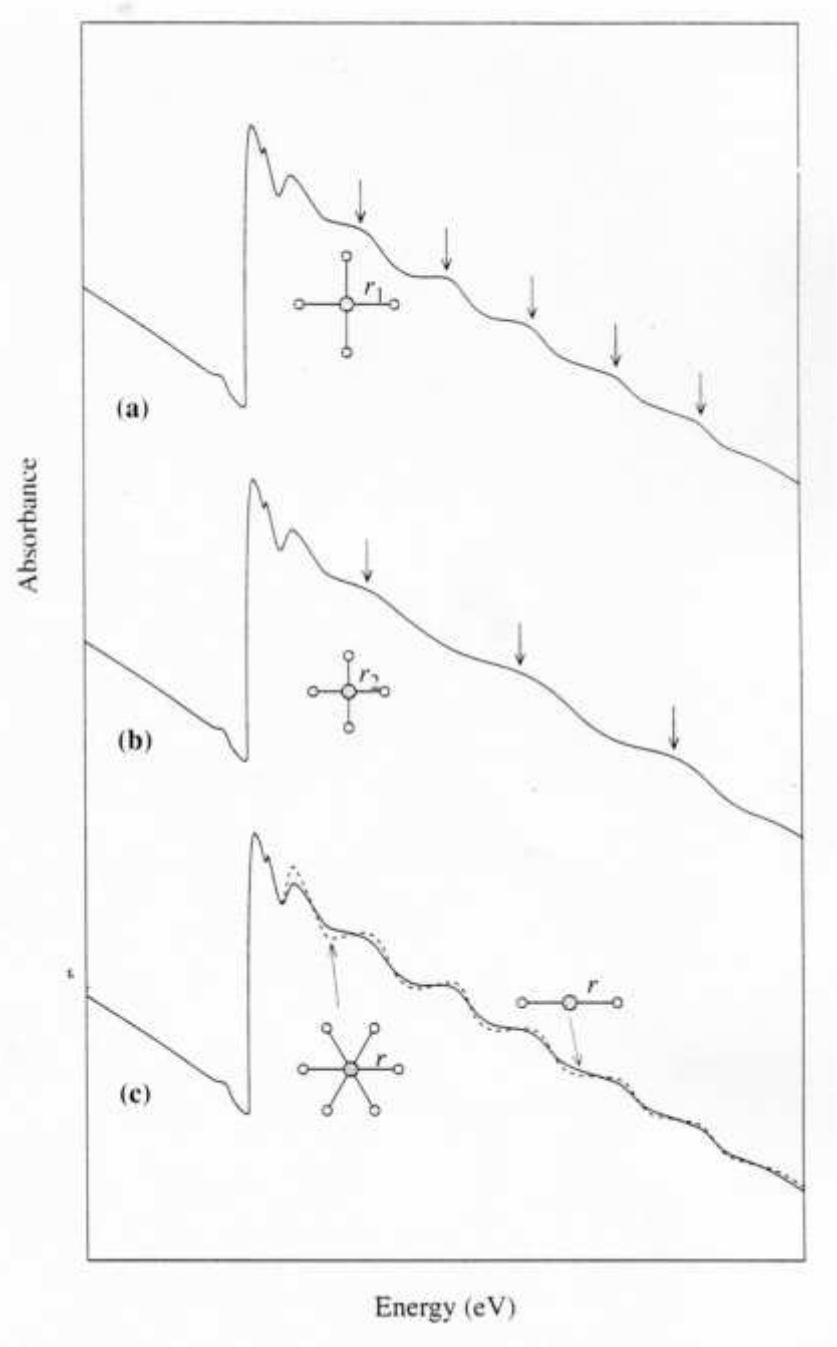
Absorbance
(a)
r_1
(b)
r_2
(c)
r
r
Energy (eV)

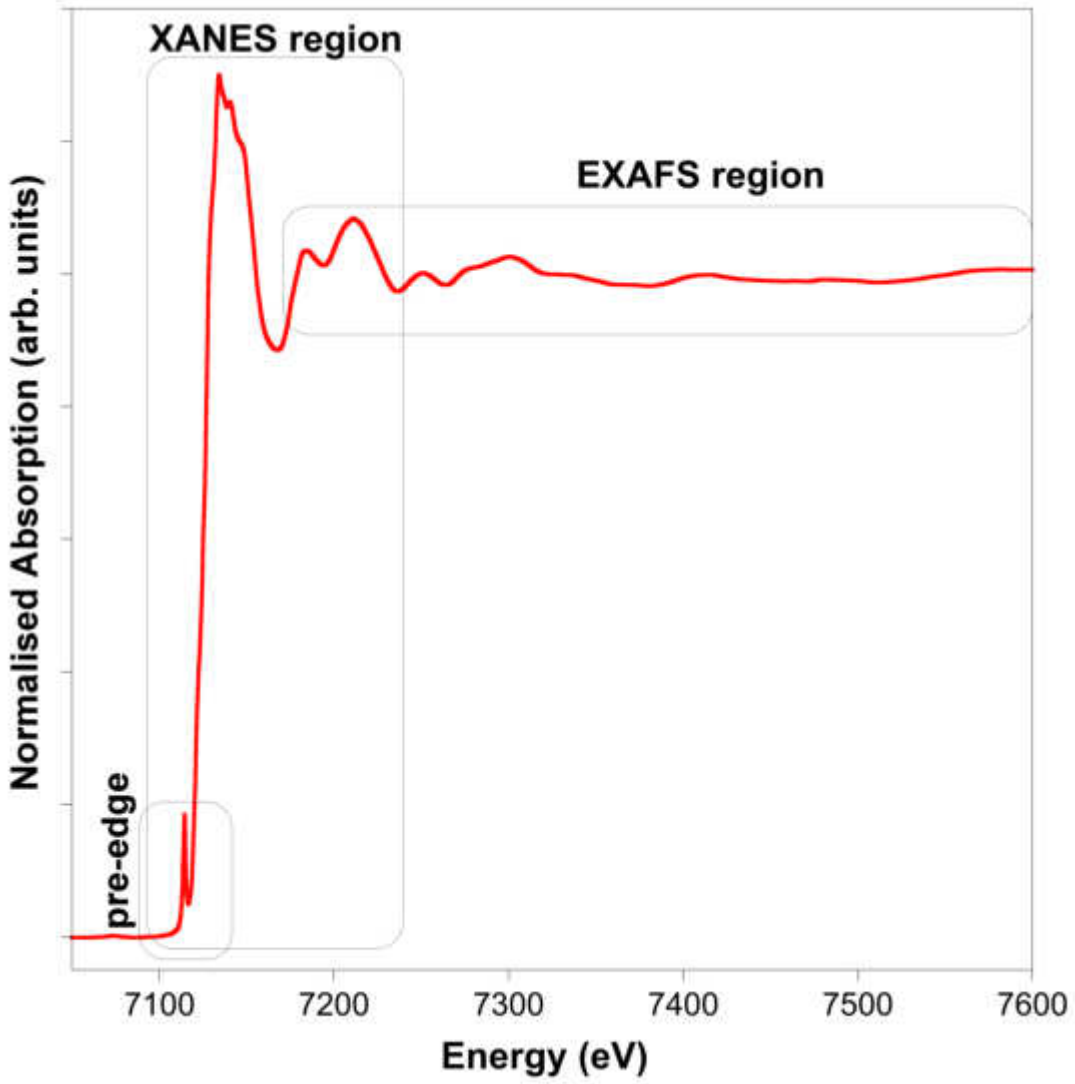

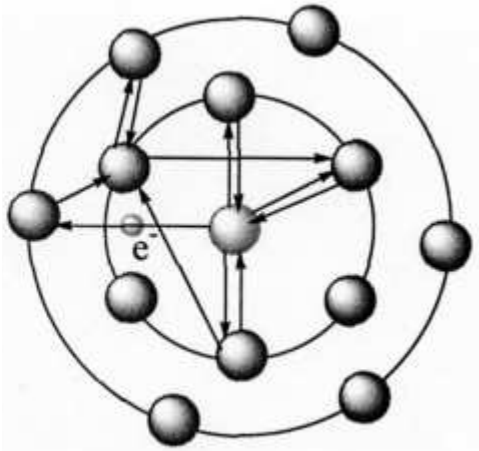

Multiple scattering

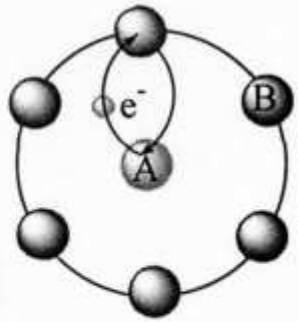

Single scattering

Oxidation state – Edge Energy

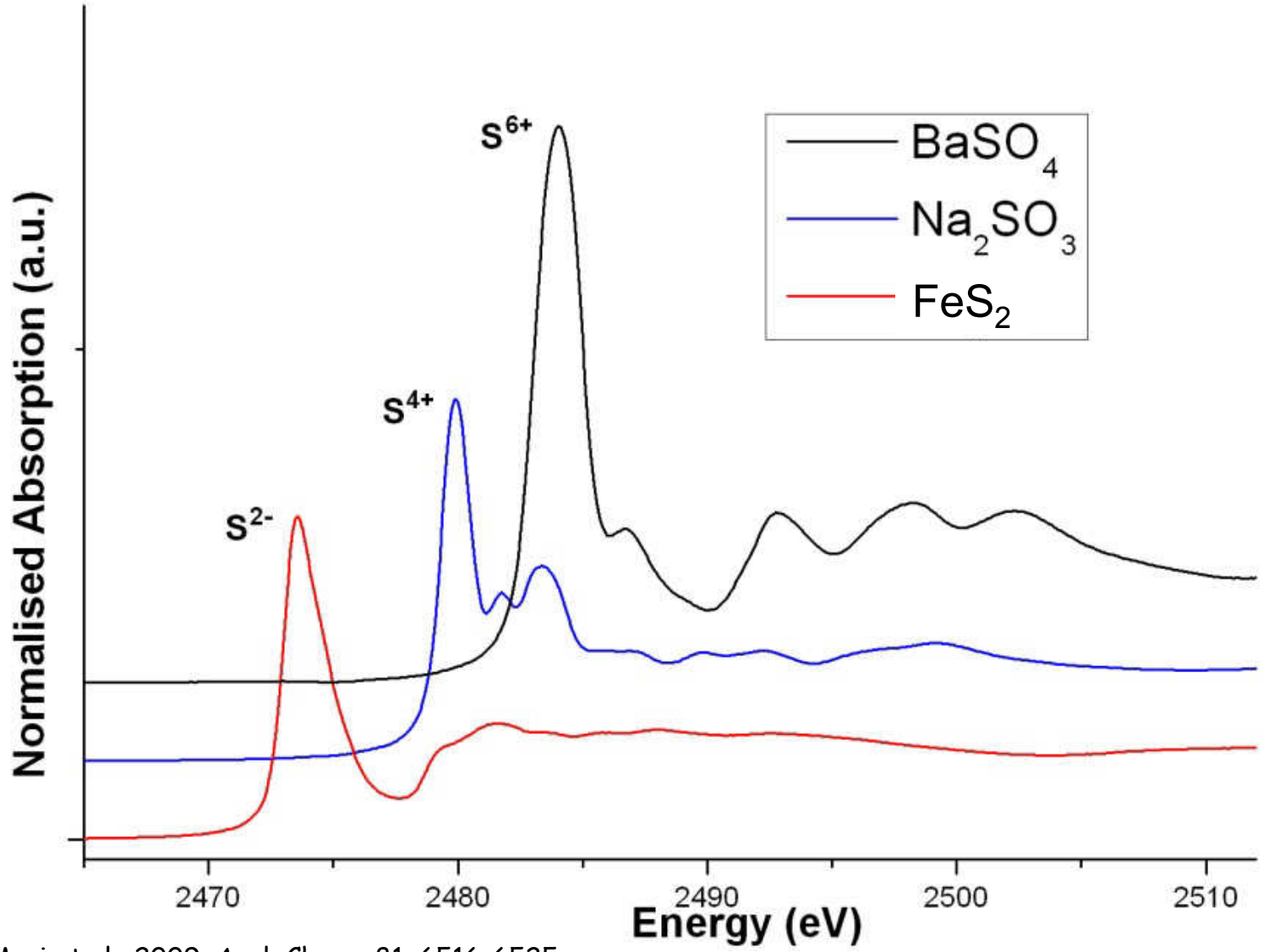

From Mori et al., 2009. Anal. Chem., 81, 6516-6525

Oxidation state – Edge Energy

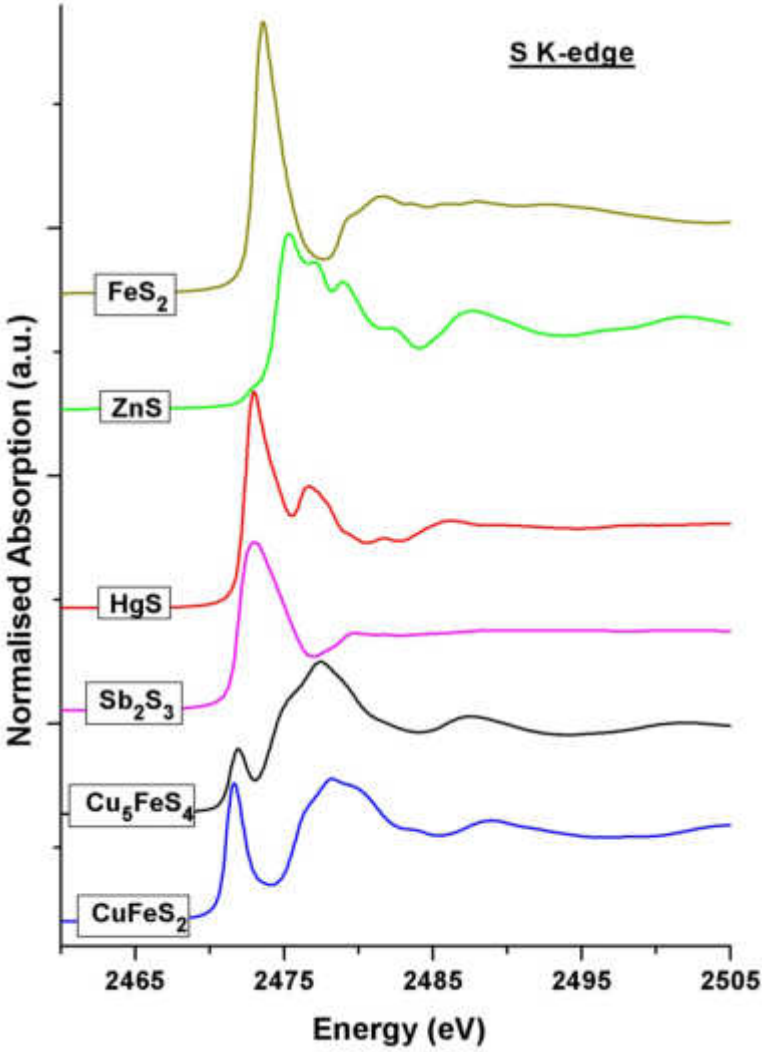

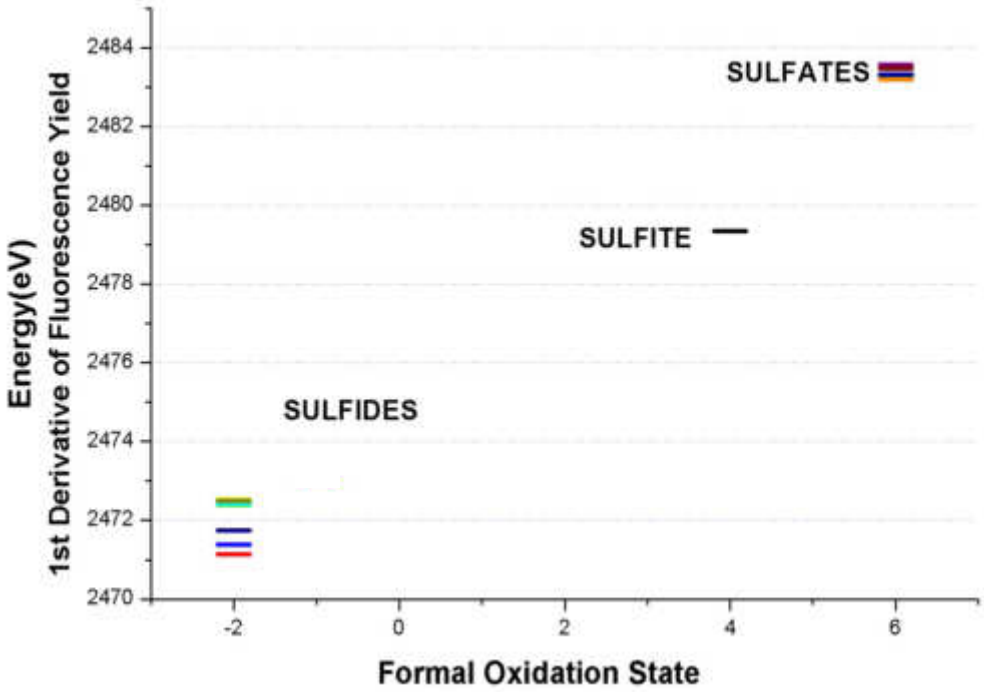

From Mori et al., 2009. Anal. Chem., 81, 6516-6525

Oxidation state – Edge Energy

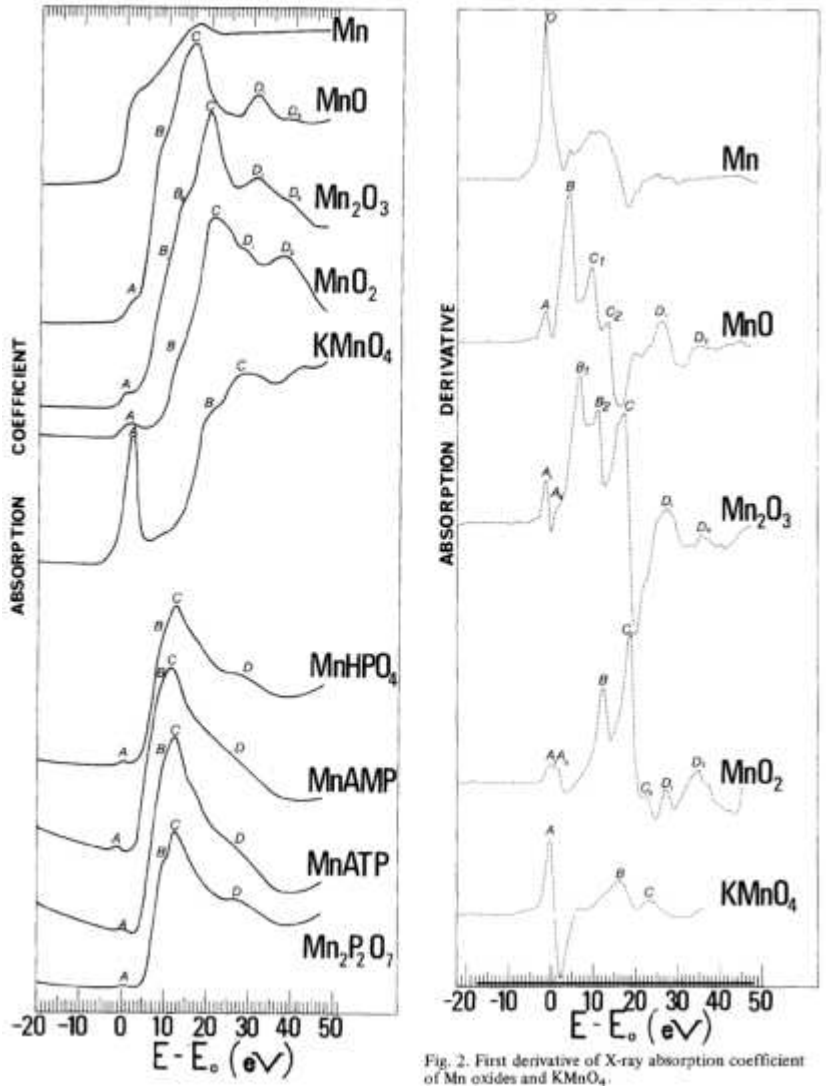

Fig. 2. First derivative of X-ray absorption coefficient of Mn oxides and $KMnO_4$.

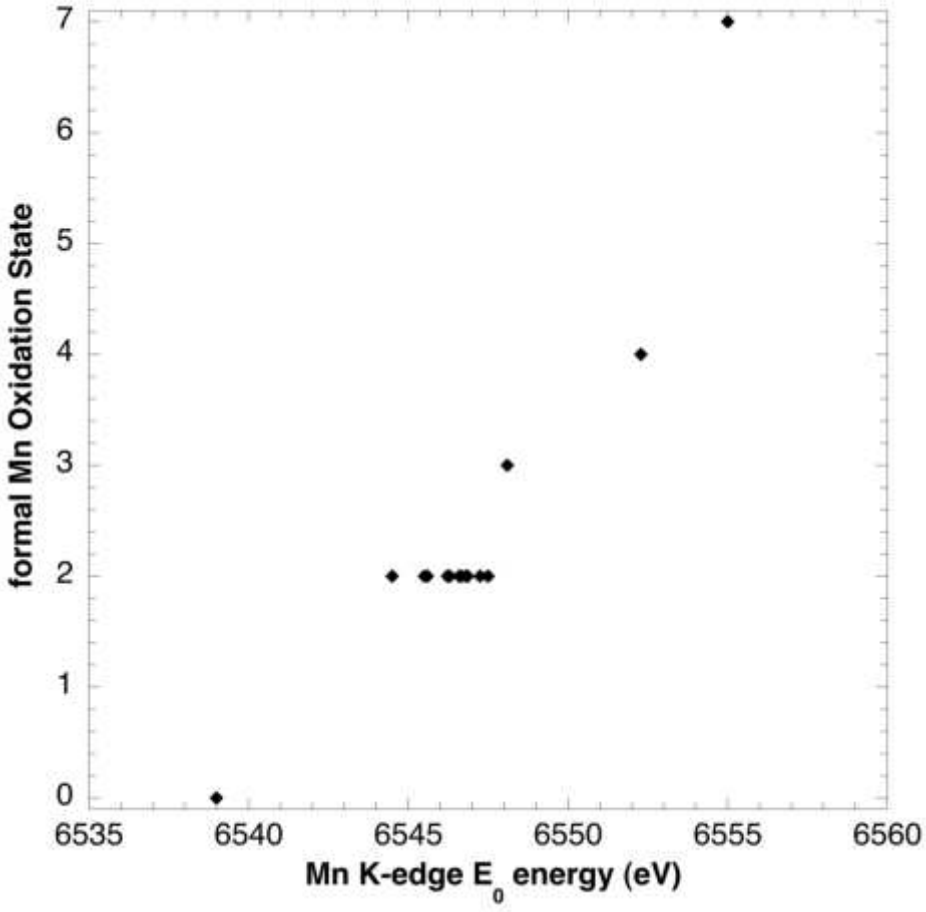

From Belli et al., 1980. Solid State Comm., 35, 355-361

Oxidation state – Edge Energy

Al^{3+}

The edge can shift:
- Bond distances
- Bonding type

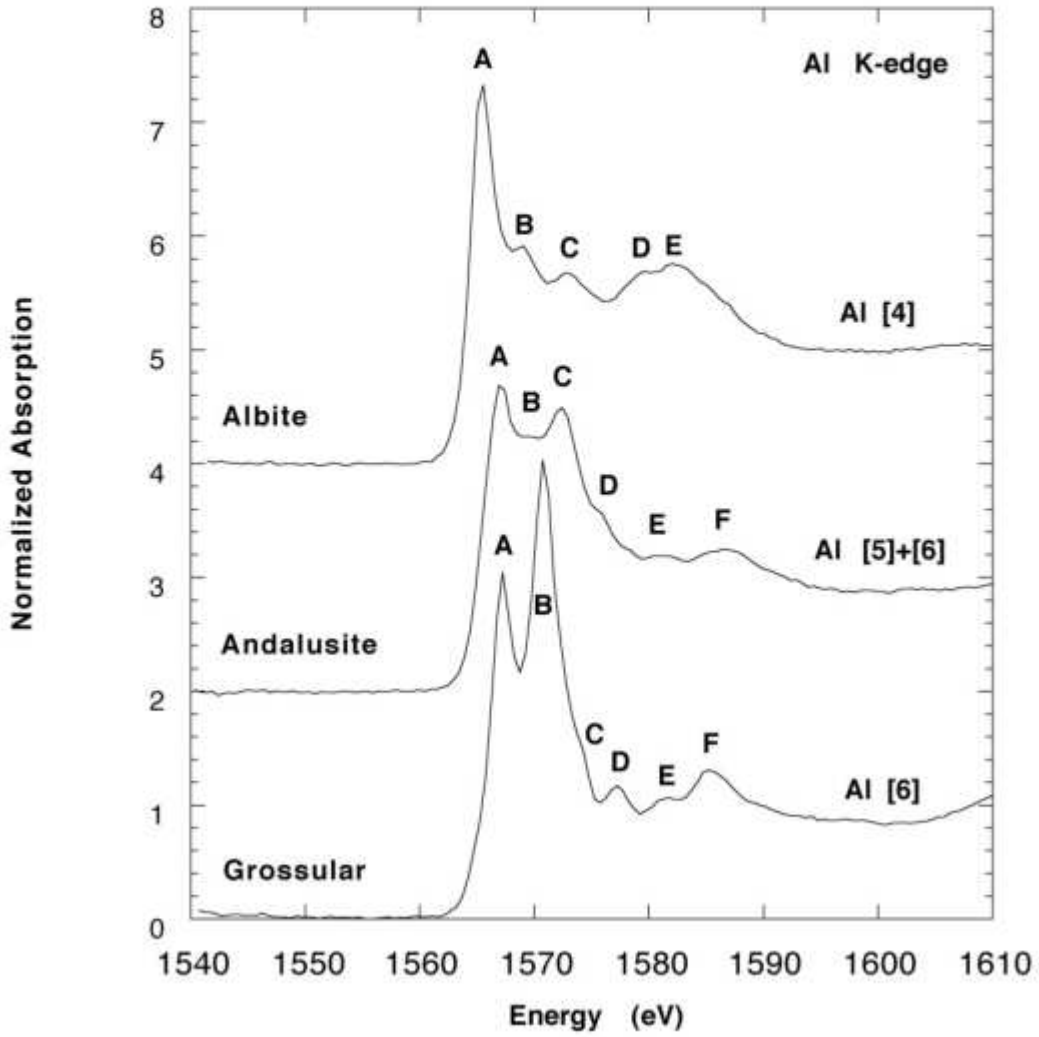

From Giuli et al., 2000. Am. Min, 85, 1172-1174

Oxidation state – Edge Energy

Fe^{2+} - Fe^{3+}

Variety of:

- coordination geometries
- bond distances

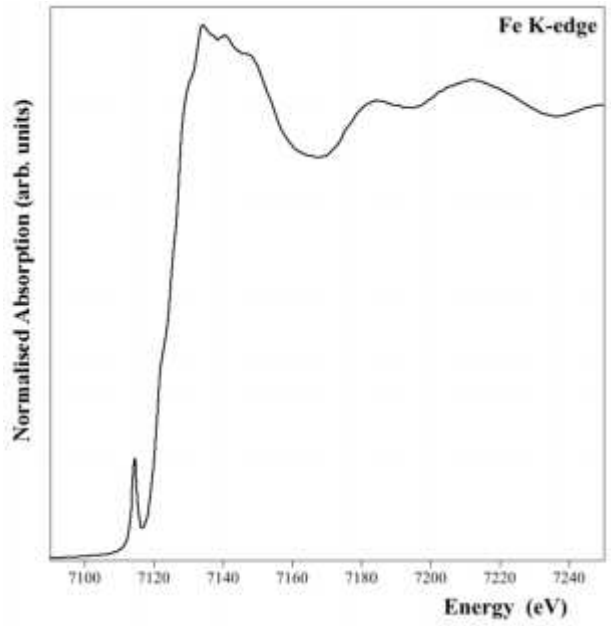

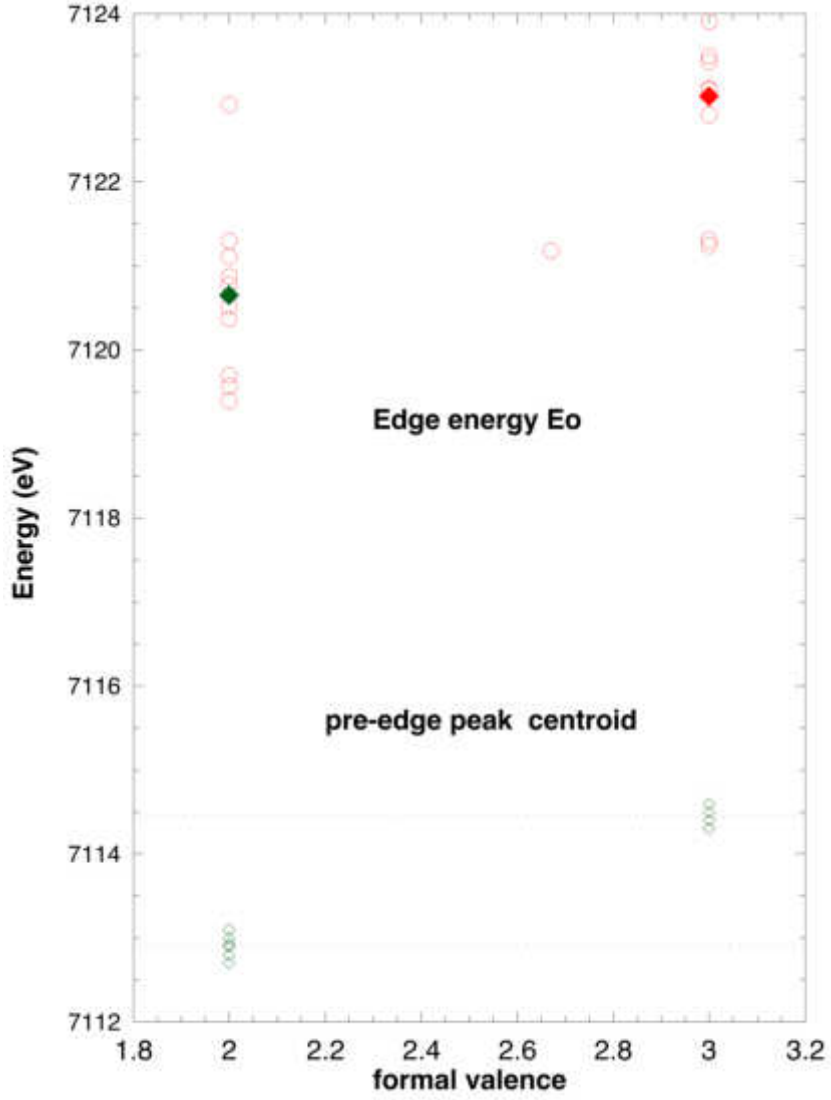

Oxidation state – pre edge peak

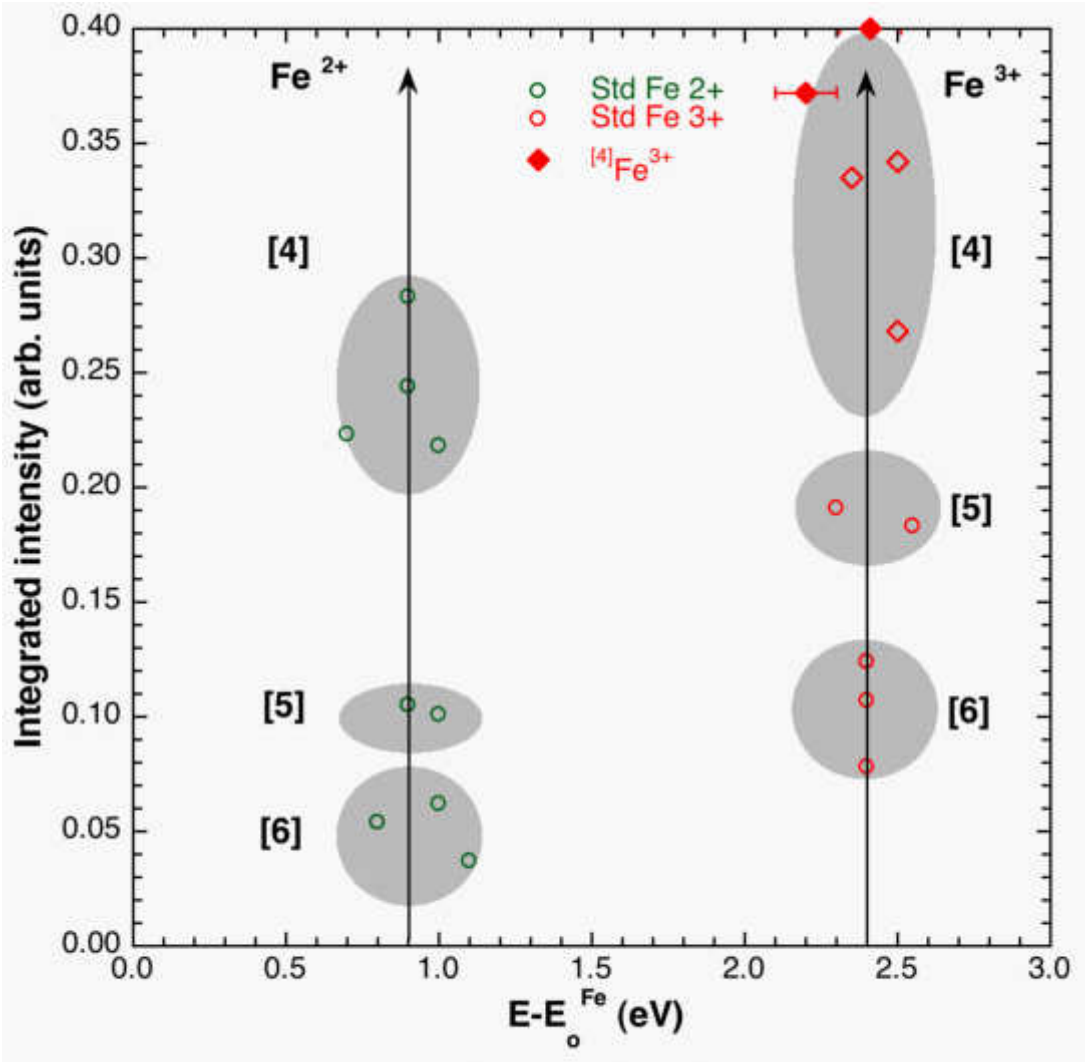

Oxidation state – pre edge peak

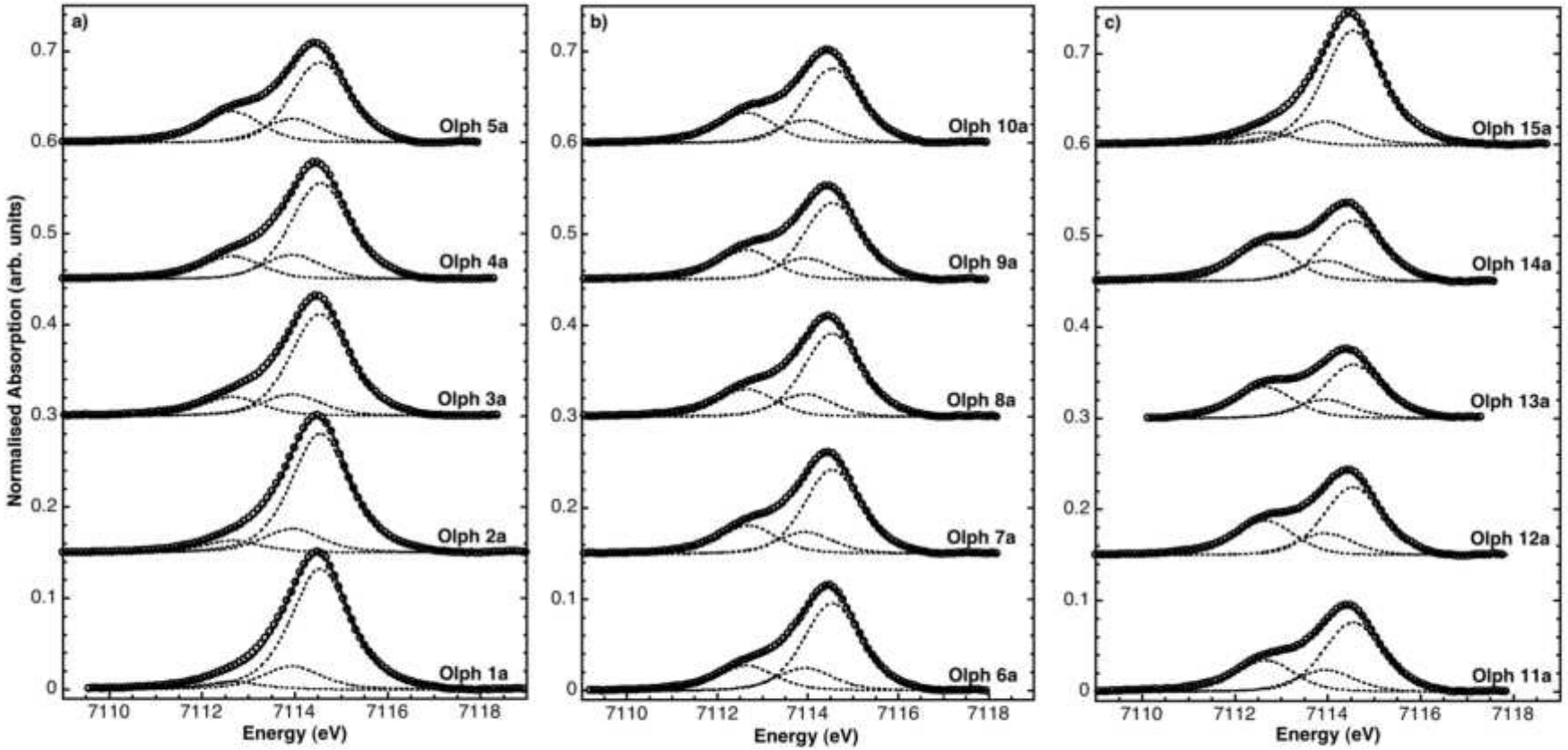

From Giuli et al., 2011, Am. Mineral., 96, 631-636

Oxidation state – pre edge peak

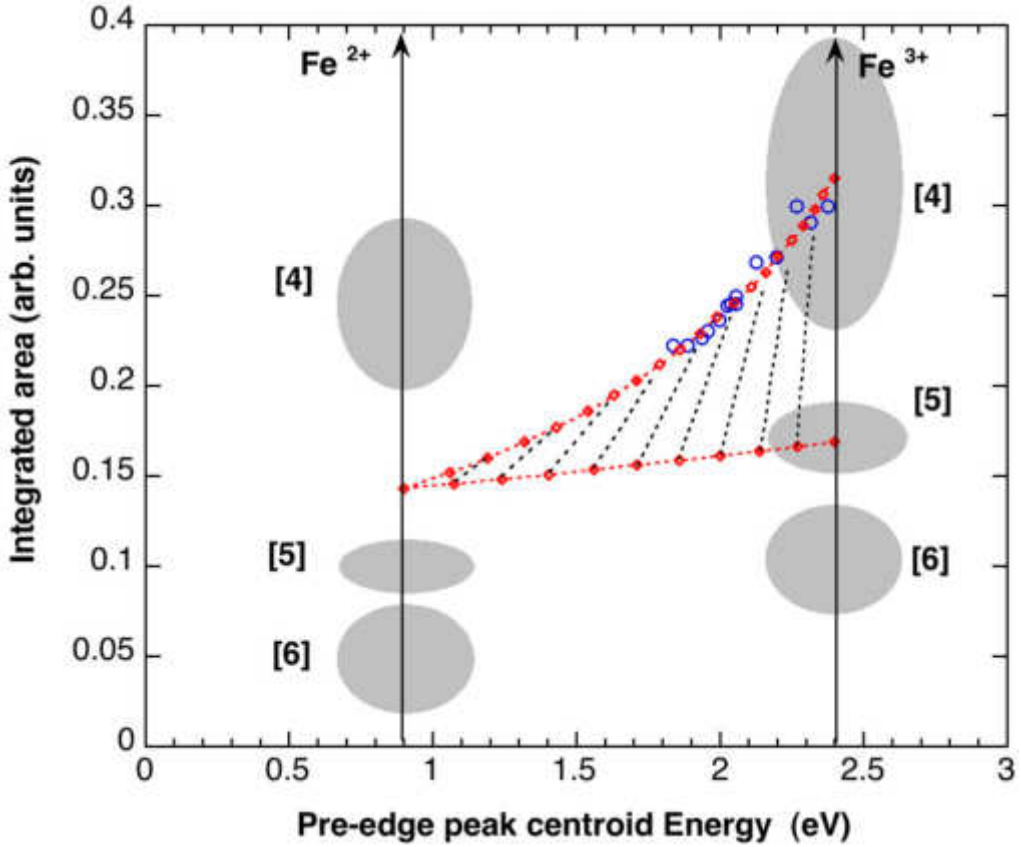

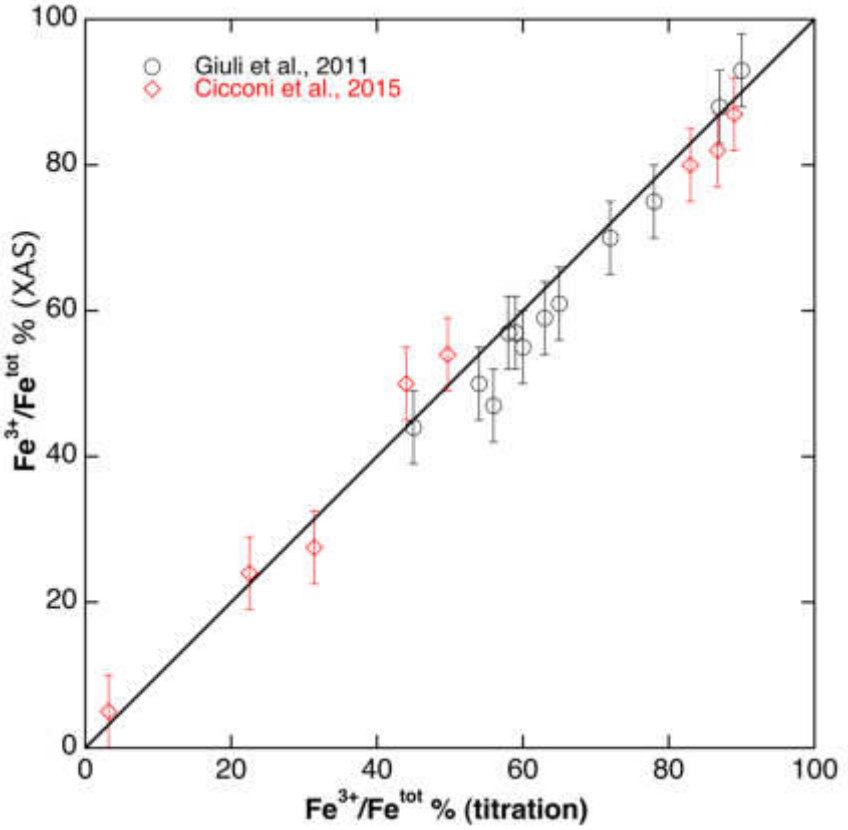

From Giuli et al., 2011, Am. Mineral., 96, 631-636

Oxidation state – pre edge peak

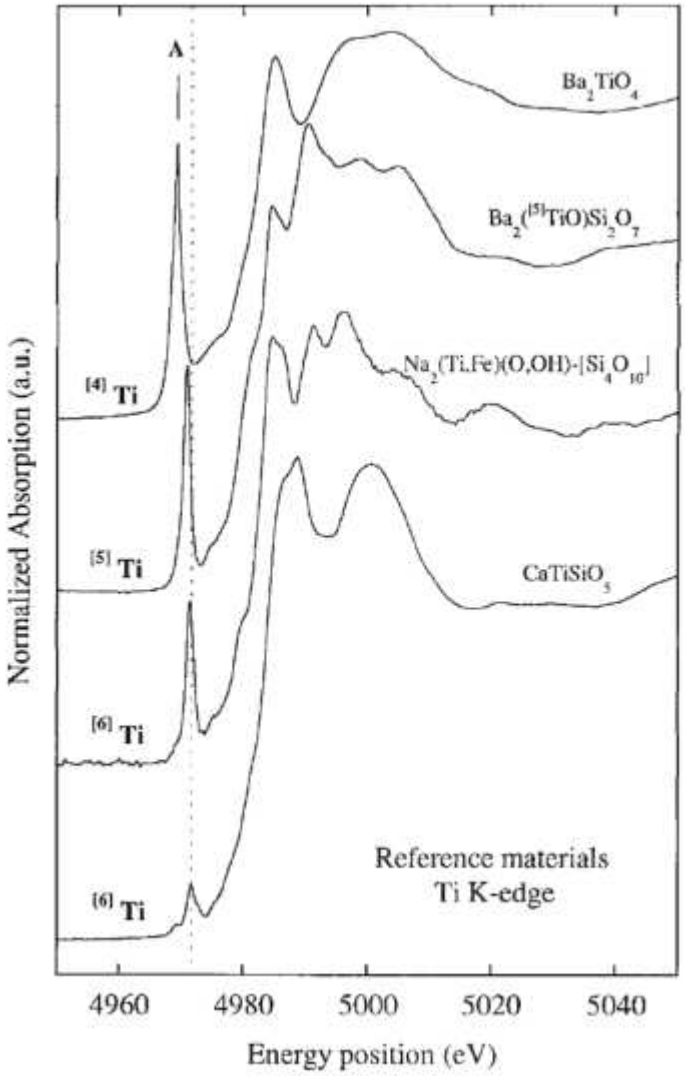

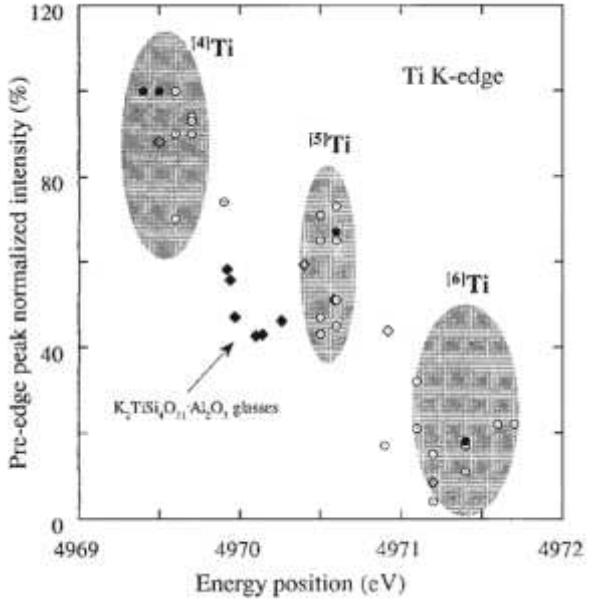

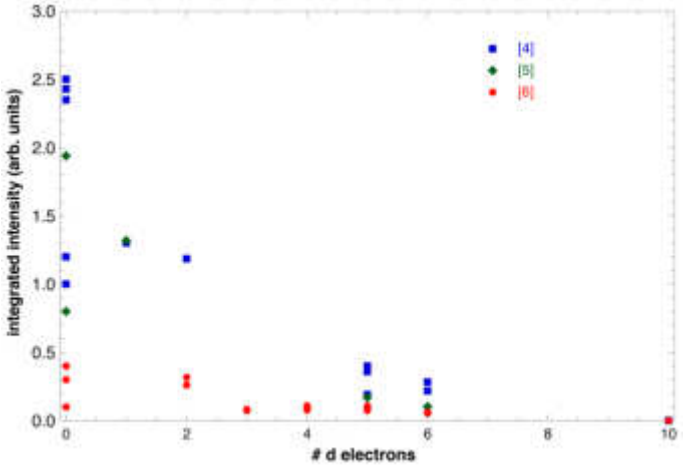

From Romano et al., 2000, Am. Mineral., 85, 108-117

Oxidation state – pre edge peak

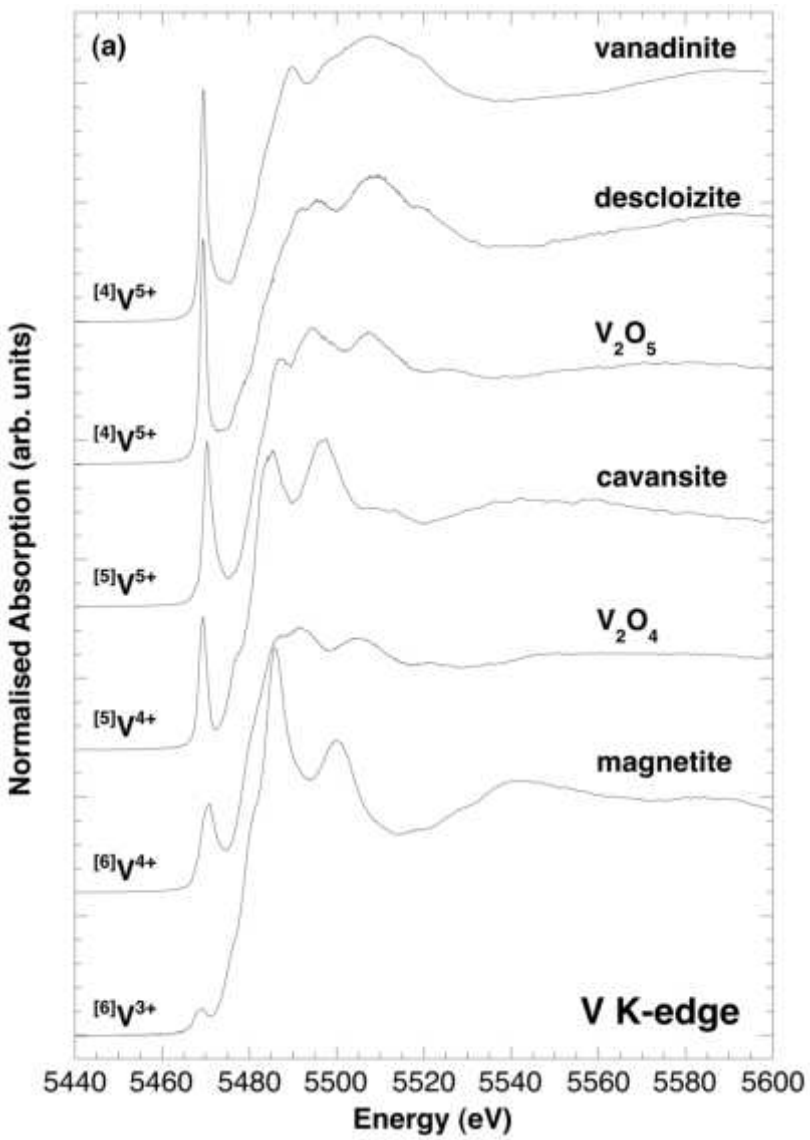

From Giuli et al., 2004, Am. Mineral., 89, 1640-1646

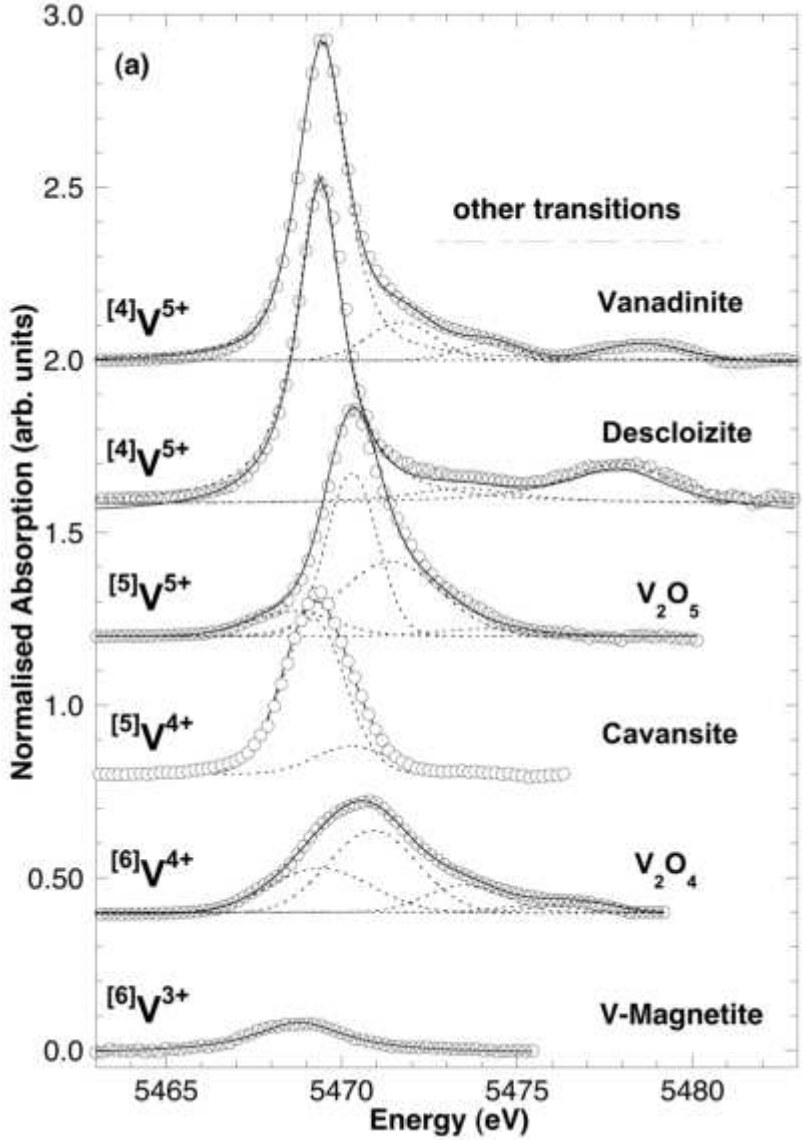

Oxidation state – pre edge peak

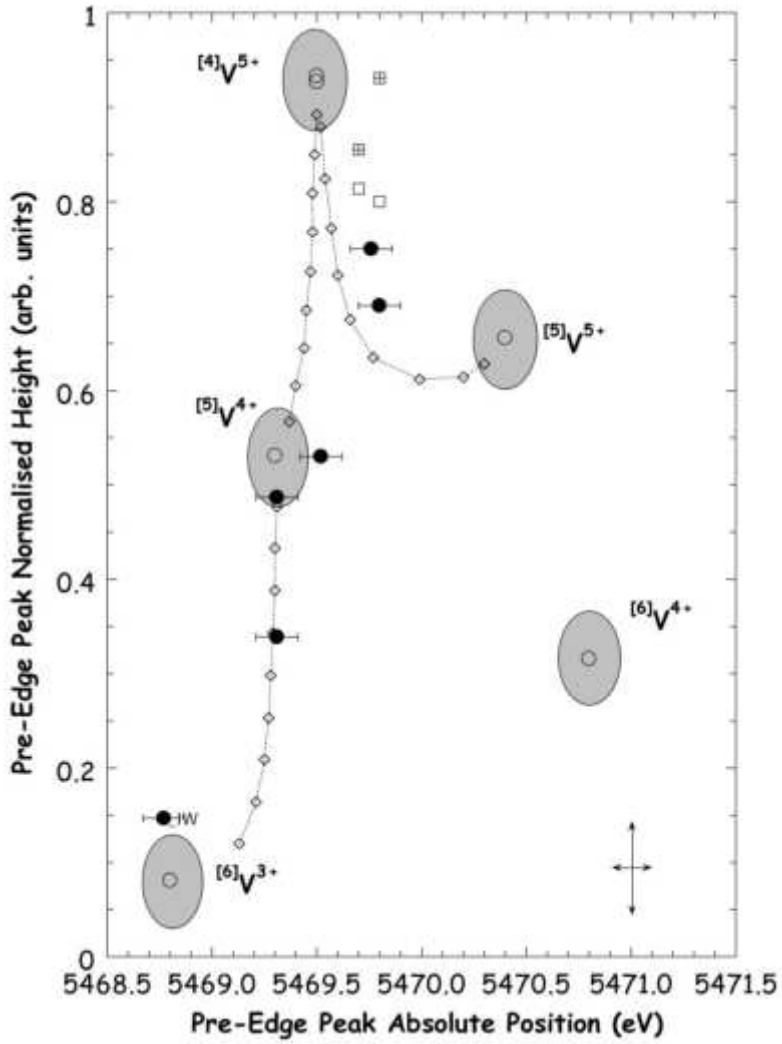

Air $^{[4]}V^{5+}$ + $^{[5]}V^{5+}$

FMQ+1 $^{[5]}V^{4+}$

FMQ

FMQ-1 $^{[5]}V^{4+}$ + $^{[6]}V^{3+}$

IW $^{[6]}V^{3+}$

Site location- XANES

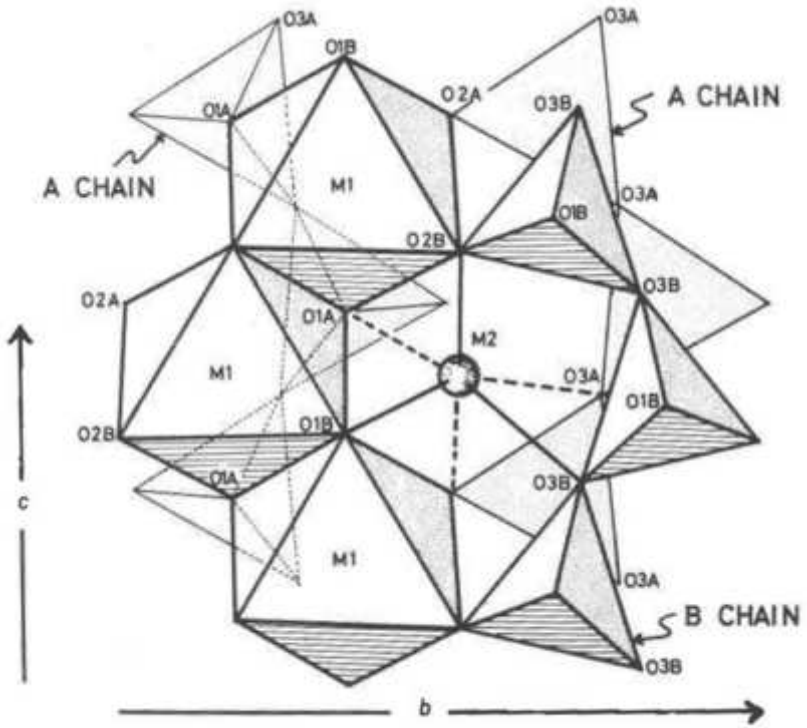

FIG. 1. Projection along a^* of part of the orthoferrosilite structure.

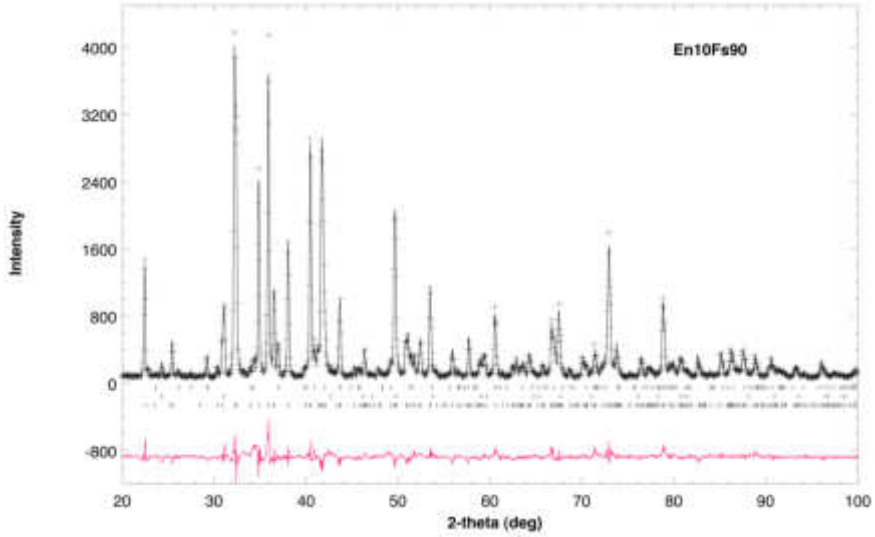

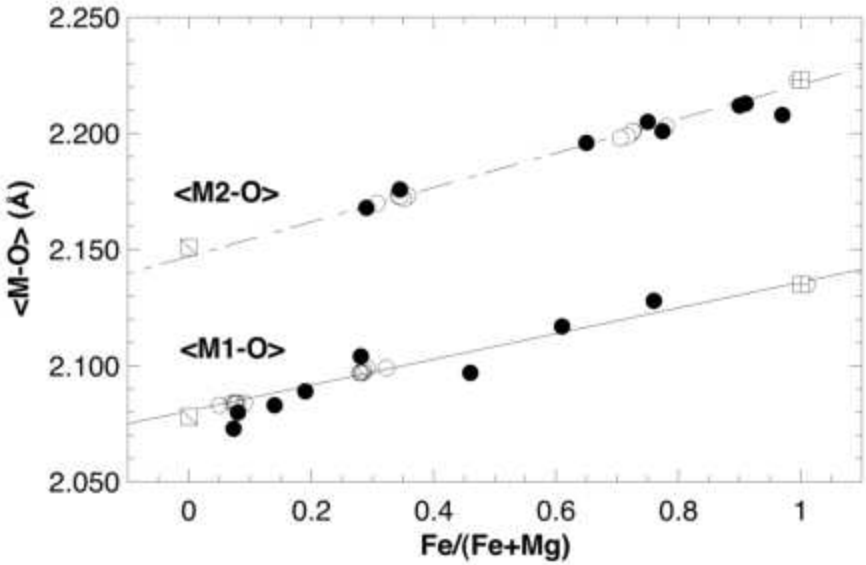

Site location- XANES

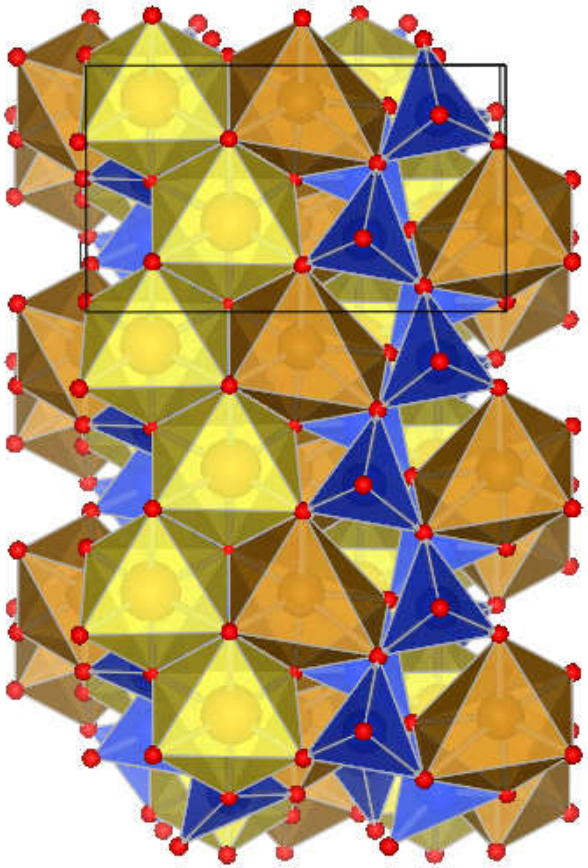

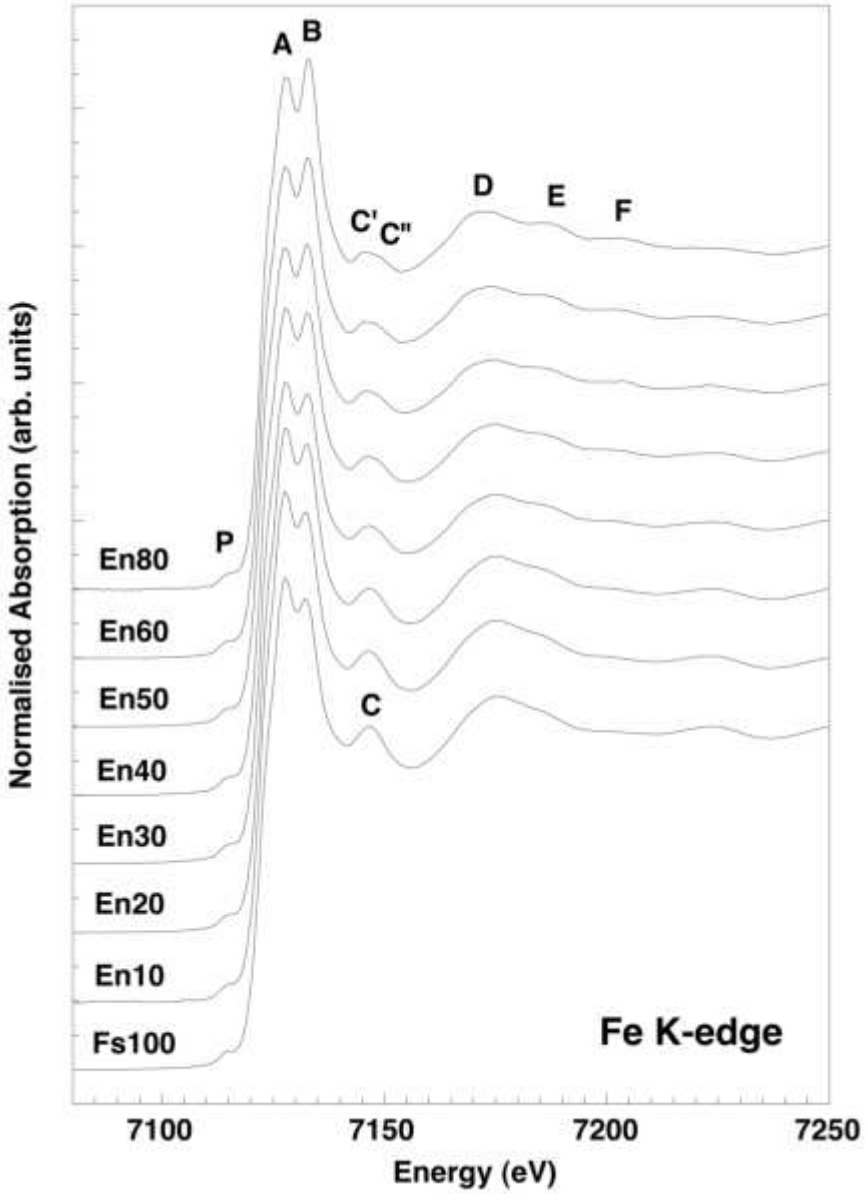

Site location- XANES

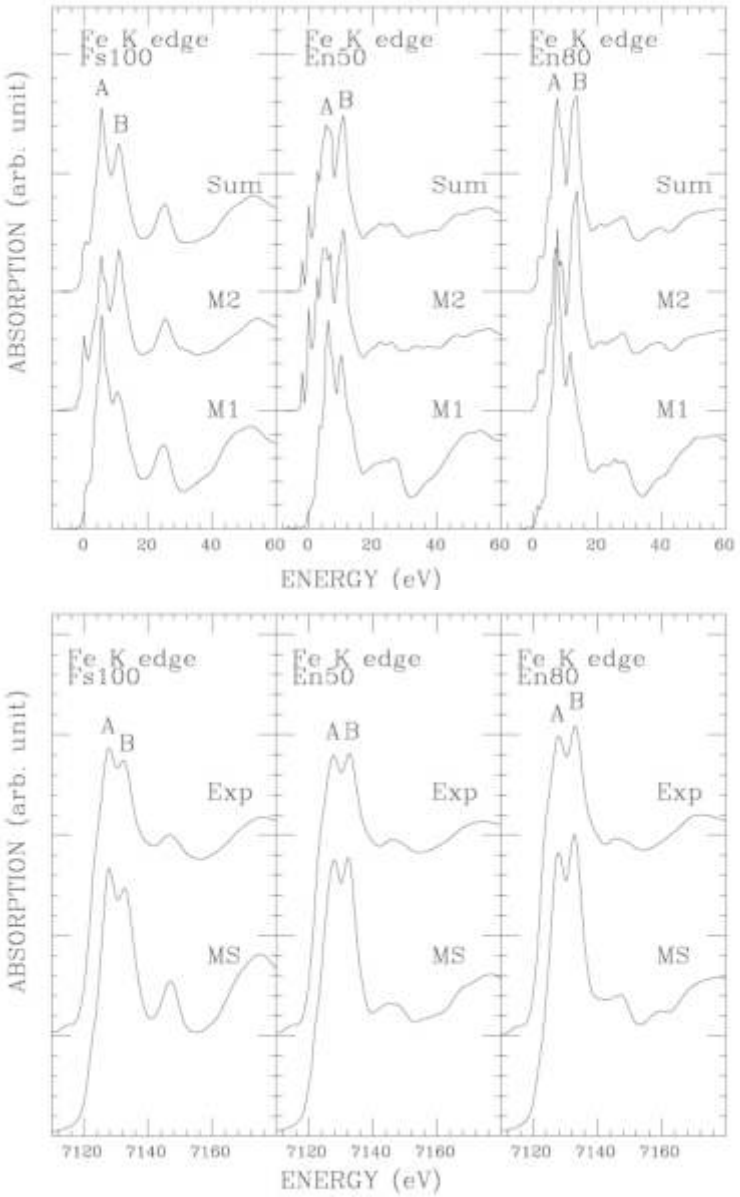

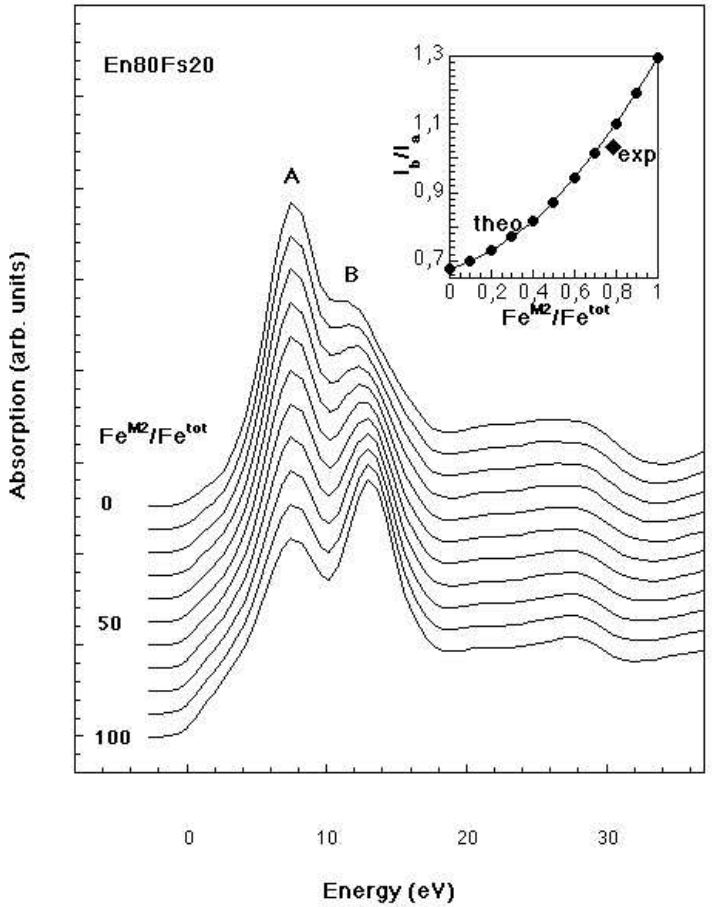

Local Geometry- EXAFS

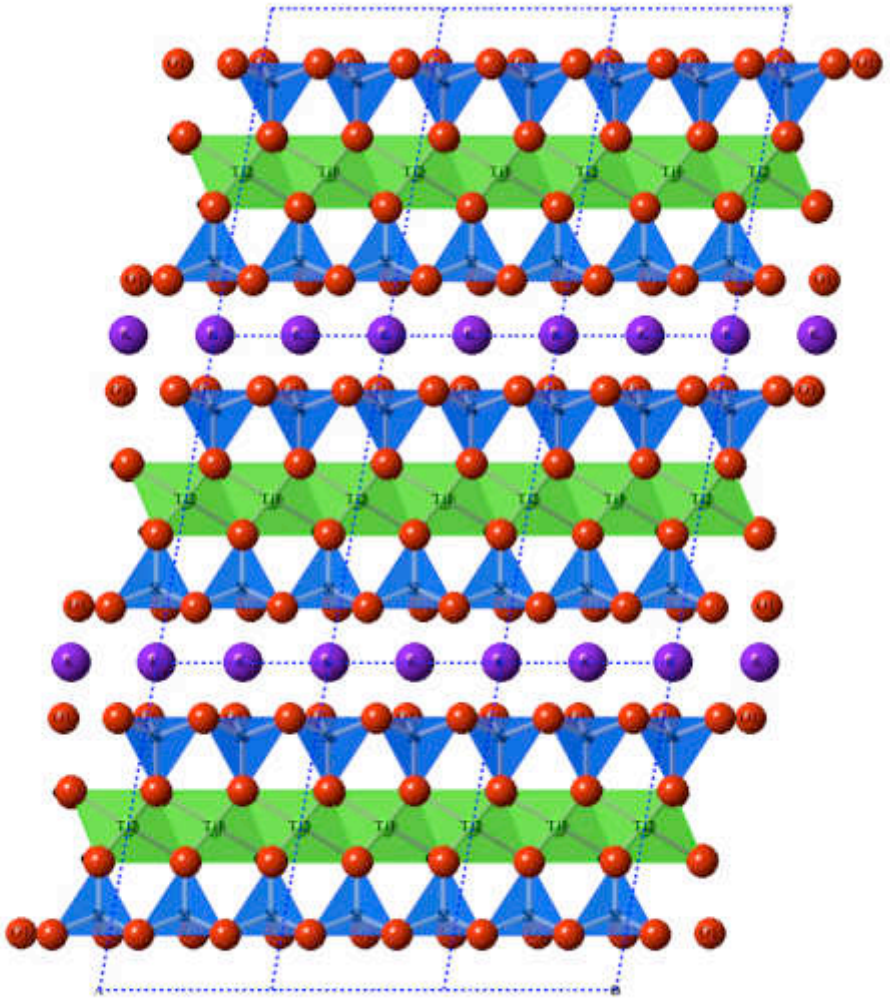

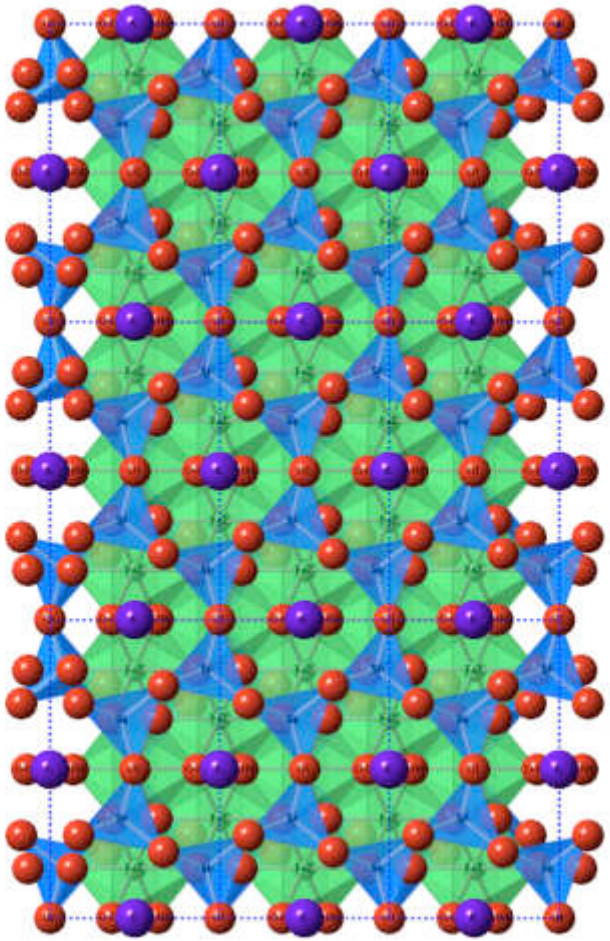

Local Geometry- EXAFS

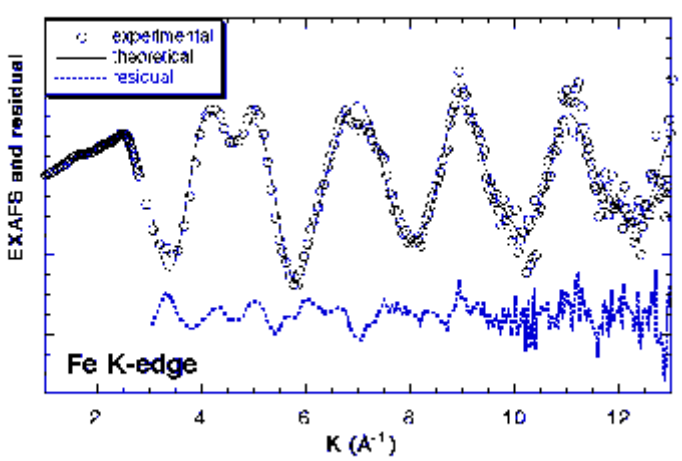

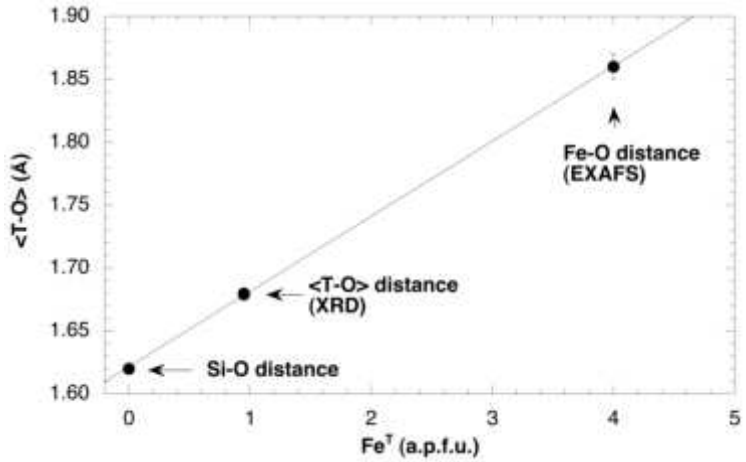

<Fe-O>= 1.86 ± 0.01 Å

<T-O>= 1.680 ± 0.002 Å

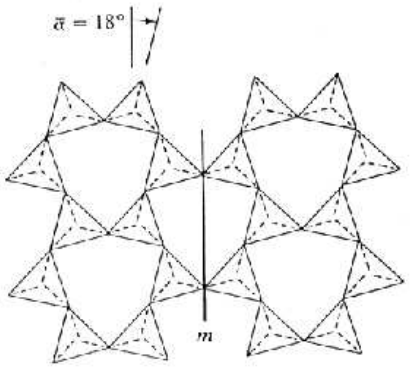

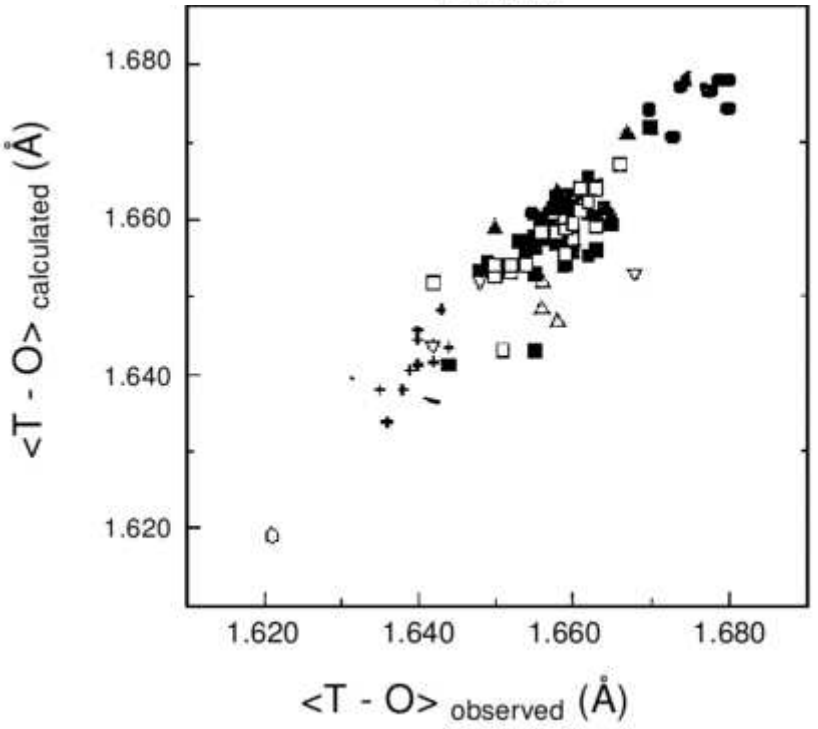

Corundum α-Al_2O_3

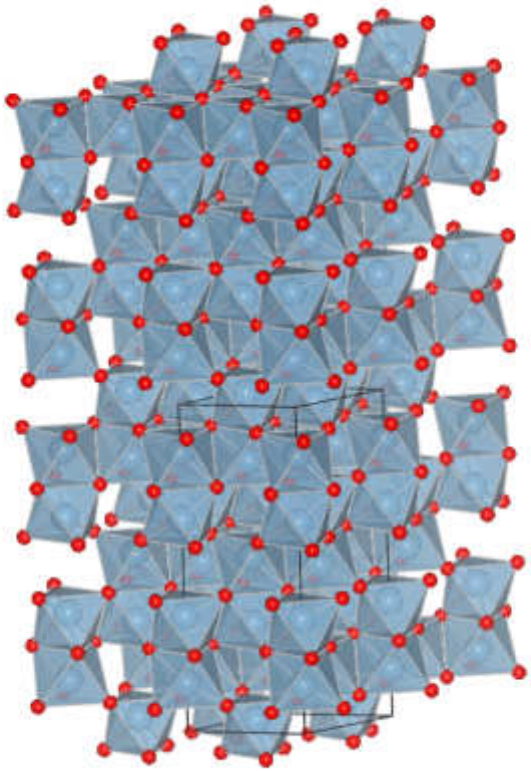

Al_2O_3	<Al-O>=	1.912 Å
Cr_2O_3	<Cr-O>=	1.985 Å
Fe_2O_3	<Fe-O>=	2.031 Å

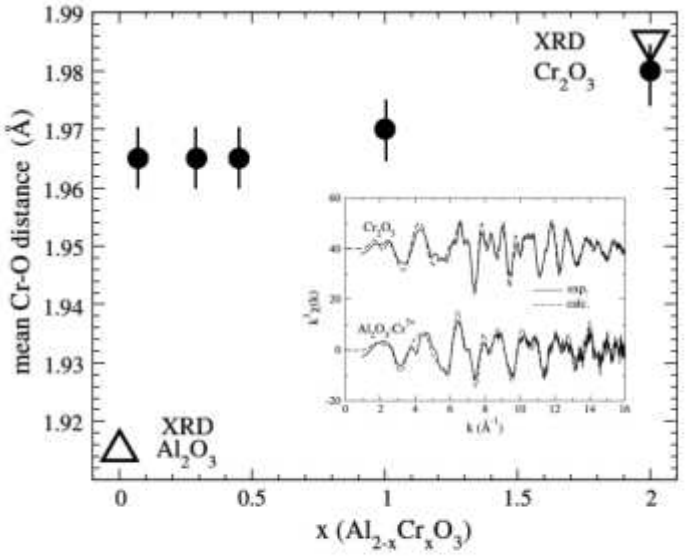

Fig. 8 Mean Cr–O distances (Å) from EXAFS analysis on $Cr_xAl_{2-x}O_3$ powders. *Black dots* are experimental points deduced from this study. *Triangles* are XRD data from Finger and Hazen (1980) and from Pearson (1962)

Corundum α-Al_2O_3

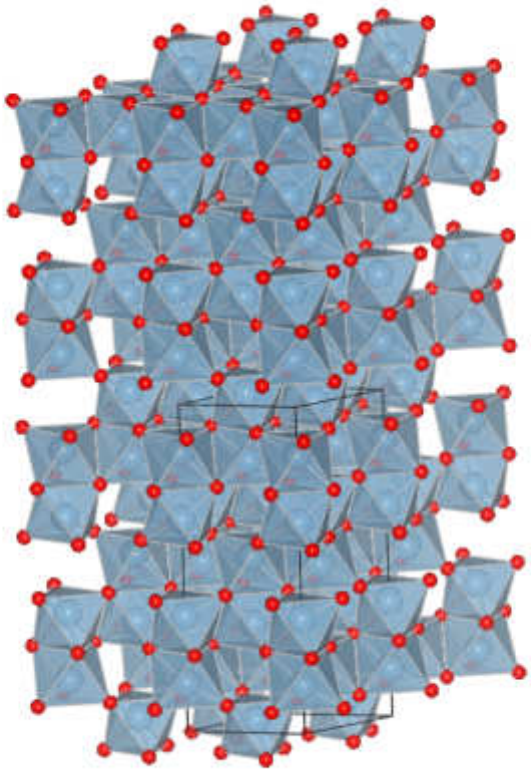

Al_2O_3 <Al-O>= 1.912 Å

Cr_2O_3 <Cr-O>= 1.985 Å

Fe_2O_3 <Fe-O>= 2.031 Å

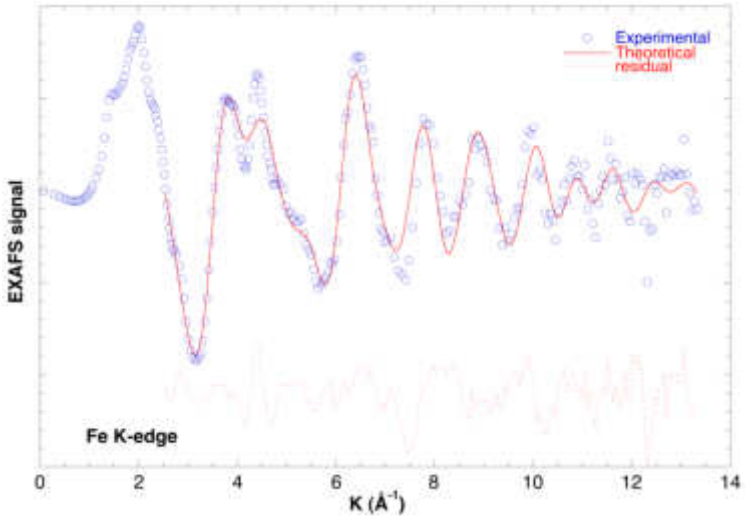

Al_2O_3 <Fe-O>= 1.947 Å

$^{[4]}Fe^{3+}$-O distance in synthetic kimzeyite garnet

$Ca_3(Zr,Ti)_2[Fe,Al,Si]_3O_{12}$

- Milton C., Ingram B.L., Blade L.V. (1961), Am. Mineral., 46, 533-548
- Ito J., and Frondel C. (1967), Am. Mineral., 52, 773-781
- Munno r., Rossi G., Tadini C. (1980), Am Mineral, 65, 188-191
- Schingaro E., Scordari F., Capitanio F., Parogi G., Smith D.C., Mottana A. (2001), Eur. J. Mineral., 13, 749-759

$^{[4]}Fe^{3+}$-O distances

Rodolicoite $FePO_4$ <Fe-O>= 1.825 Å
Arnold, 1986 Zeit. Krist., 177, 139-142

Tetra-Ferriphlogopite <Fe-O> = 1.86 ± 0.01 Å
Giuli et al., 2001, Eur. J. Min., 13, 1099-1108

Quartz (Fe^{3+} + Fe^{4+}?) <Fe-O> = 1.78 ± 0.02 Å
Di Benedetto et al., 2010, Phys. Chem. Min., 37,283-289

Phonolitic glass <Fe-O> = 1.85 ± 0.01 Å
Giuli et al., 2011, Amer. Miner., 96,

Rhyolitic glass <Fe-O> = 1.84 ± 0.01 Å
Giuli et al., 2011, Amer. Miner. (in press)

PXRD

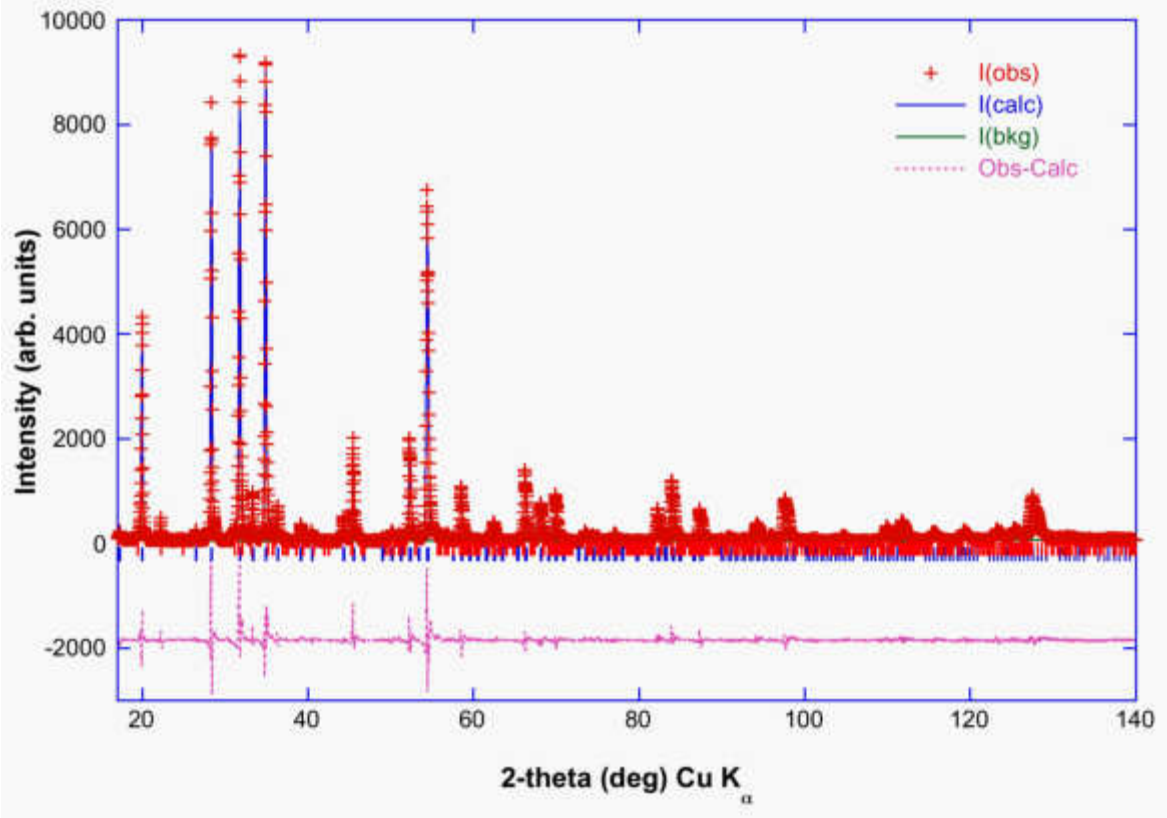

wRp = 16.22
Rp = 12.74
R_F =0.044

$I\,a\bar{3}d$

a_0=12.6250 ± 0.0001 Å

O_X= 0.034971
O_Y= 0.049655
O_Z= 0.654231

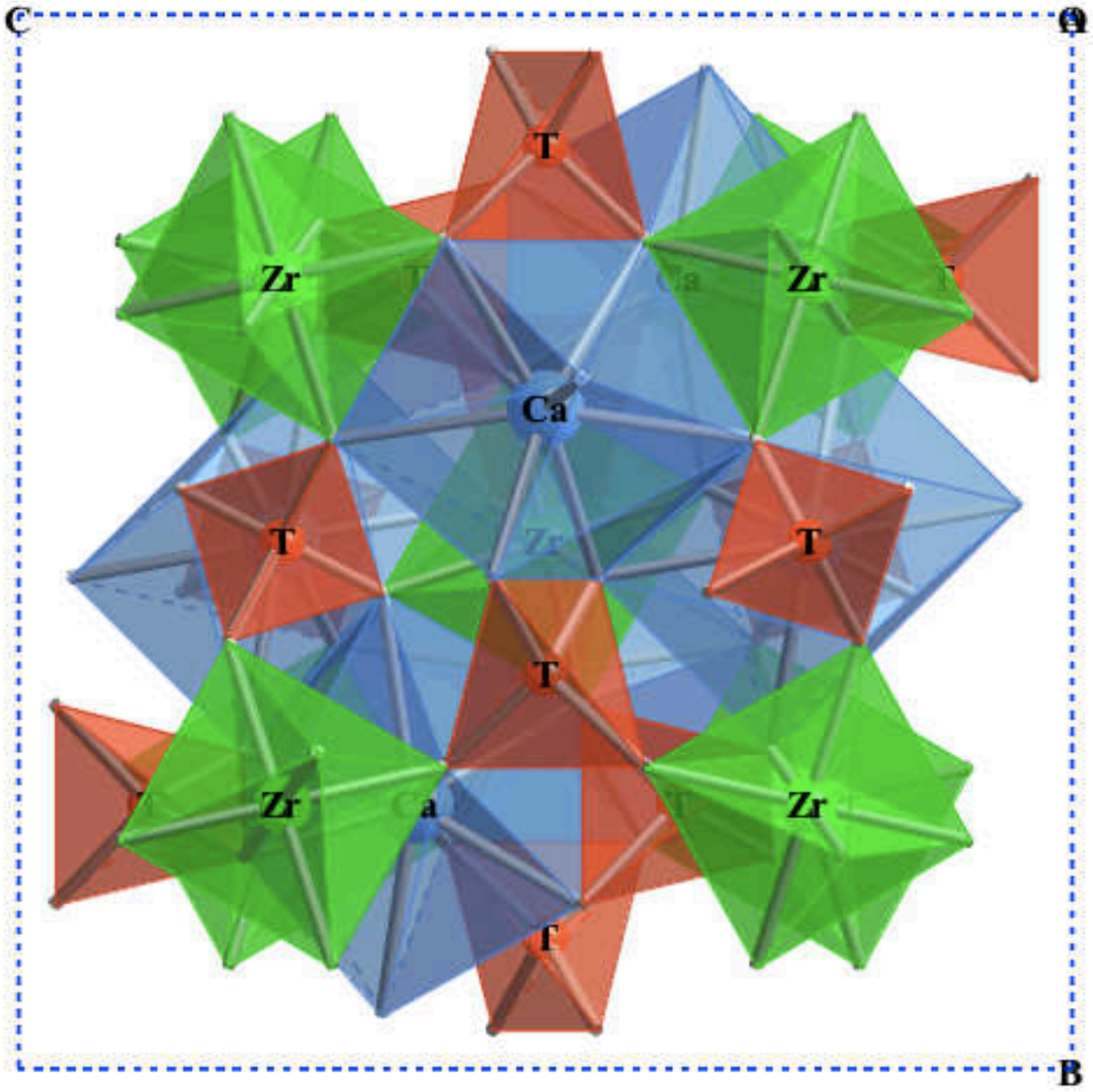

2.436 Å

Ca-O

2.594 Å

<Ca-O> = 2.515 Å

<Zr-O> = 2.093 Å

<T-O> = 1.774 Å

XANES

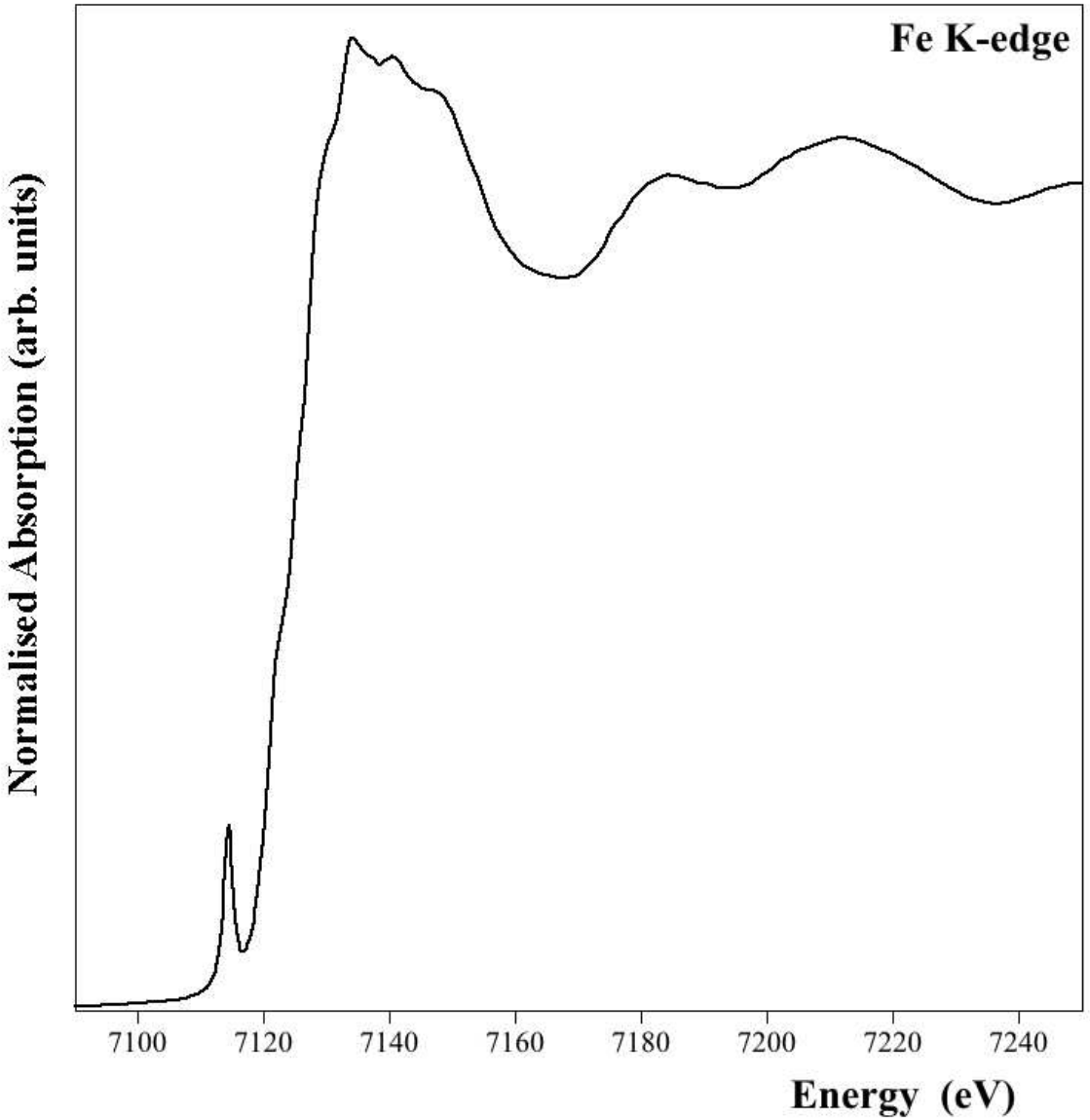
Fe K-edge
Normalised Absorption (arb. units)
7100
7120
7140
7160
7180
7200
7220
7240
Energy (eV)

XANES pre-edge

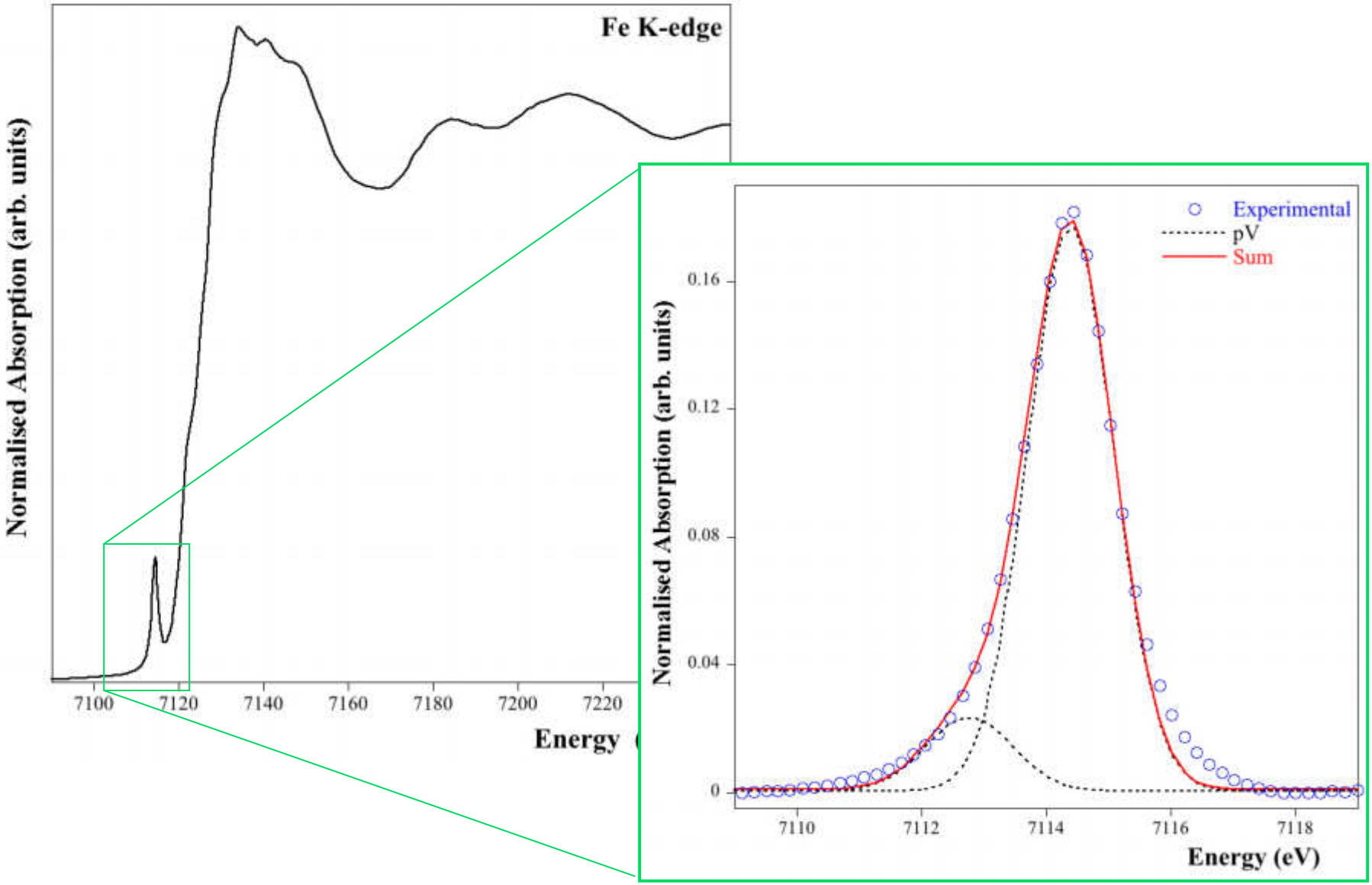

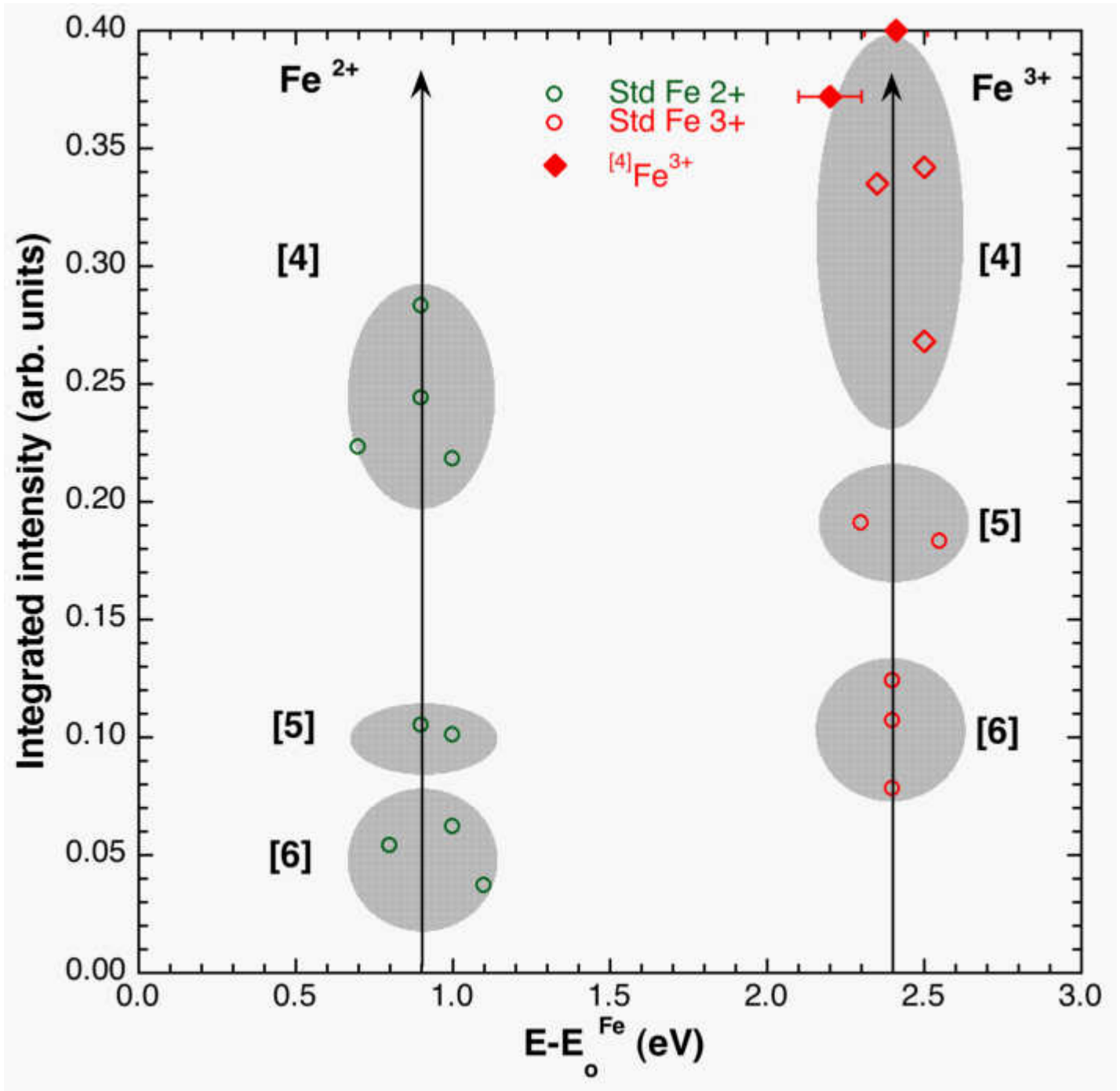
Fe 2+
Fe 3+
Std Fe 2+
Std Fe 3+
[4]Fe3+
[4]
[5]
[6]
[4]
[5]
[6]
Integrated intensity (arb. units)
E-E o Fe (eV)
0.00
0.05
0.10
0.15
0.20
0.25
0.30
0.35
0.40
0.0
0.5
1.0
1.5
2.0
2.5
3.0

EXAFS

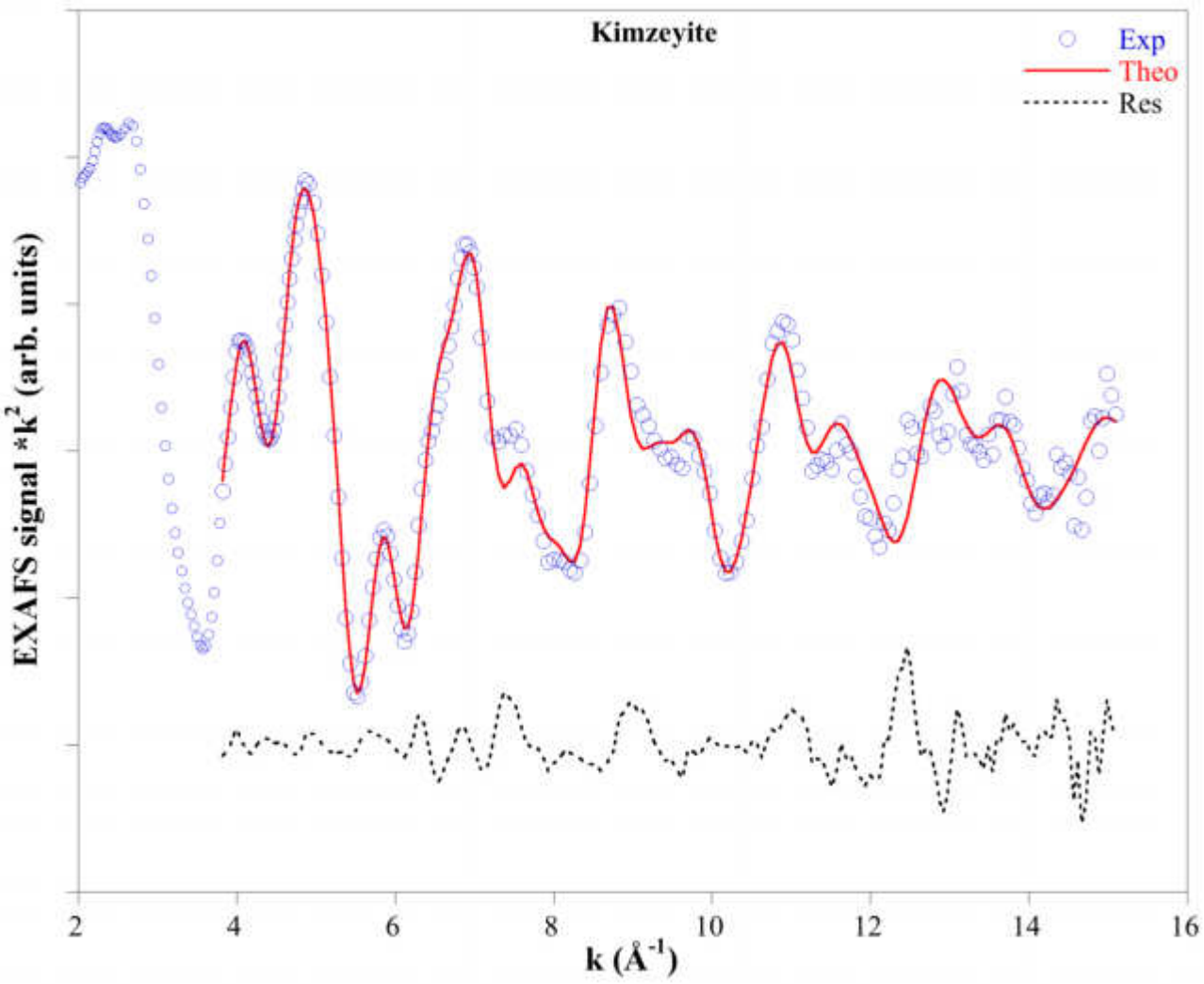

Fe-O
1.845 ± 0.01 Å

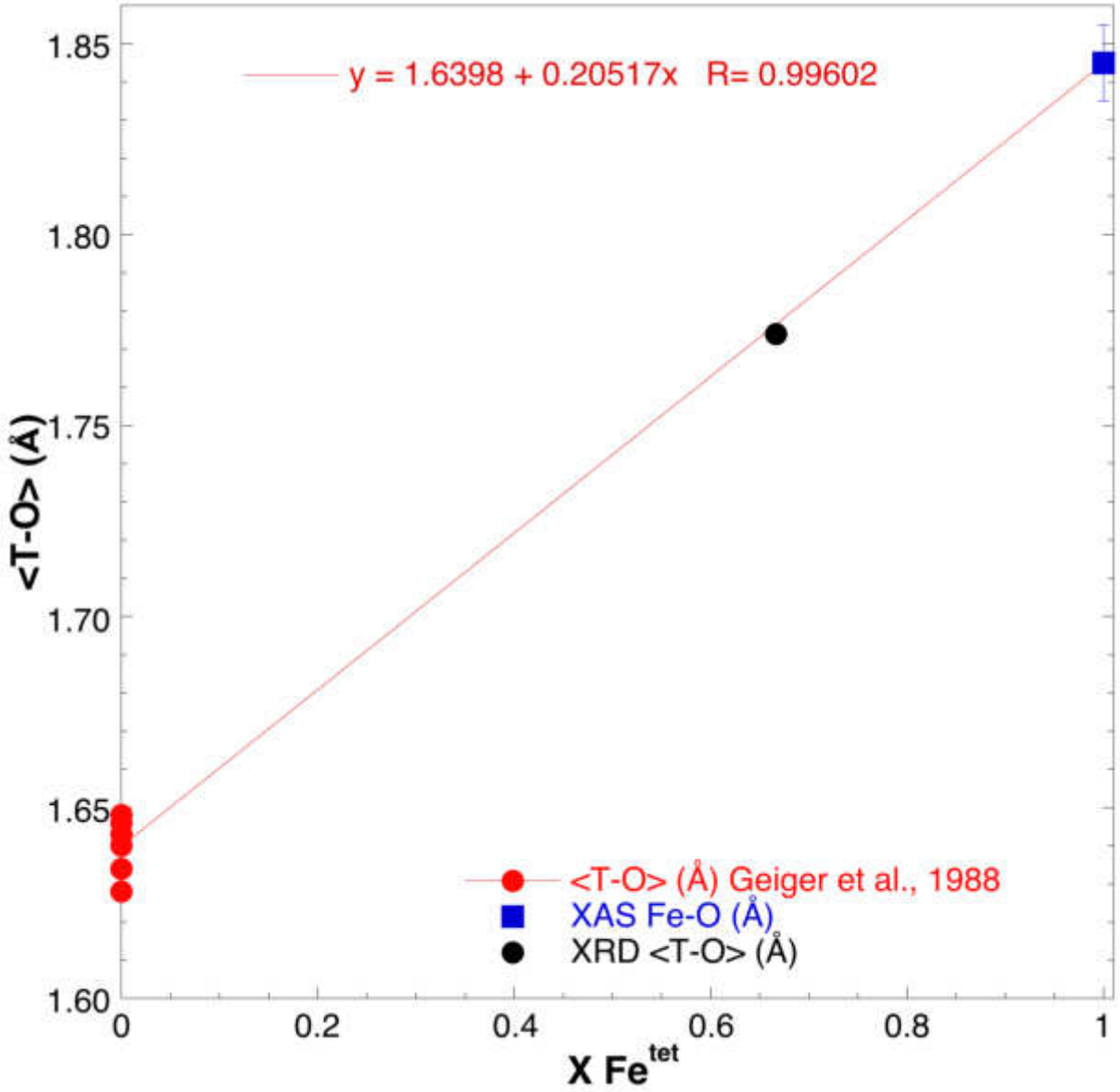
y = 1.6398 + 0.20517x R= 0.99602
<T-O> (Å) Geiger et al., 1988
XAS Fe-O (Å)
XRD <T-O> (Å)
<T-O> (Å)
X Fe^tet
1.85
1.80
1.75
1.70
1.65
1.60
0
0.2
0.4
0.6
0.8
1

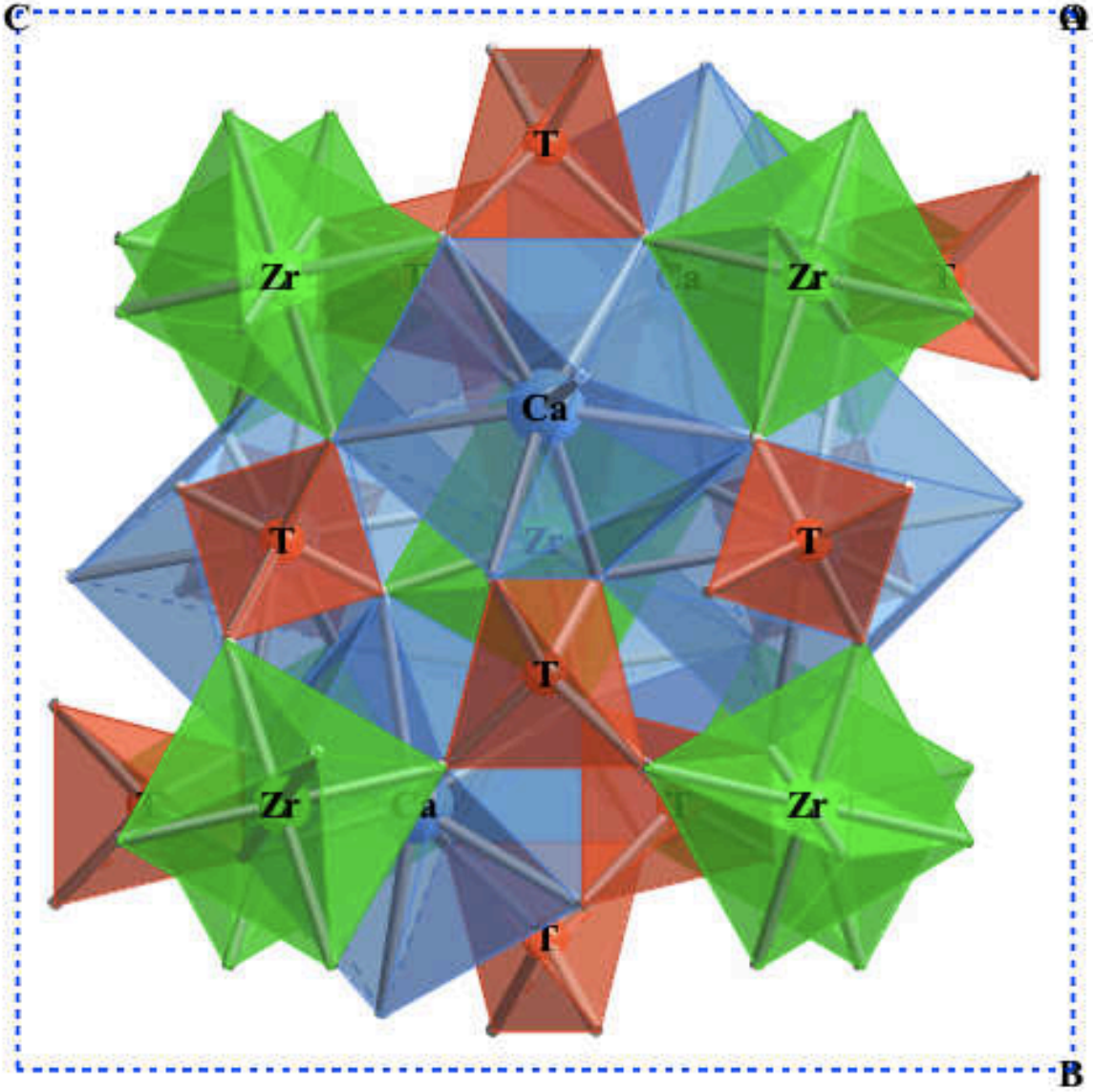

2.436 Å

Ca-O

2.594 Å

<Ca-O> = 2.515 Å

<Zr-O> = 2.093 Å

Fe-O 1.845 Å

Si-O 1.640 Å (?)

<T-O> = 1.774 Å

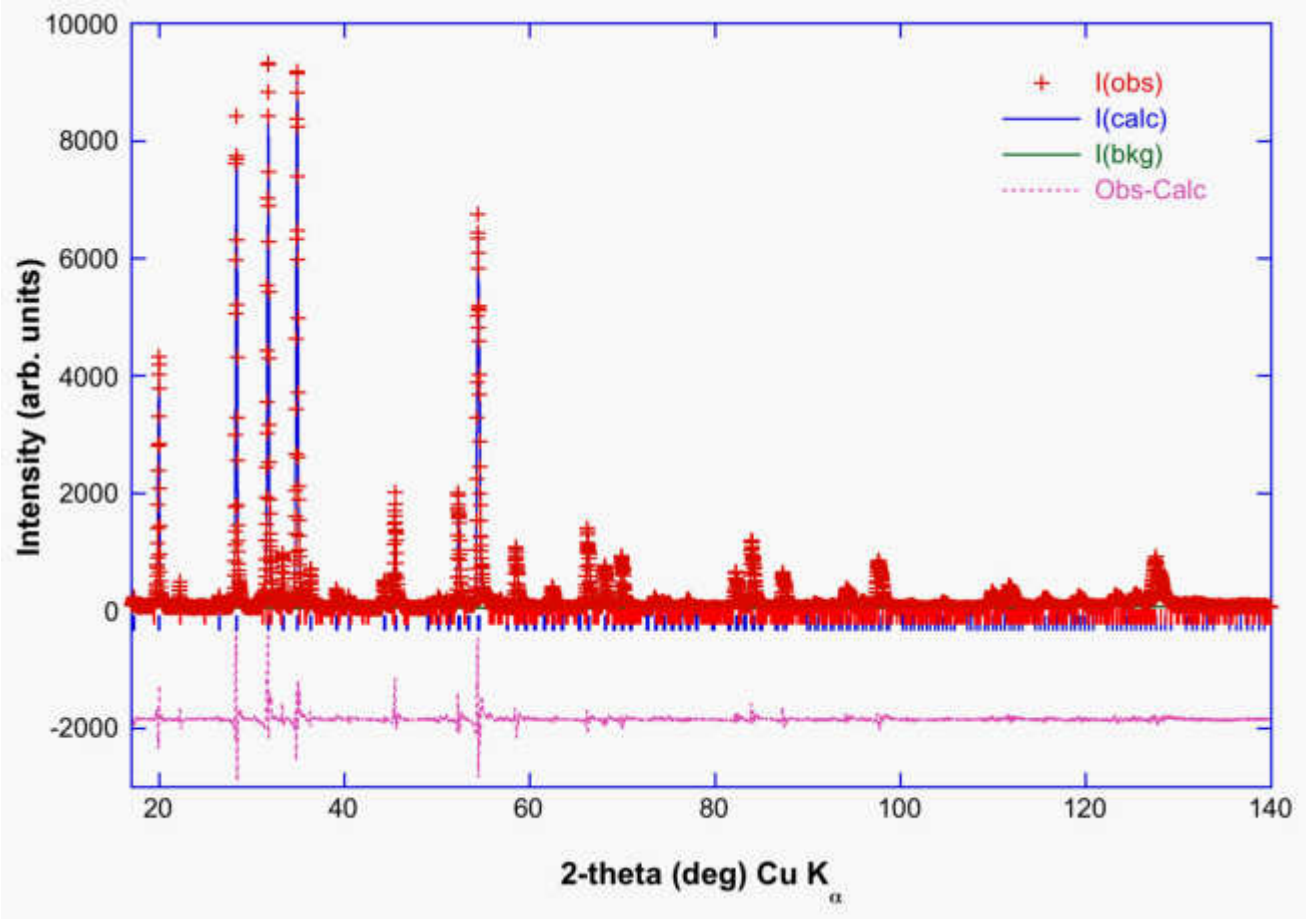

wRp = 16.22
Rp = 12.74
R_F =0.043

$I\,a\bar{3}d$

O_X= 0.027924
O_y= 0.049962
O_Z= 0.652805

a_0=12.6250 ± 0.0001 Å

O_X= 0.053236
O_y= 0.048514
O_Z= 0.656799

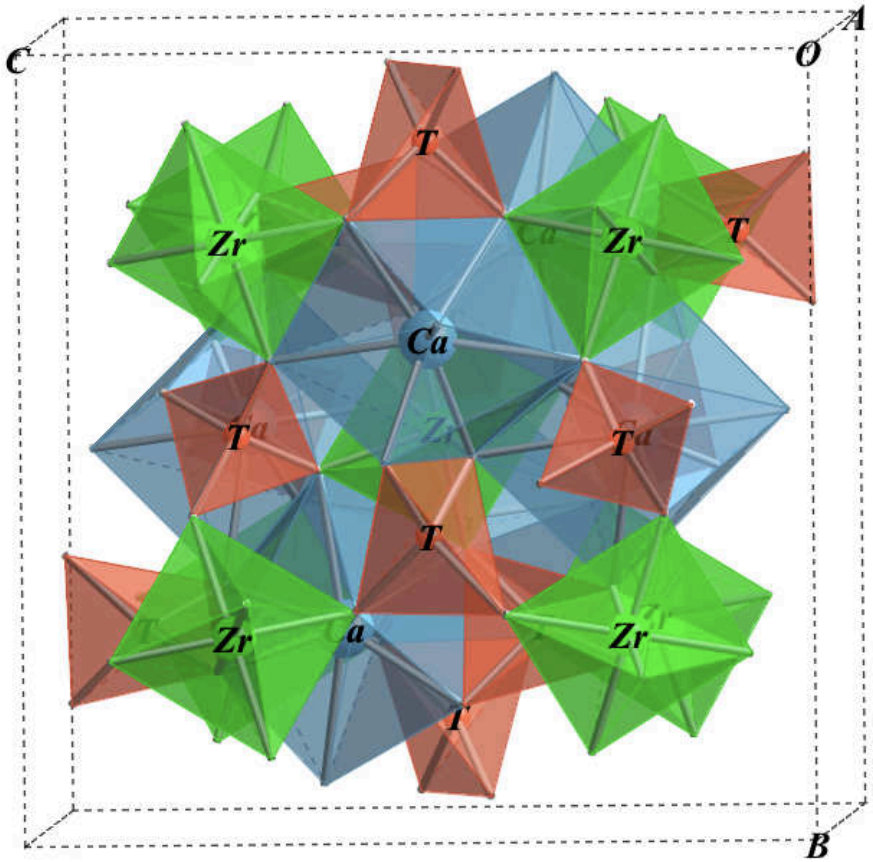

T-O = 1.845 Å
Zr-O = 2.060 Å
<Ca-O> = 2.473 Å

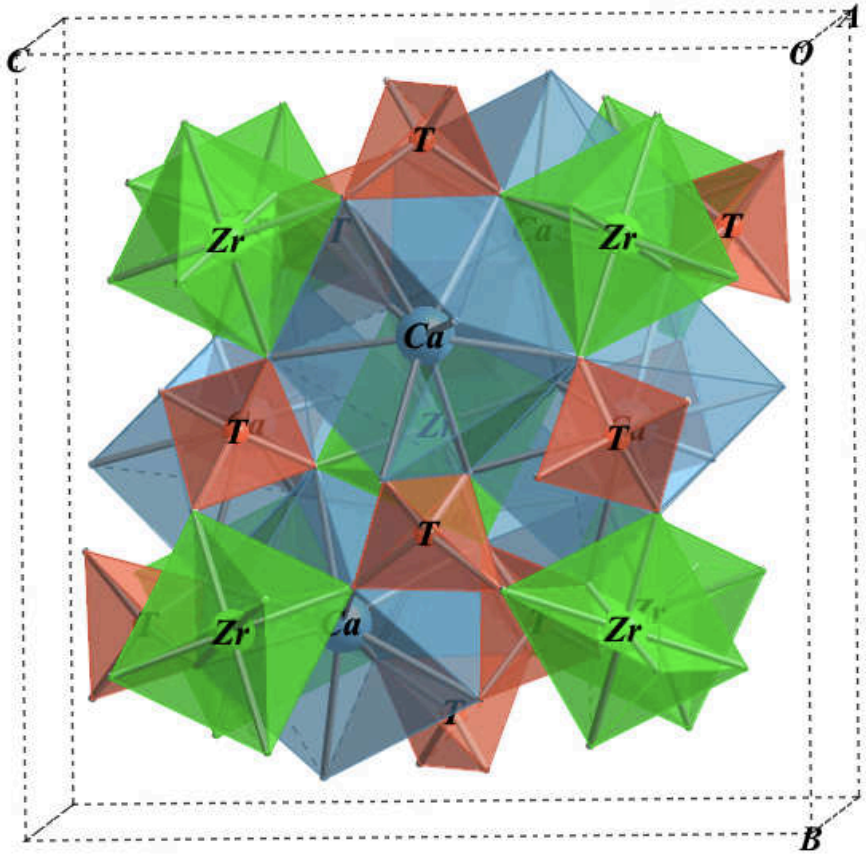

T-O = 1.606 Å
Zr-O = 2.179 Å
<Ca-O> = 2.637 Å

$^{[4]}Fe^{3+}$ in garnet

$^{[4]}Fe^{3+}$-O distance

1.845 ± 0.015 Å in kimzeyite garnet

Possible splitting of the O position ?

- *More accurate PXRD data collection*

or

- *Single-crystal synthesis*

How do these different structural units coexhist?

- *TEM work*

AMORPHOUS SAMPLES

Cu-peptides

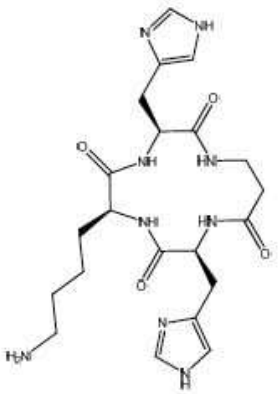

1. cyclo(Lys-His-βAla-His)

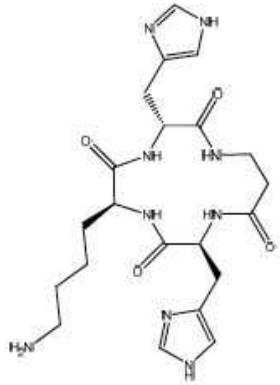

2. cyclo(Lys-DHis-βAla-His)

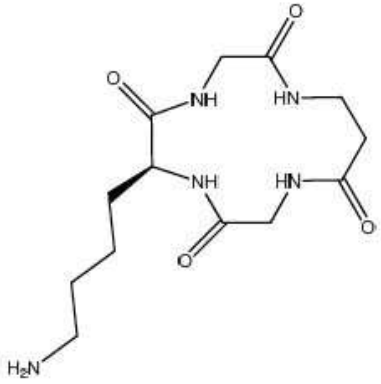

3. cyclo(Gly-βAla-Gly-Lys)

Cu OXIDATION STATE

Cu SITE GEOMETRY

Amorphous samples

Stability under the beam?

Cu-peptides

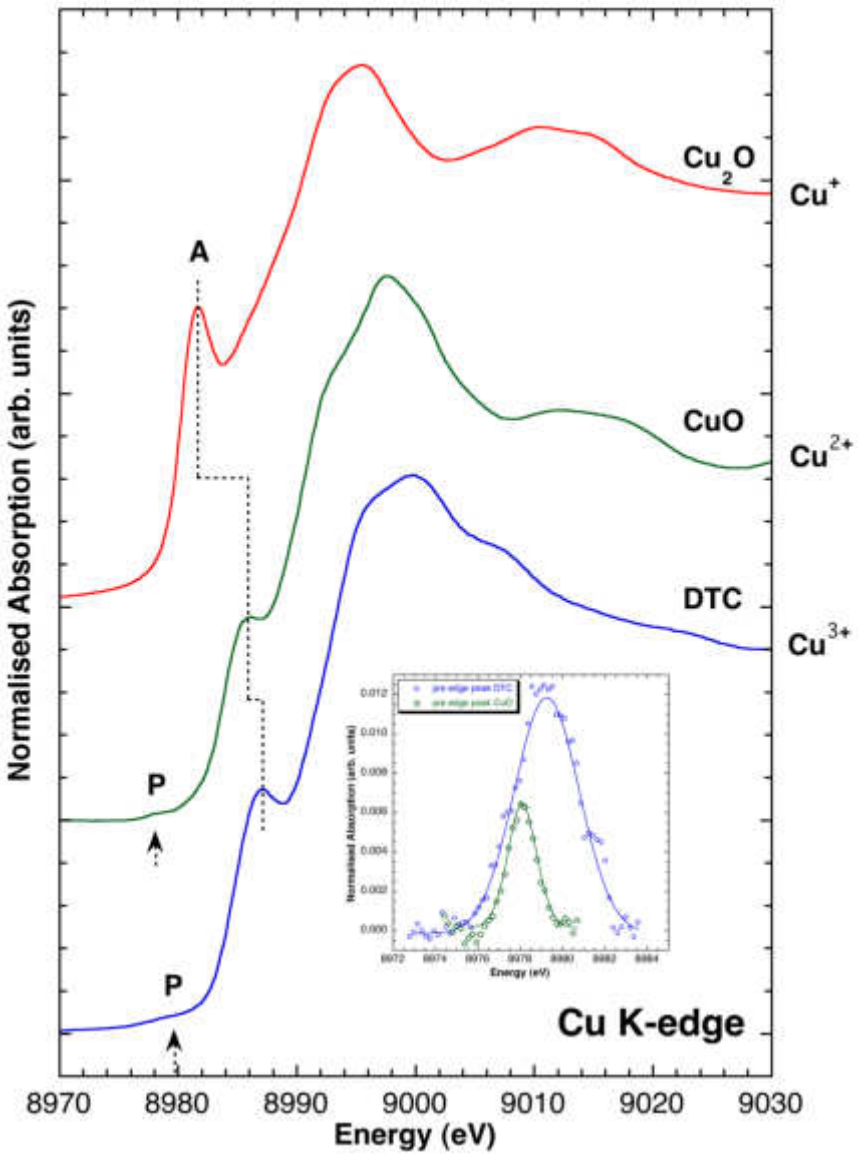
Cu2O
Cu+
A
CuO
Cu2+
DTC
Cu3+
P
P
Cu K-edge
Normalised Absorption (arb. units)
8970
8980
8990
9000
9010
9020
9030
Energy (eV)

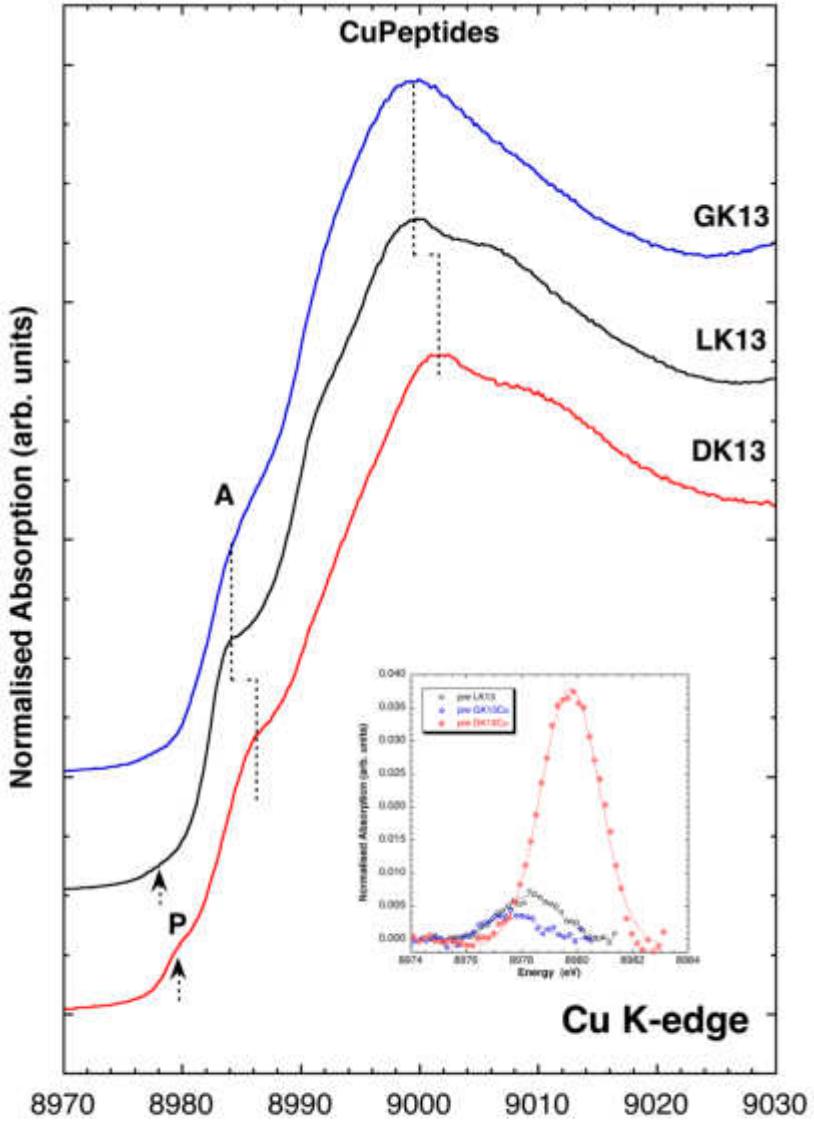
CuPeptides
GK13
LK13
DK13
A
P
Cu K-edge
Normalised Absorption (arb. units)
8970
8980
8990
9000
9010
9020
9030
Energy (eV)

Cu-peptides EXAFS vs XANES

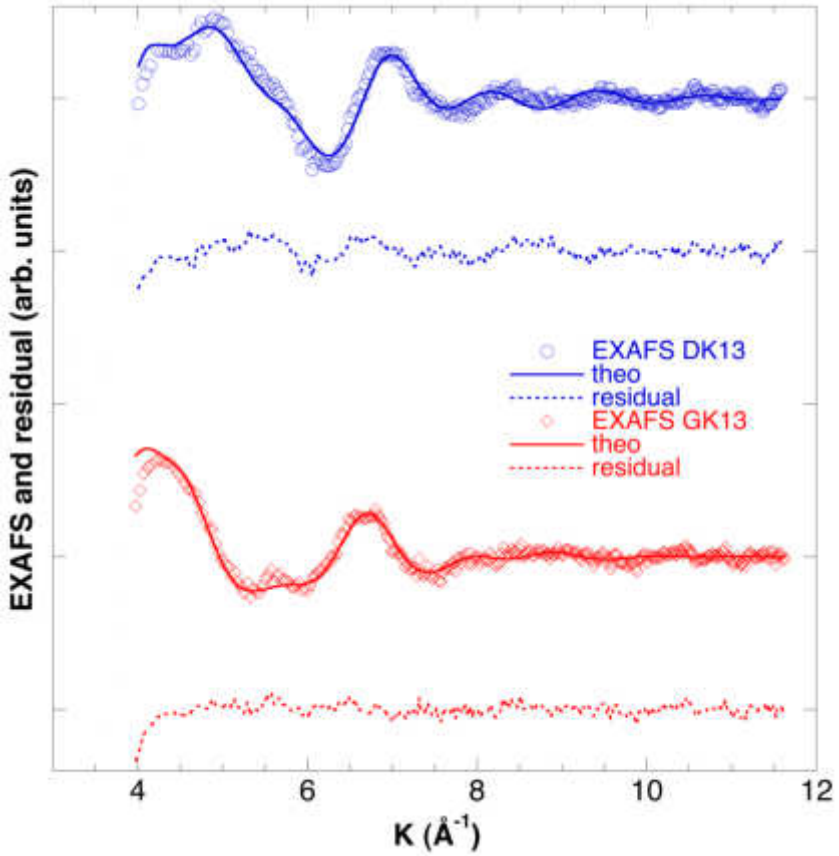

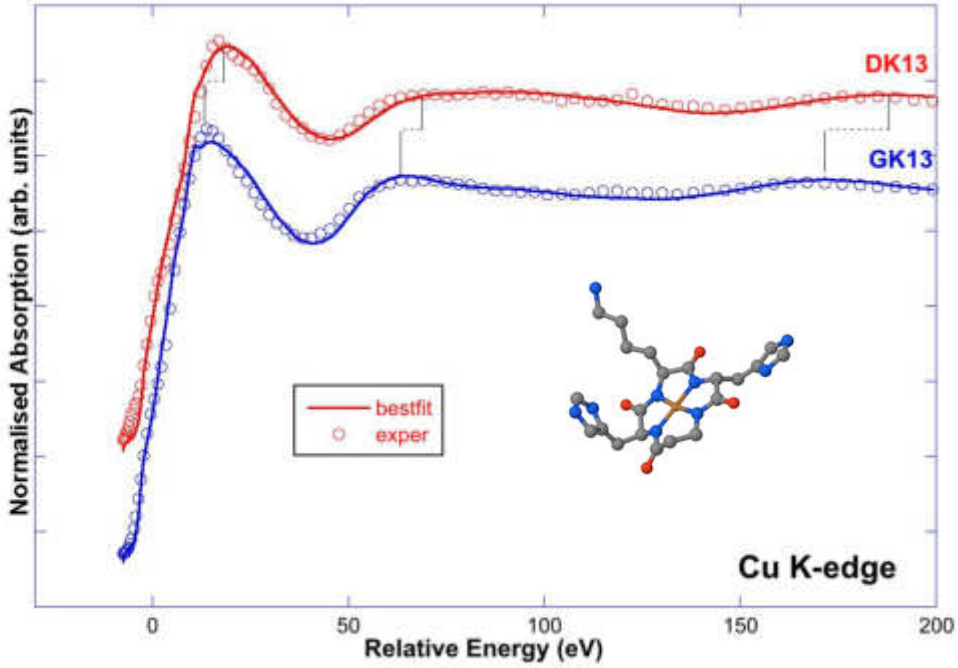

<Cu-N> = 1.90 Å Cu^{II}
<Cu-C> = 2.88 Å
<Cu-N> = 1.79 Å Cu^{III}
<Cu-C> = 2.78 Å

^{XANES}<Cu-N> = ^{EXAFS}<Cu-N>

Also hints on local geometry
(sq. coord. Non centrosymmetric)

Structure of silicate glasses

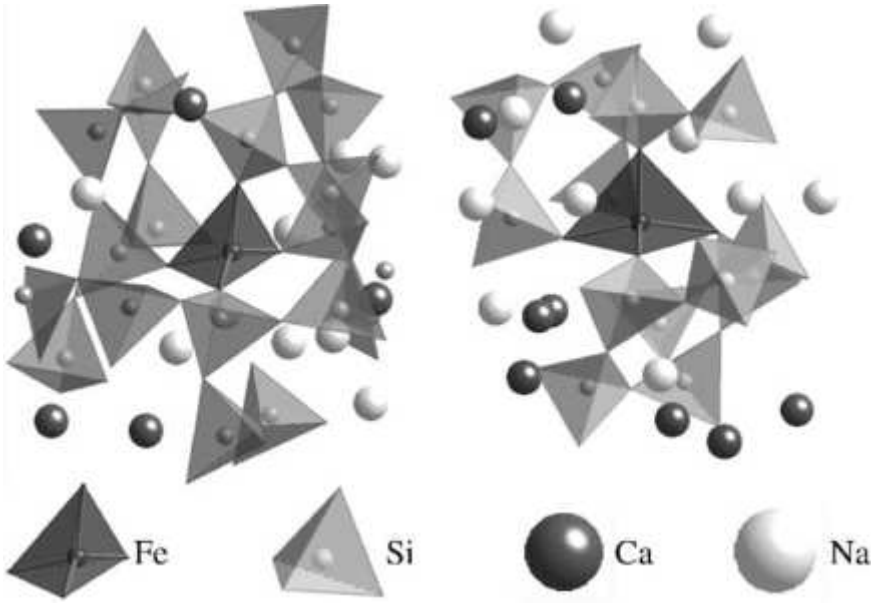

Fe role?:

- Polimerisation?
- Bonding?
- To which units is Fe bonded?

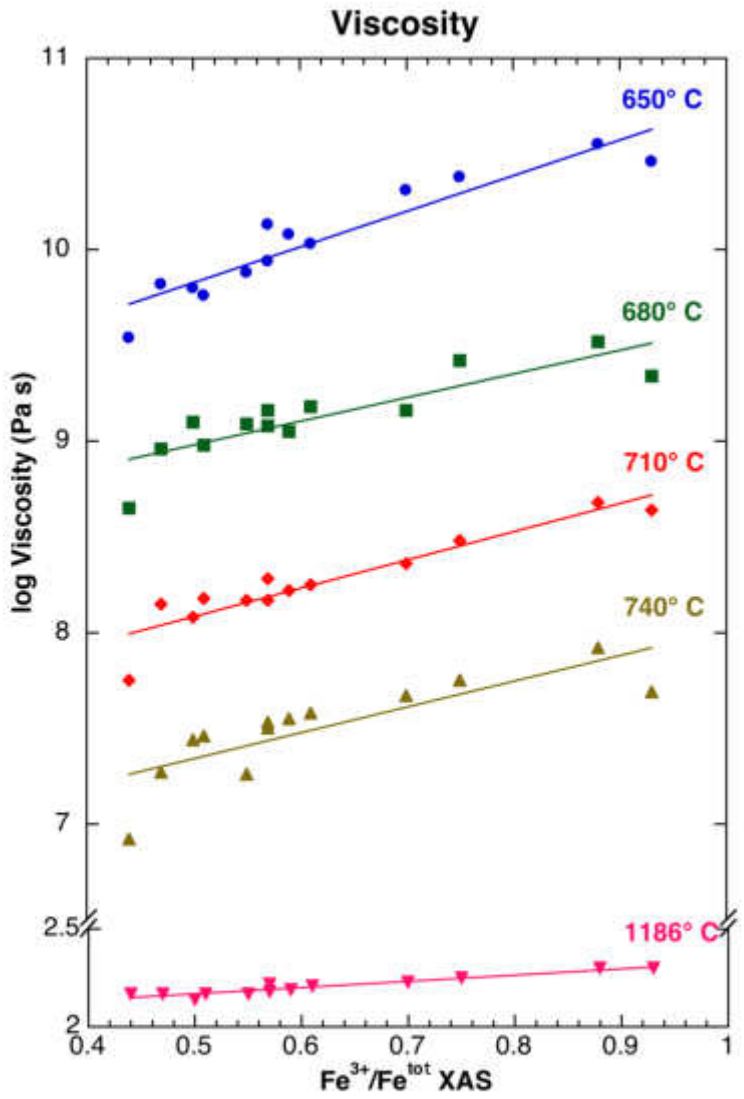

From Dingwell et a. et al., in preparation

Structure of silicate glasses

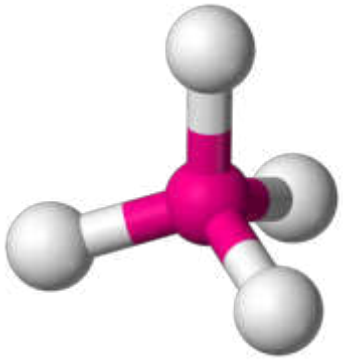

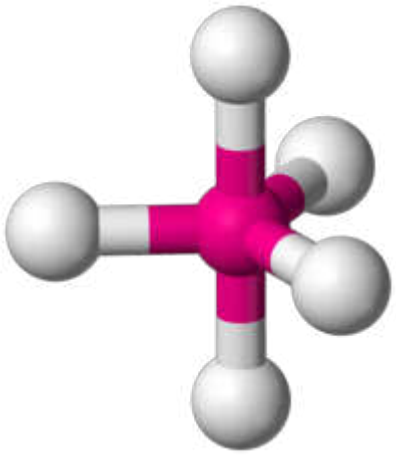

Fe^{2+}

[4]

<Fe-O>~2.00 Å

[5]

<Fe-O>~2.07 Å

Fe^{3+}

[4]

<Fe-O>~1.85 Å

[5]

<Fe-O>~1.94 Å

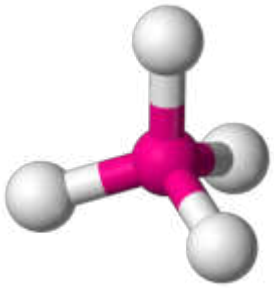

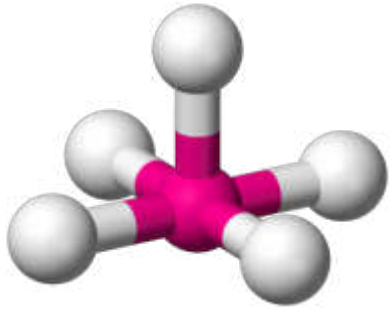

Structure of silicate glasses

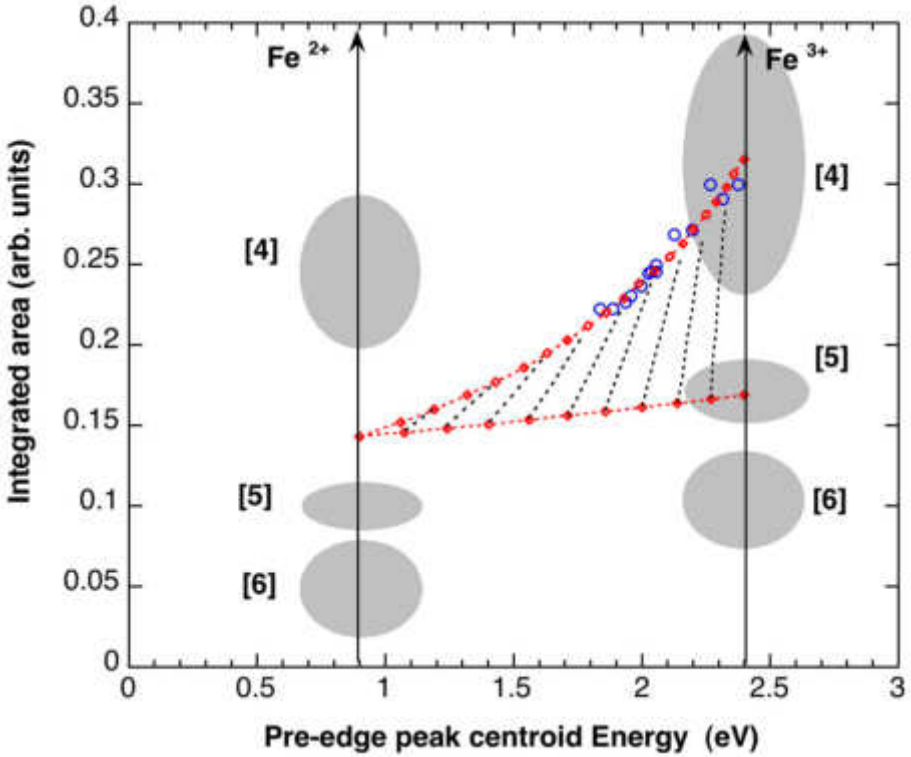

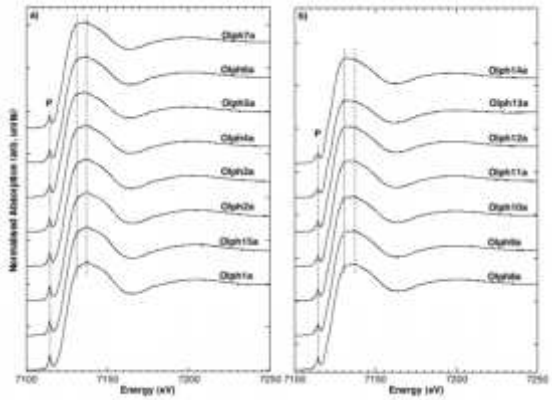

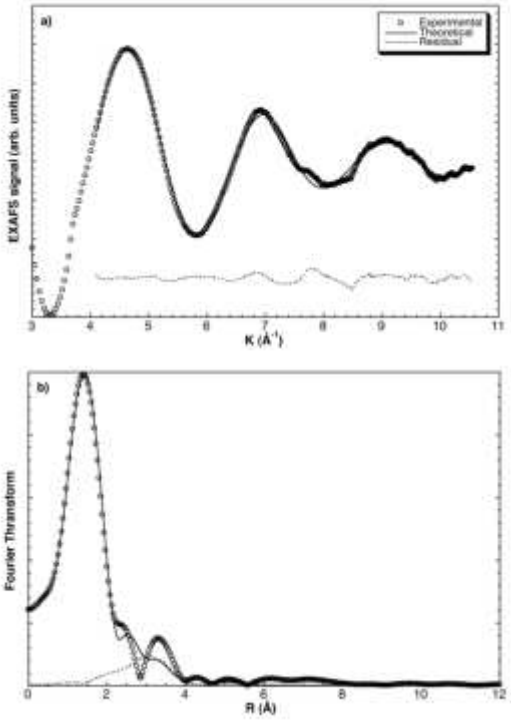

Fe-O distances

air $^{[4]}Fe^{3+}$ <Fe-O>=1.86 Å

FMQ $^{[4]}Fe^{2+}$, $^{[5]}Fe^{2+}$, $^{[4]}Fe^{3+}$

IW $^{[4]}Fe^{2+}$ and $^{[5]}Fe^{2+}$
<Fe-O>=2.01 Å

The case of doped $LiFePO_4$, ZnO, SnO_2

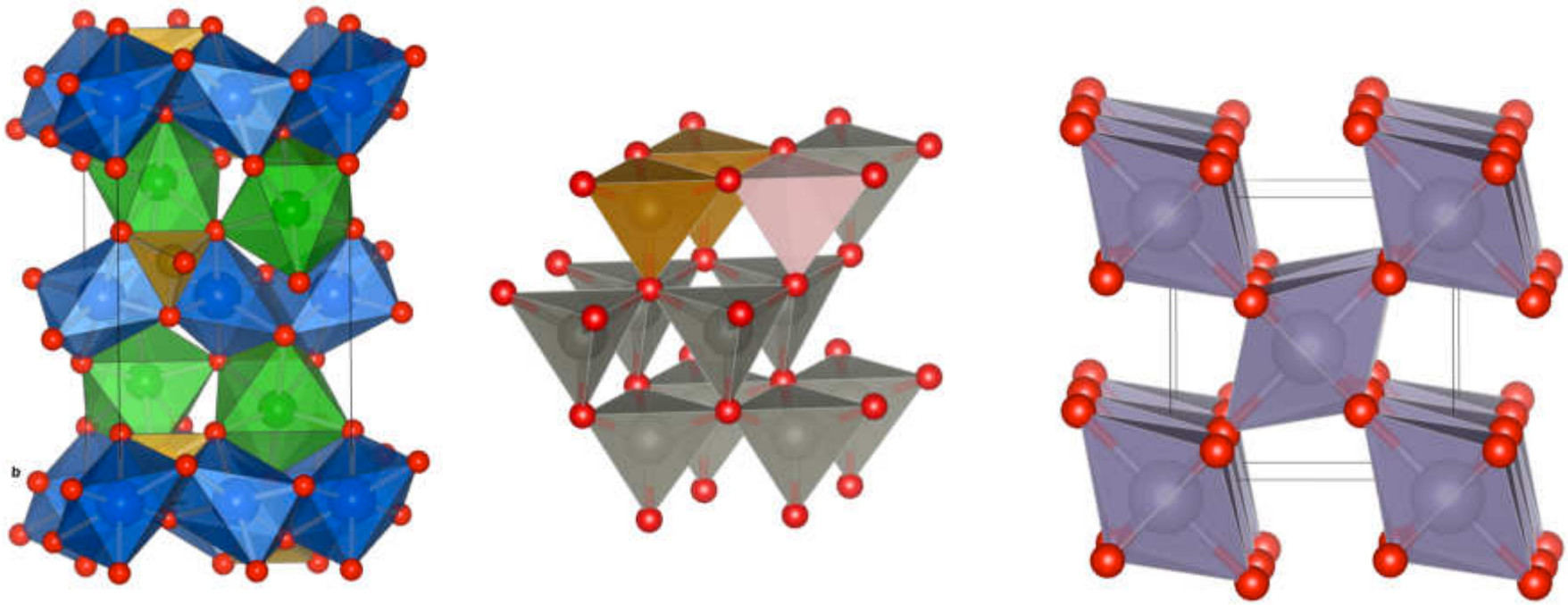

Effect of V doping in $LiFePO_4$

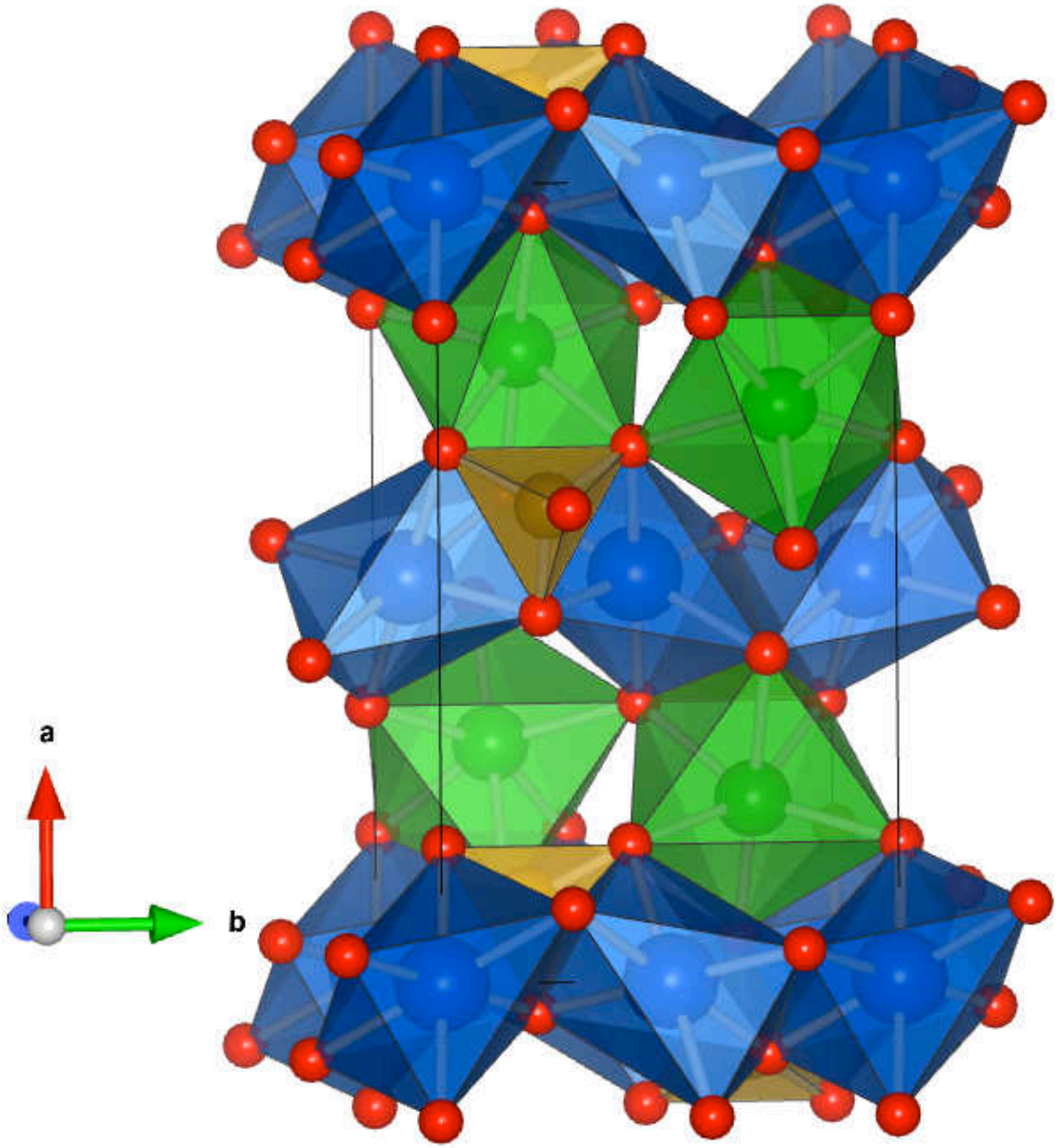

$^{[6]}Li^{+}$ in **M1**

$^{[6]}Fe^{2+}$ in **M2**

$^{[4]}P^{5+}$ in **T**

Effect of V doping in $LiFePO_4$

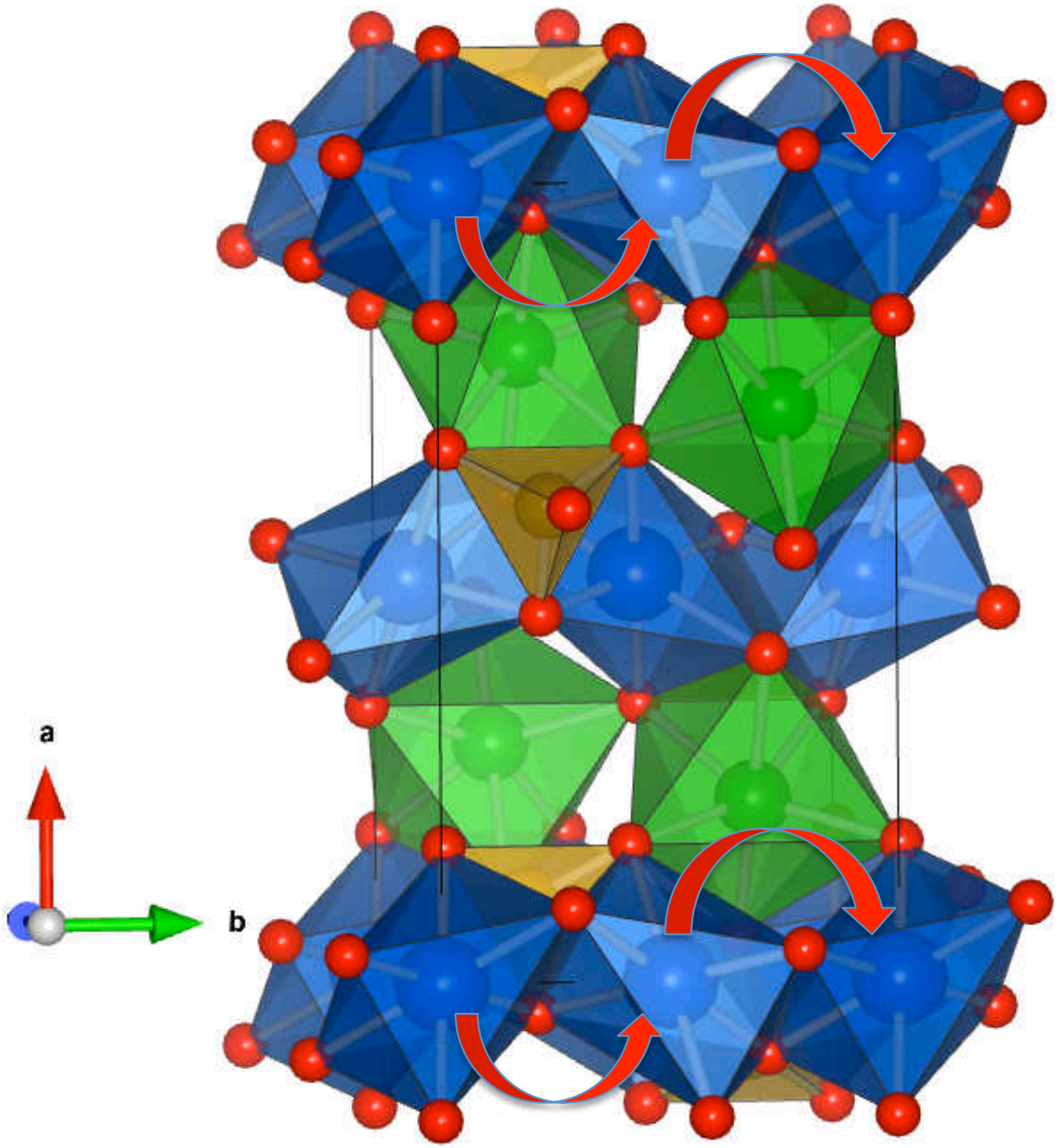

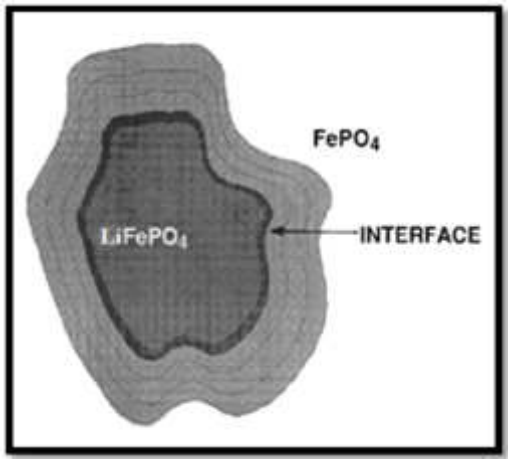

Core-shell model

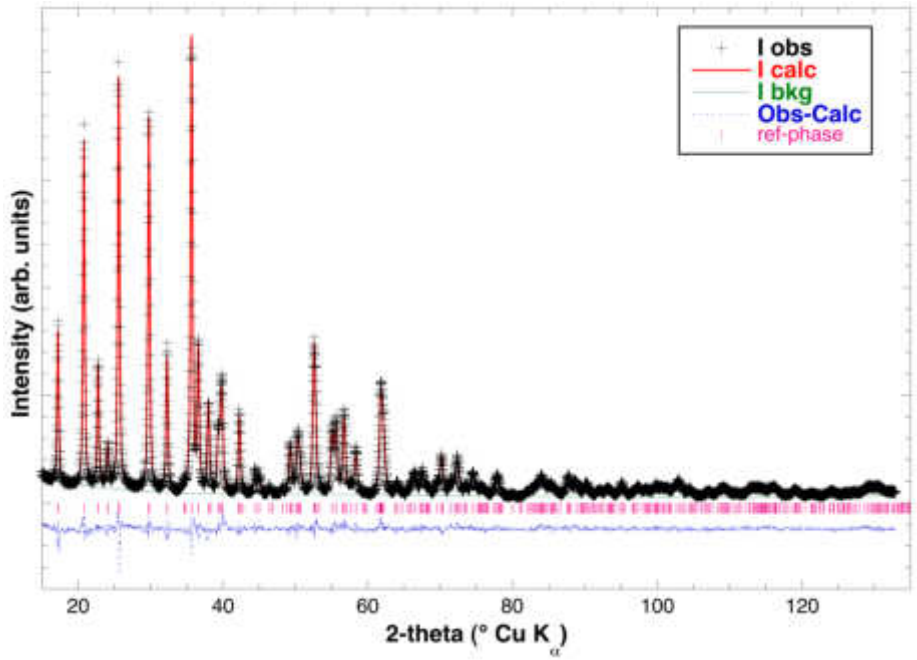
I obs
I calc
I bkg
Obs-Calc
ref-phase
Intensity (arb. units)
20
40
60
80
100
120
2-theta (° Cu K α)

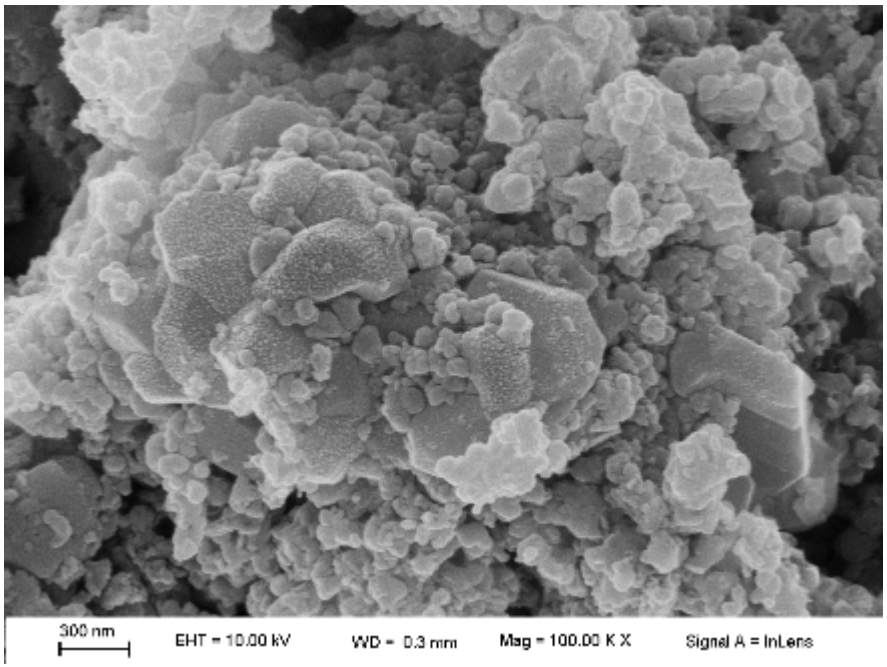
300 nm
EHT = 10.00 kV
WD = 0.3 mm
Mag = 100.00 K X
Signal A = InLens

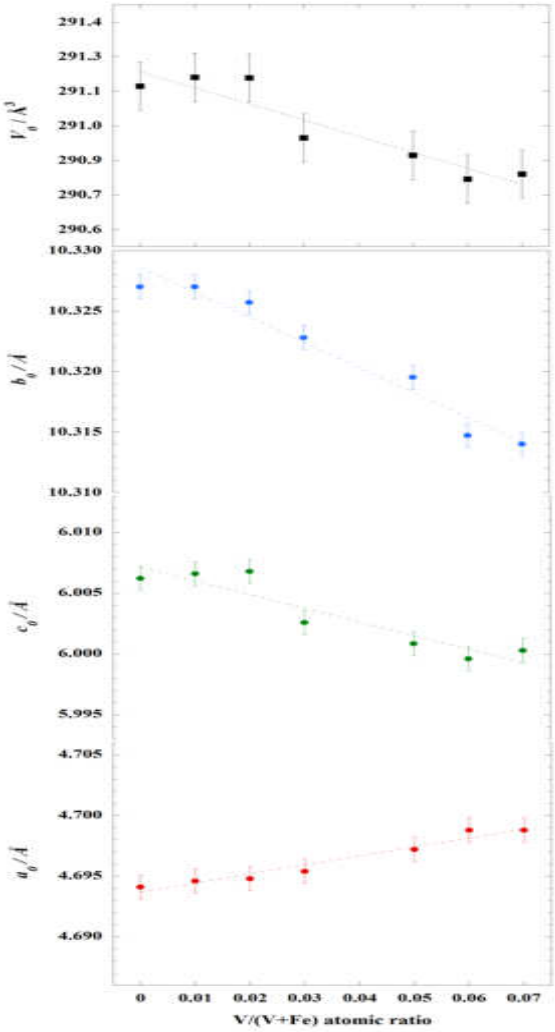
291.4
291.3
291.1
291.0
290.9
290.7
290.6
V_θ / Å^3
10.330
10.325
10.320
10.315
10.310
b_θ / Å
6.010
6.005
6.000
5.995
c_θ / Å
4.705
4.700
4.695
4.690
a_θ / Å
0
0.01
0.02
0.03
0.04
0.05
0.06
0.07
V/(V+Fe) atomic ratio

V K-edge XAS $LiFePO_4$

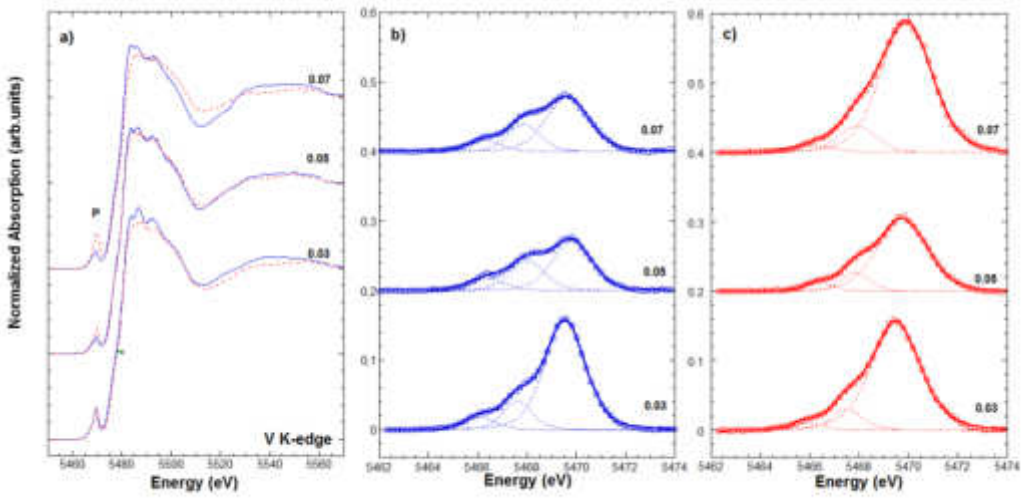

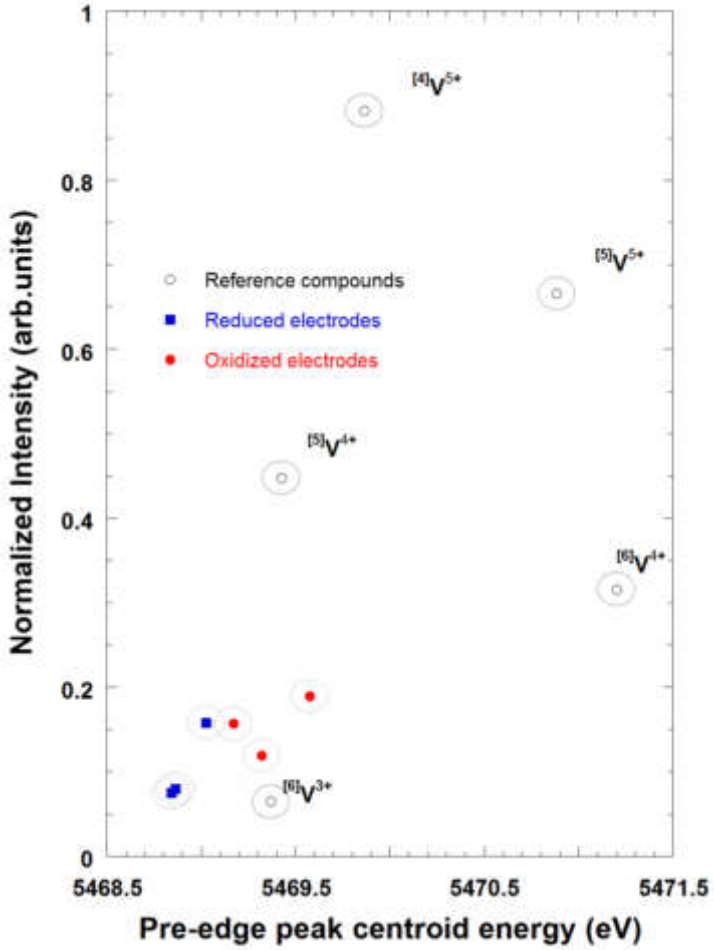

Fe K-edge XAS $LiFePO_4$

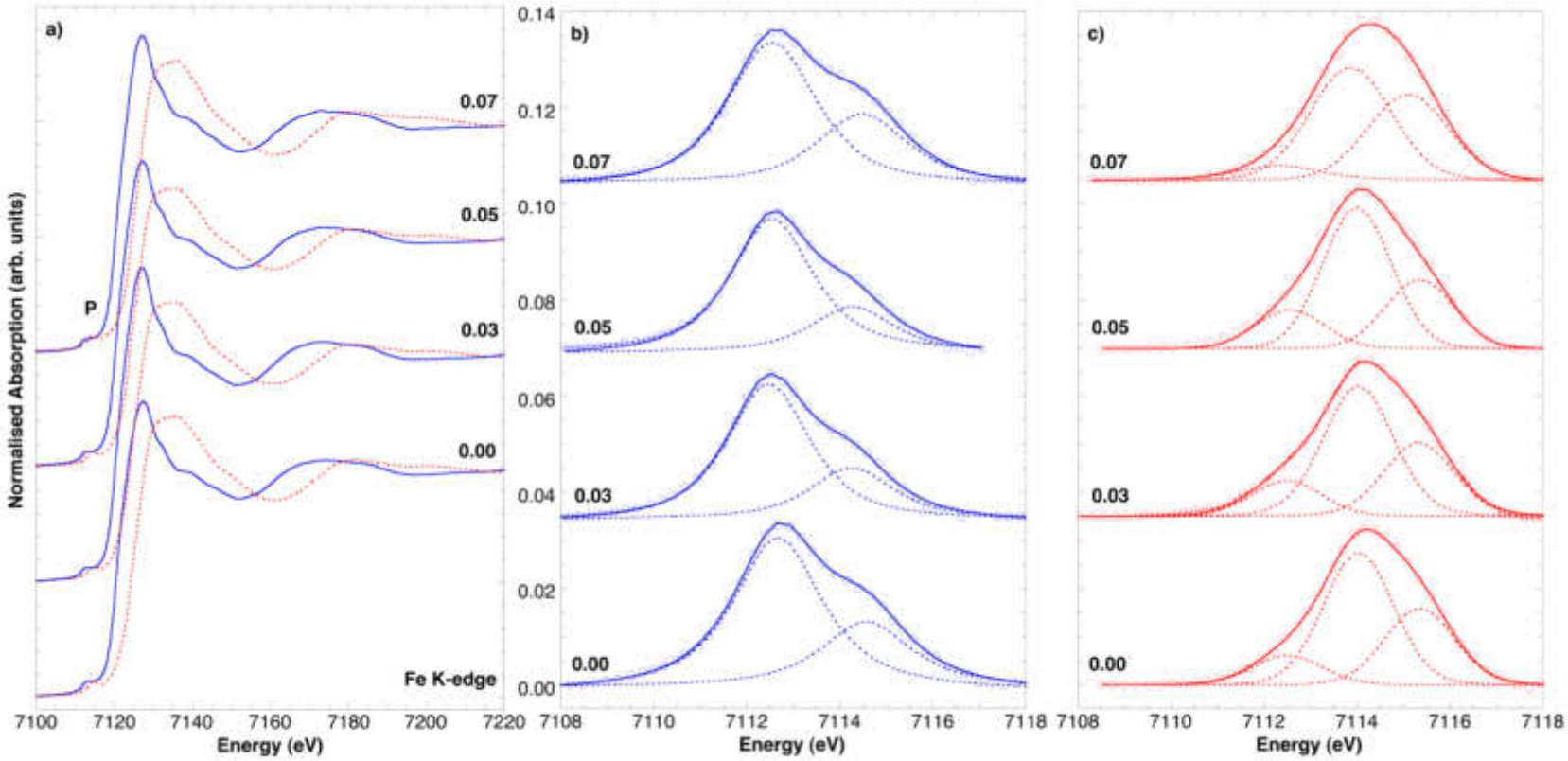

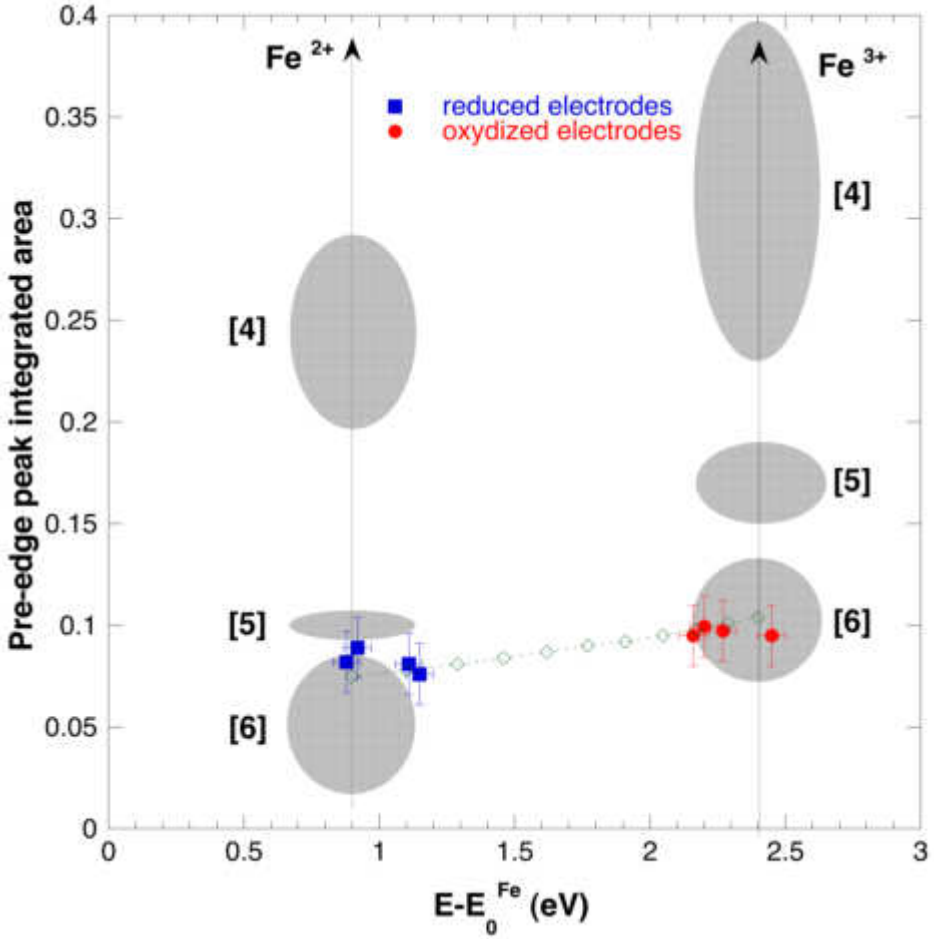
Fe 2+
Fe 3+
reduced electrodes
oxydized electrodes
[4]
[4]
[5]
[5]
[6]
[6]
Pre-edge peak integrated area
E-E0 Fe (eV)
0
0.05
0.1
0.15
0.2
0.25
0.3
0.35
0.4
0
0.5
1
1.5
2
2.5
3

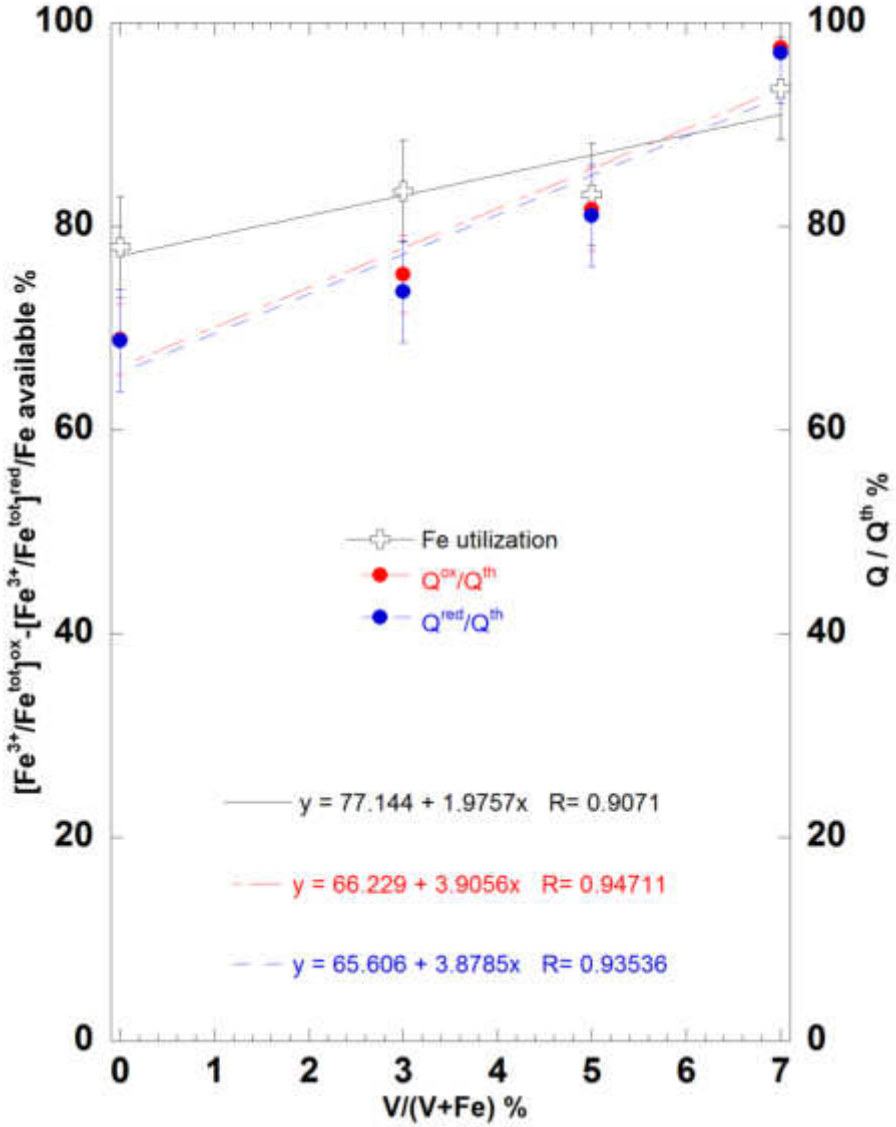
[Fe3+/Fetot]ox-[Fe3+/Fetot]red/Fe available %
Q / Qth %
V/(V+Fe) %
Fe utilization
Qox/Qth
Qred/Qth
y = 77.144 + 1.9757x R= 0.9071
y = 66.229 + 3.9056x R= 0.94711
y = 65.606 + 3.8785x R= 0.93536
0
20
40
60
80
100
0
1
2
3
4
5
6
7

- **V successfully inserted in the M2 site;**
- **V^{3+} significantly affects cell size, crystallinity and strain;**
- **V^{3+} imply Li vacancy at M1;**
- **V do not participates to reduction/oxidation, but greatly enhances efficiency of Fe oxidation/reduction.**

Moretti et al., 2013, J. Electrochem. Soc., 160(6), A940-A949

Structure of Fe- and Co- doped ZnO as anode material for Li-ion batteries

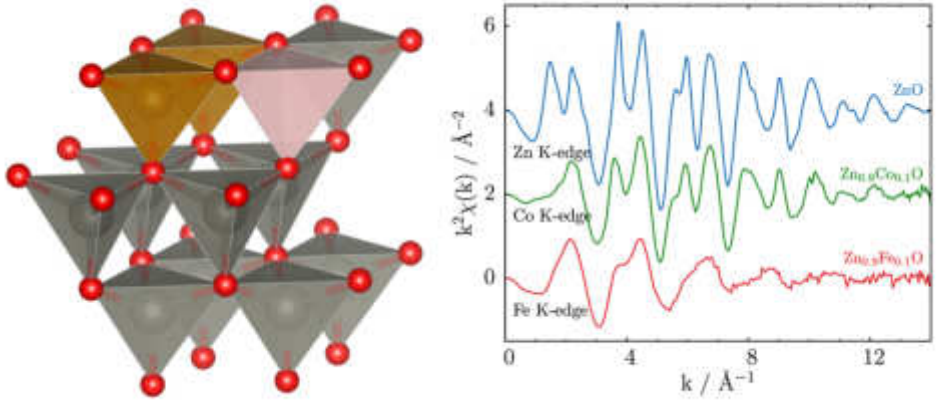

AIMS

- Characterise average and local structure
- Build the basis for *in-situ in-operando* studies during cycling

ZnO

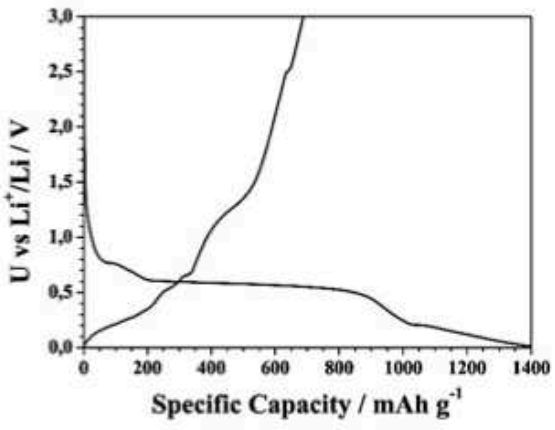

$Fe_{0.1}Zn_{0.9}O$

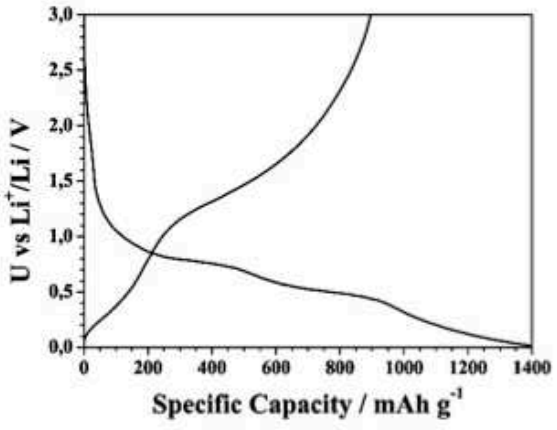

$Co_{0.1}Zn_{0.9}O$

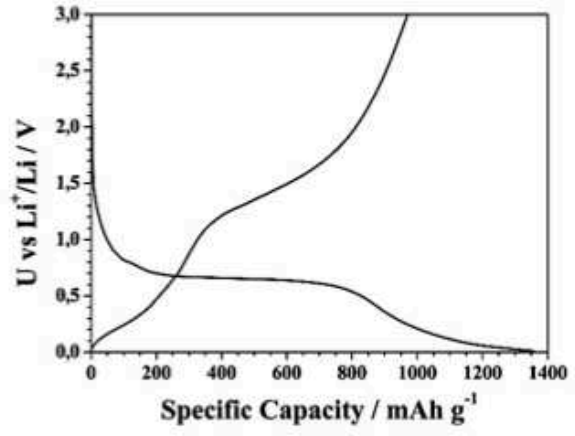

Synthesis

1) Dissolving (Zn, ±Co ± Fe) gluconate in ultra pure water.
2) the 0.2M solution was added to 1.2M solution of sucrose
3) heated at 160° C for 15' (drying)
4) T increased up to 300 °C (decomposition of sucrose)
5) Held at 450 °C for 3 hours

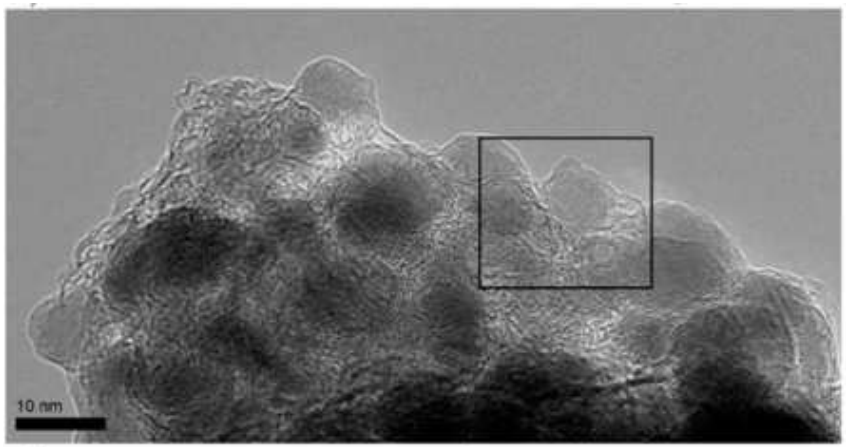

f)

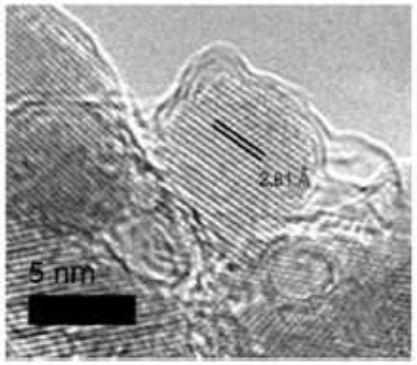

g)

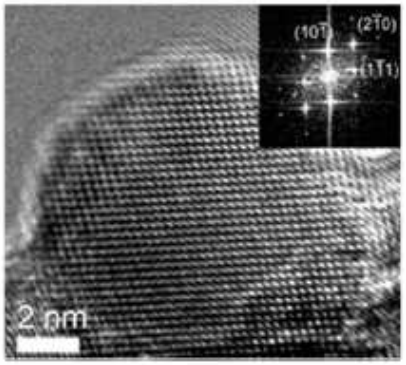

XRD results

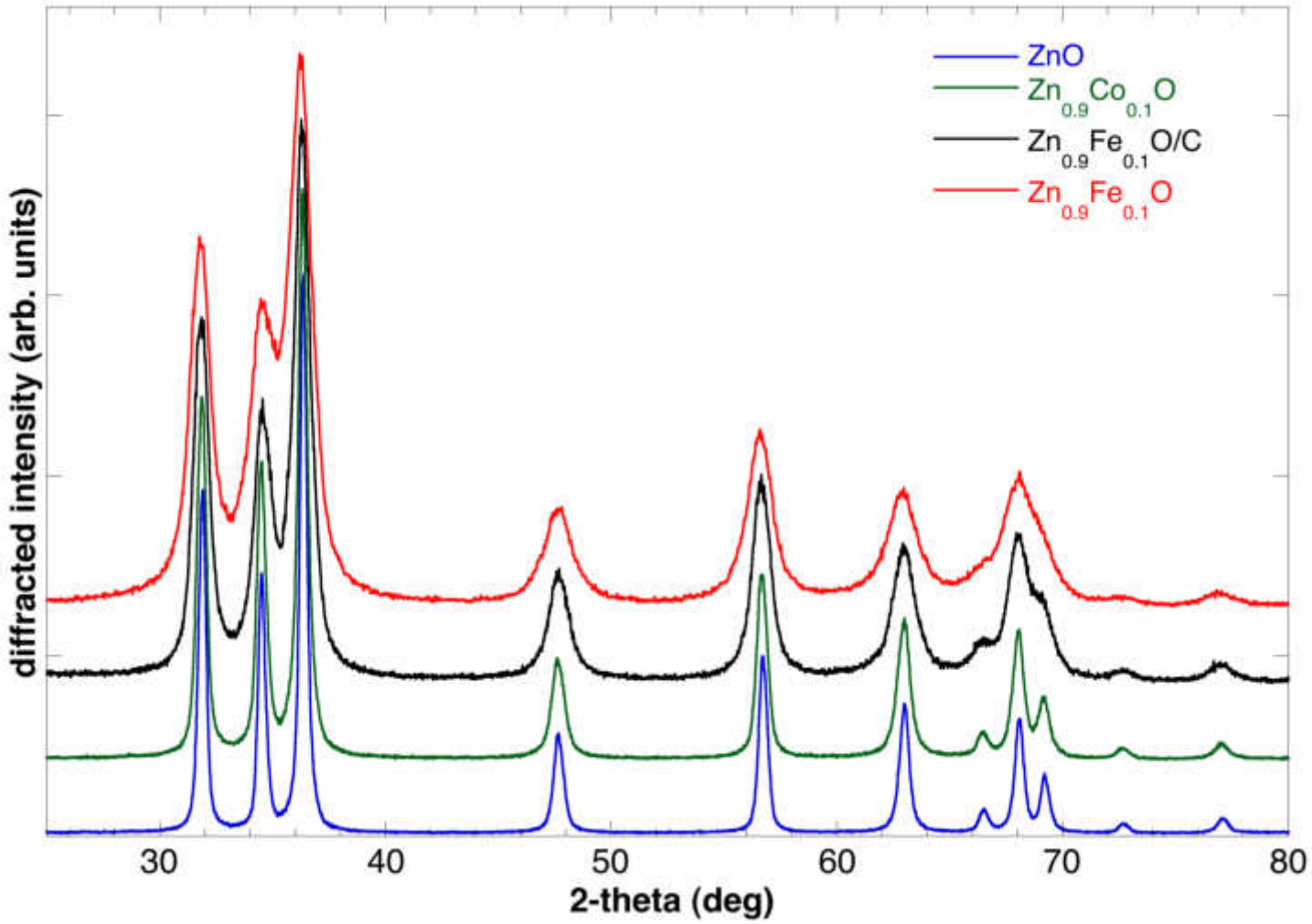
ZnO
Zn0.9Co0.1O
Zn0.9Fe0.1O/C
Zn0.9Fe0.1O
diffracted intensity (arb. units)
30
40
50
60
70
80
2-theta (deg)

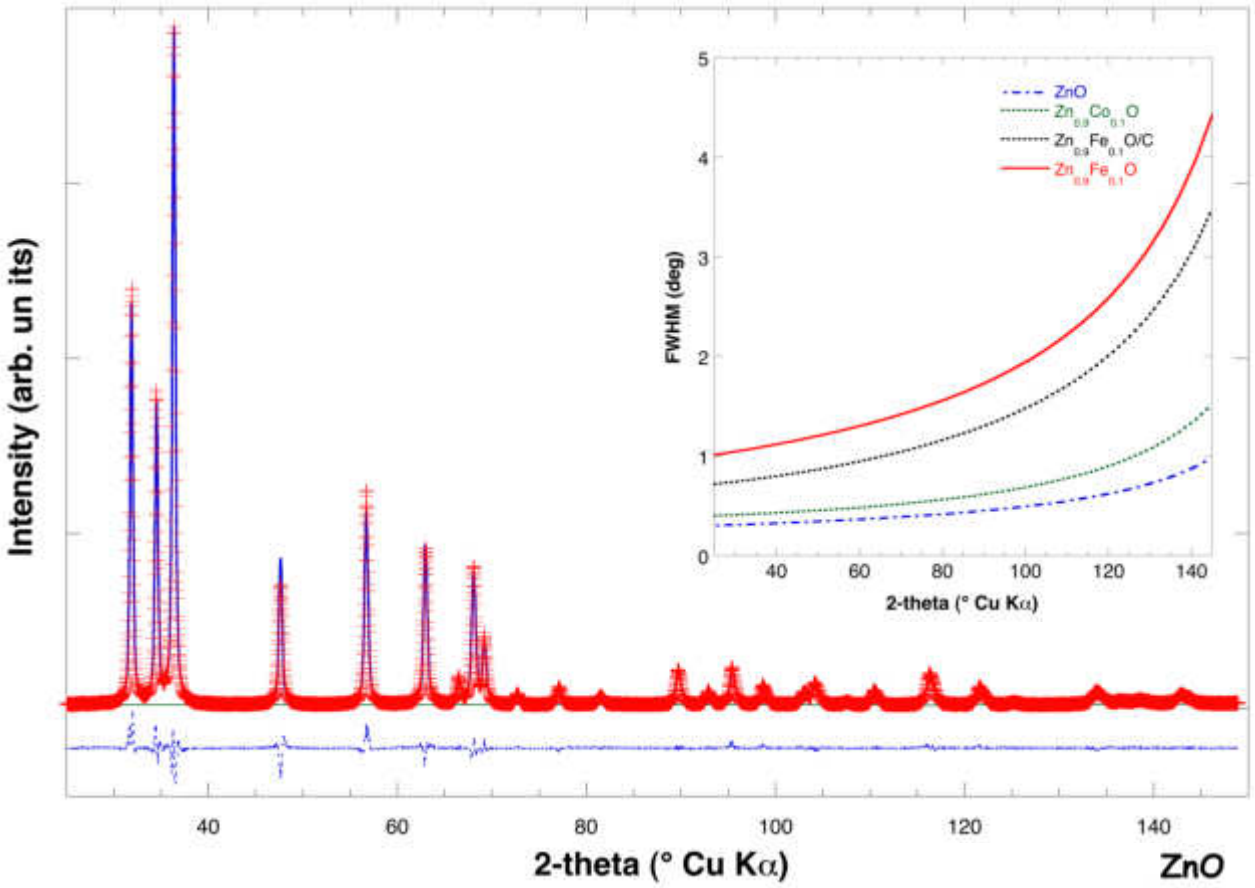

XRD results

1) No impurities
2) No dopants in the interstitial sites
3) Effect on crystallinity and strain

	ZnO	$Zn_{0.9}Co_{0.1}O$	$Zn_{0.9}Fe_{0.1}O$	$Zn_{0.9}Fe_{0.1}O/C$
a_0 (Å)	3.2511(3)	3.2523(1)	3.2552(2)	3.2547(1)
c_0 (Å)	5.2098 (1)	5.2095(1)	5.2043(4)	5.2045)2)
V_0 (Å^3)	47.687 (1)	47.721(1)	47.760(5)	47.746(2)
R_F^2	3.49	3.69	4.19	4.09
R_F	1.92	1.87	2.30	2.22
Crystallite size (nm)	42	29	13	15

XANES results

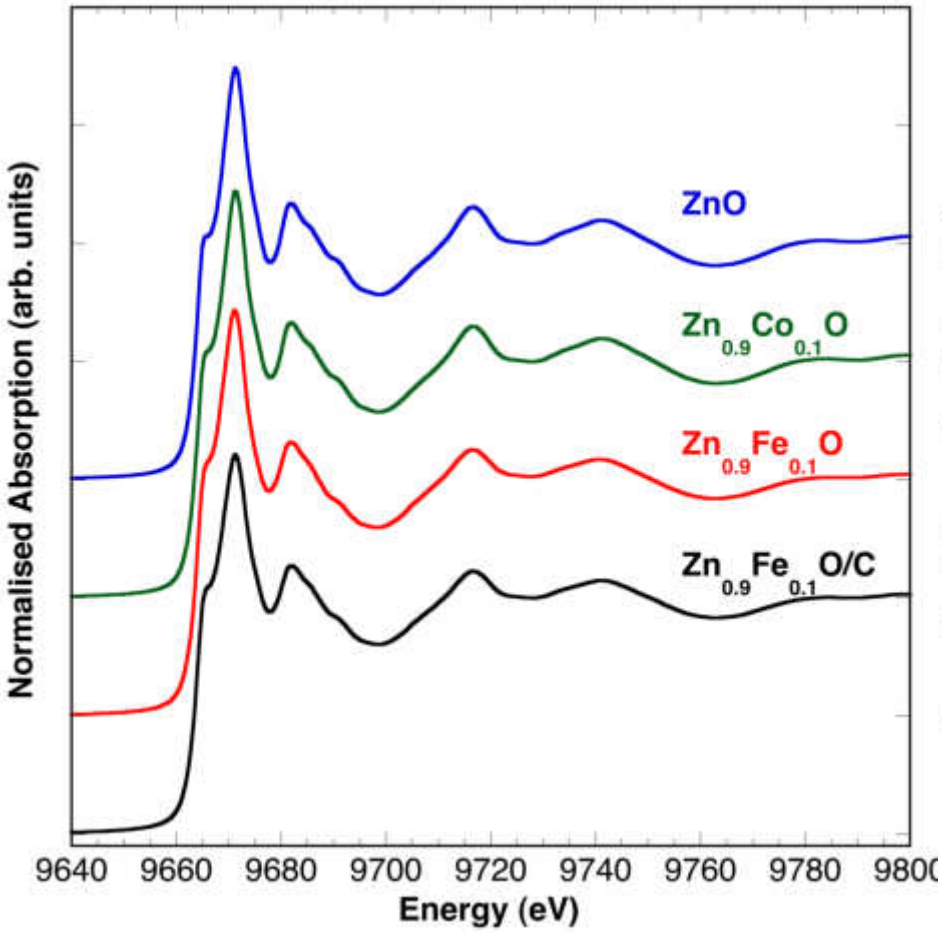

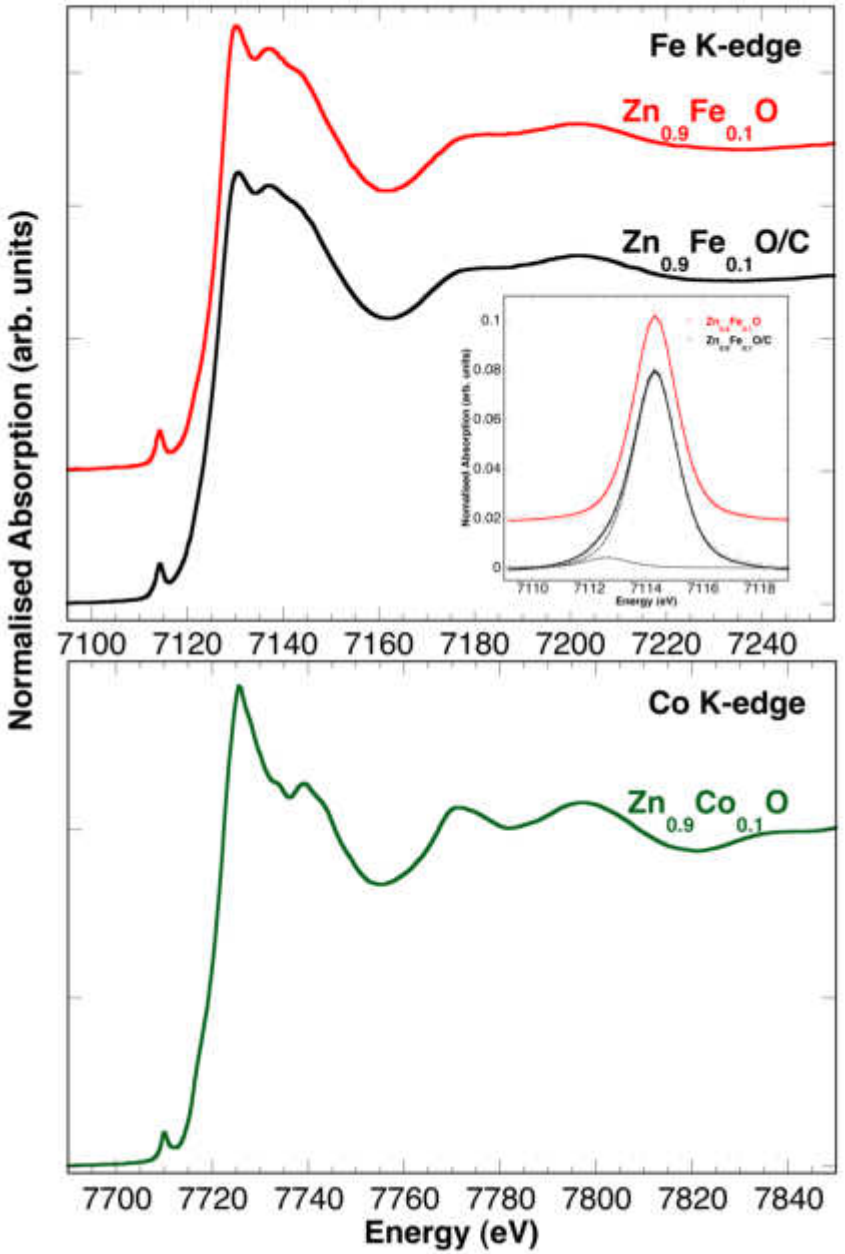

1) Zn local environment does not change
2) Fe is mostly trivalent [4]
3) Co is divalent [4]

EXAFS results

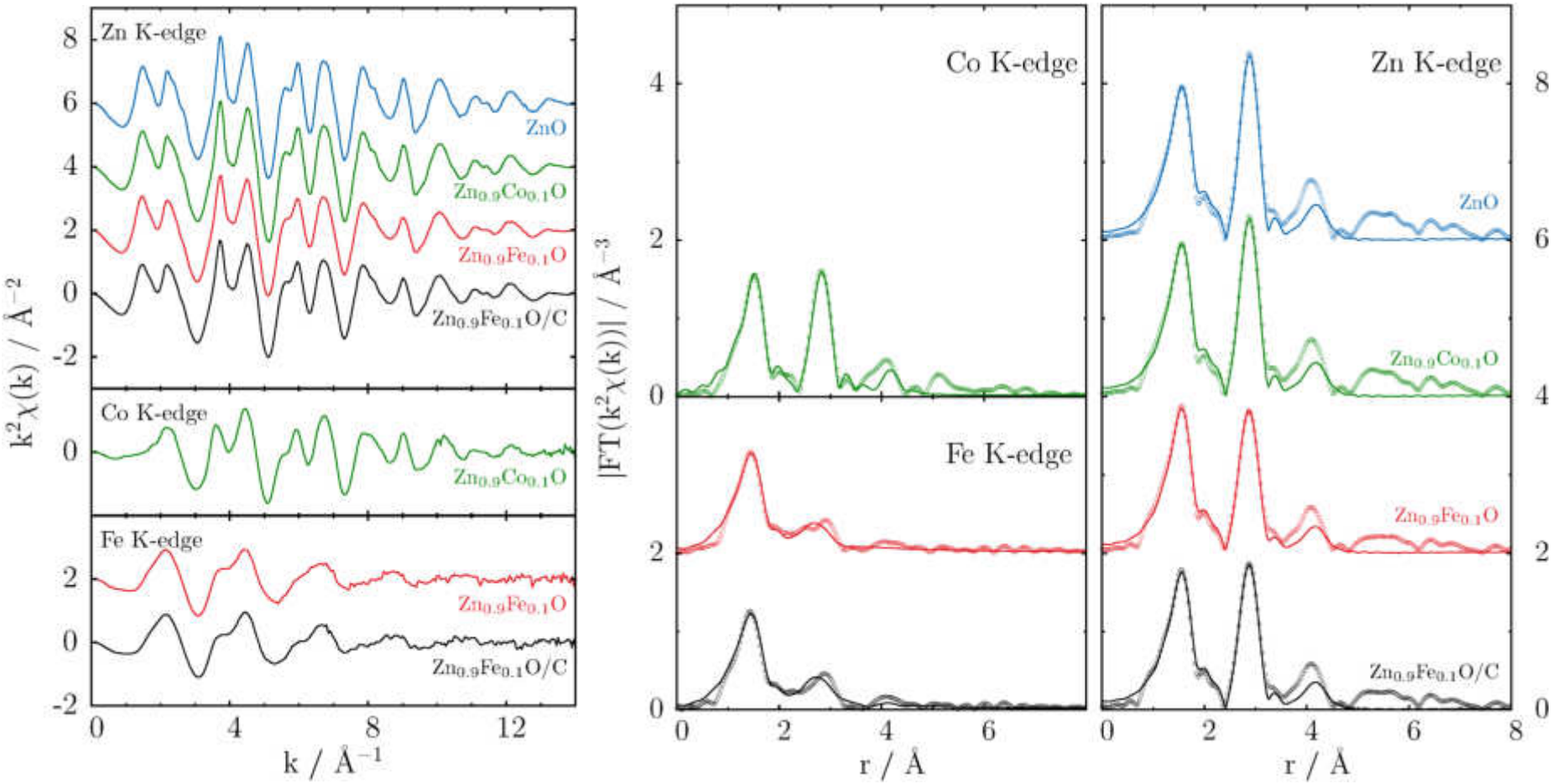

1) <Zn-O> = 1.98 Å in all samples;
2) <Co-O> = 1.97 Å;
3) <Fe-O> = 1.93 and 1.94 Å (much larger than 1.85-1.86 found in silicates*);
4) Fe oscillations are damped (possibly due to vacancies)

- Fe and Co successfully inserted in the Zn sites
- Co^{2+} only slightly affects cell size, crystallinity and strain
- Fe^{3+} greatly affects strain and crystallinity:
  - ➡ Possibly introducing ^{Zn}V or interstitial oxygens;
- 1 vacancy (or interstitial oxygen) compensates 2 Fe sites
  - ➡ Possible formation of FeO_4 dimers or oligomers

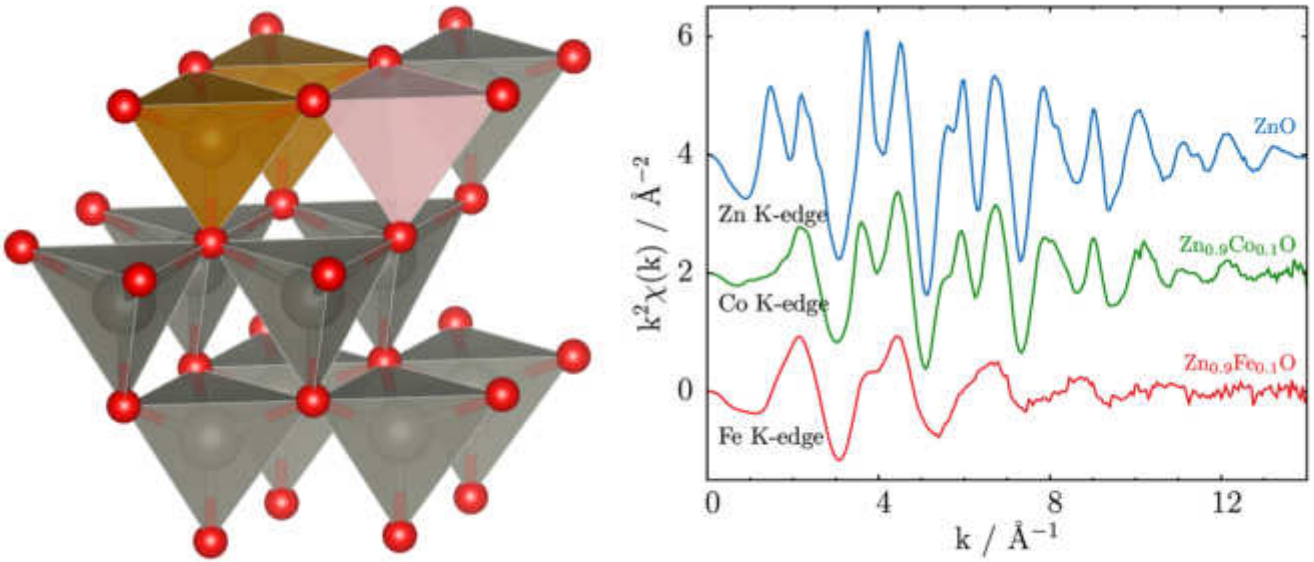

Giuli et al., 2015, Inorg. Chem., 54, 9393-9400

In-situ (operando) experiments

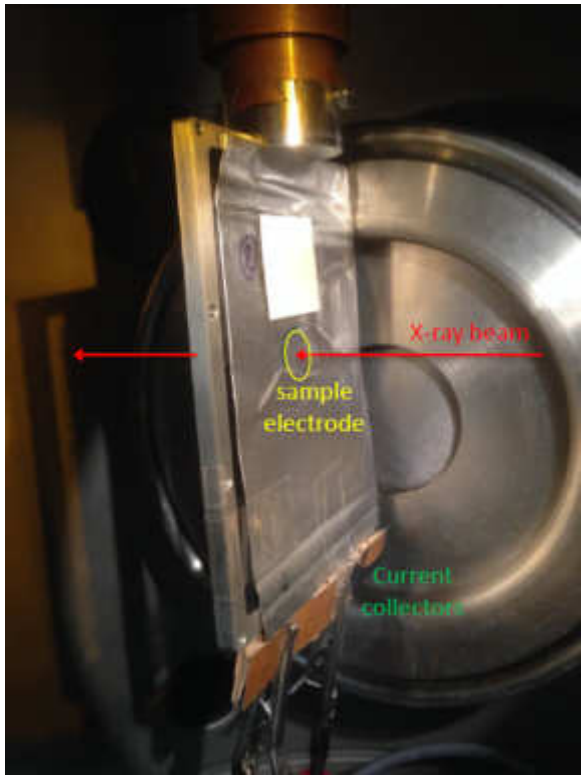

XAS on a working pouch cell
(BM08)

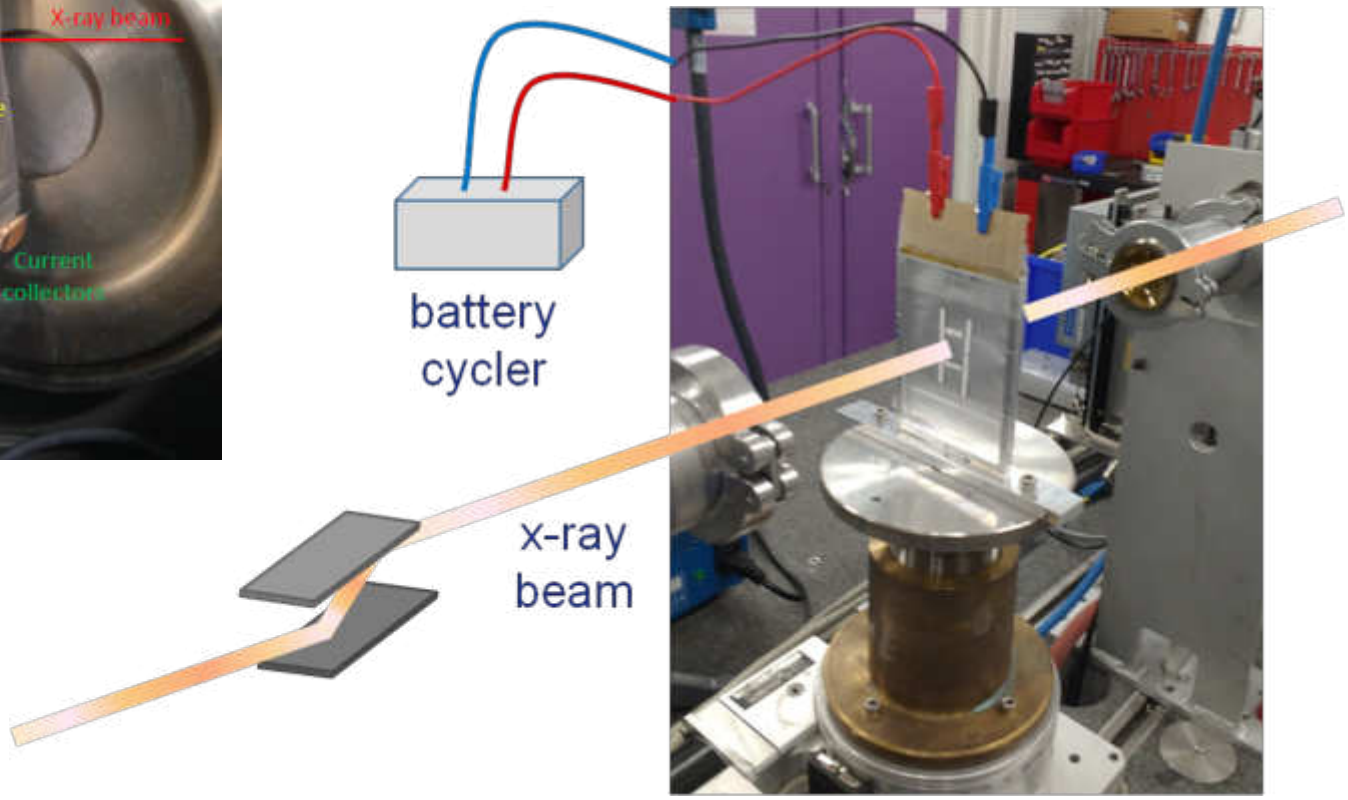

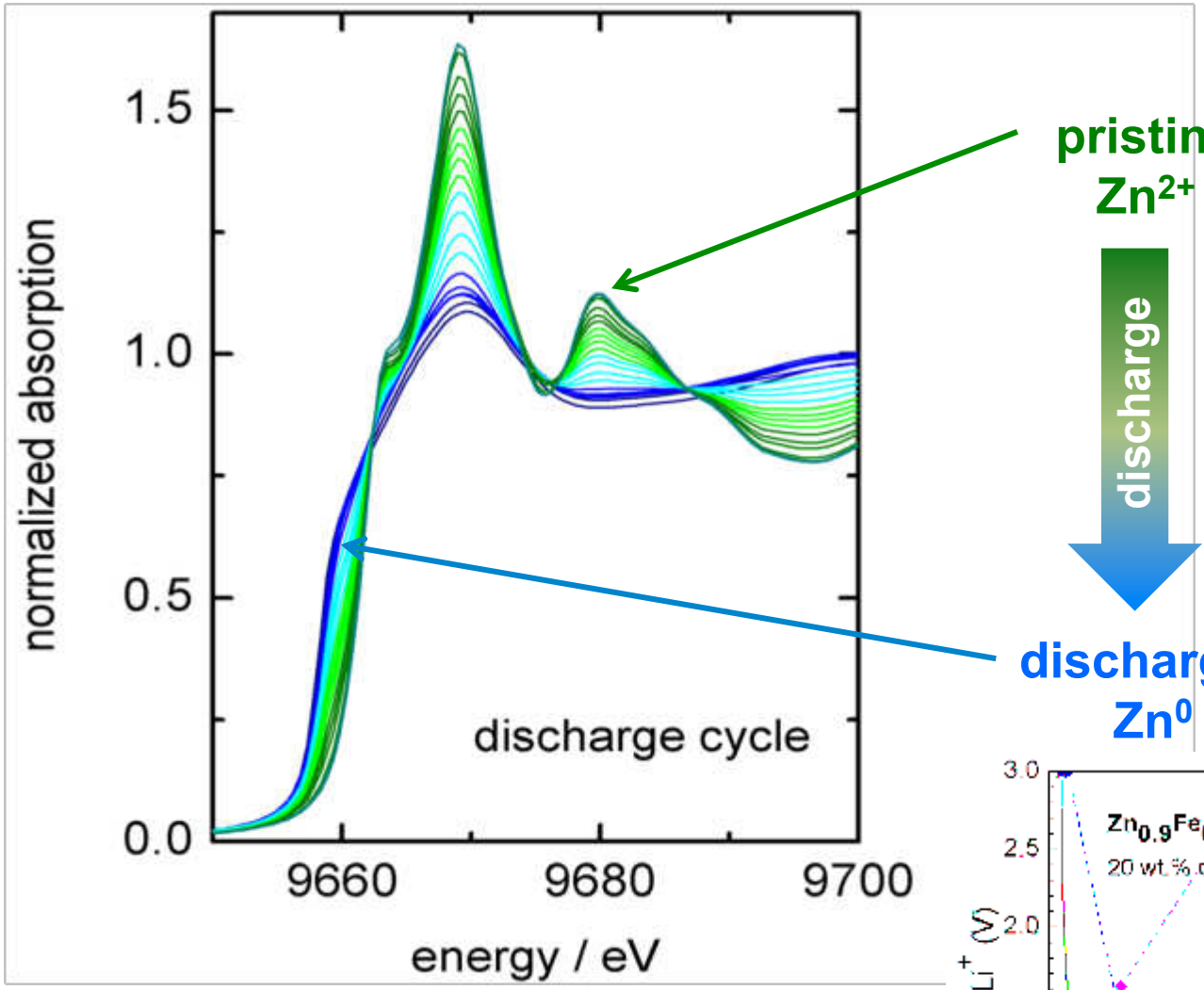

pristine Zn^{2+}

discharge

discharged Zn^0

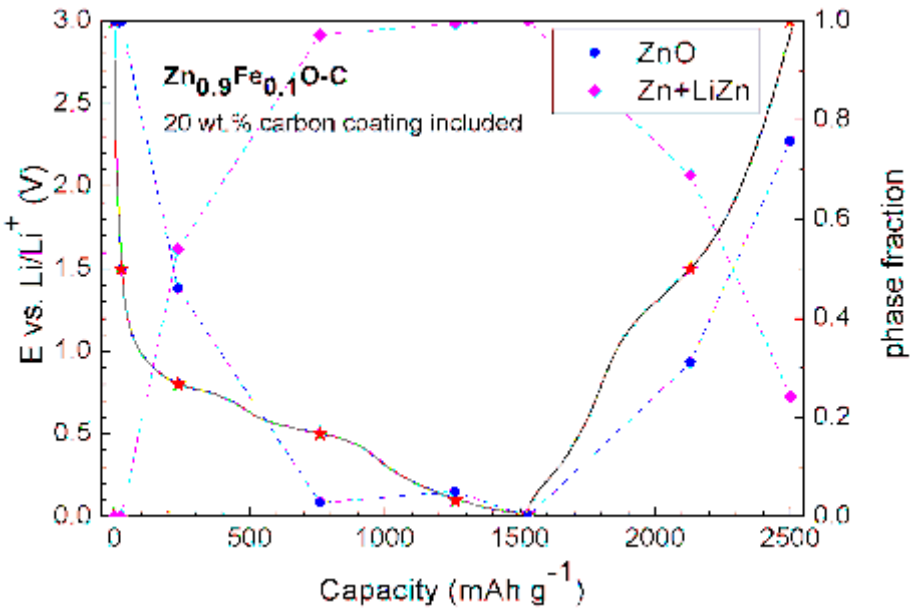

Trapananti et al., 2018, in prep.

Effect of varying the Fe content

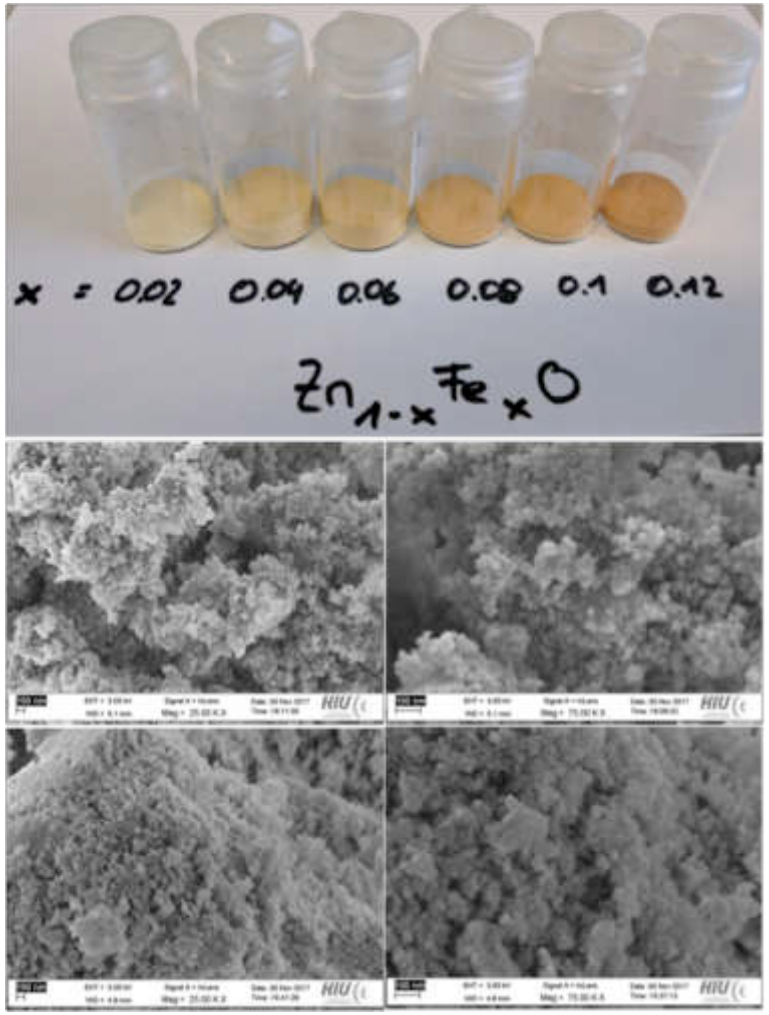

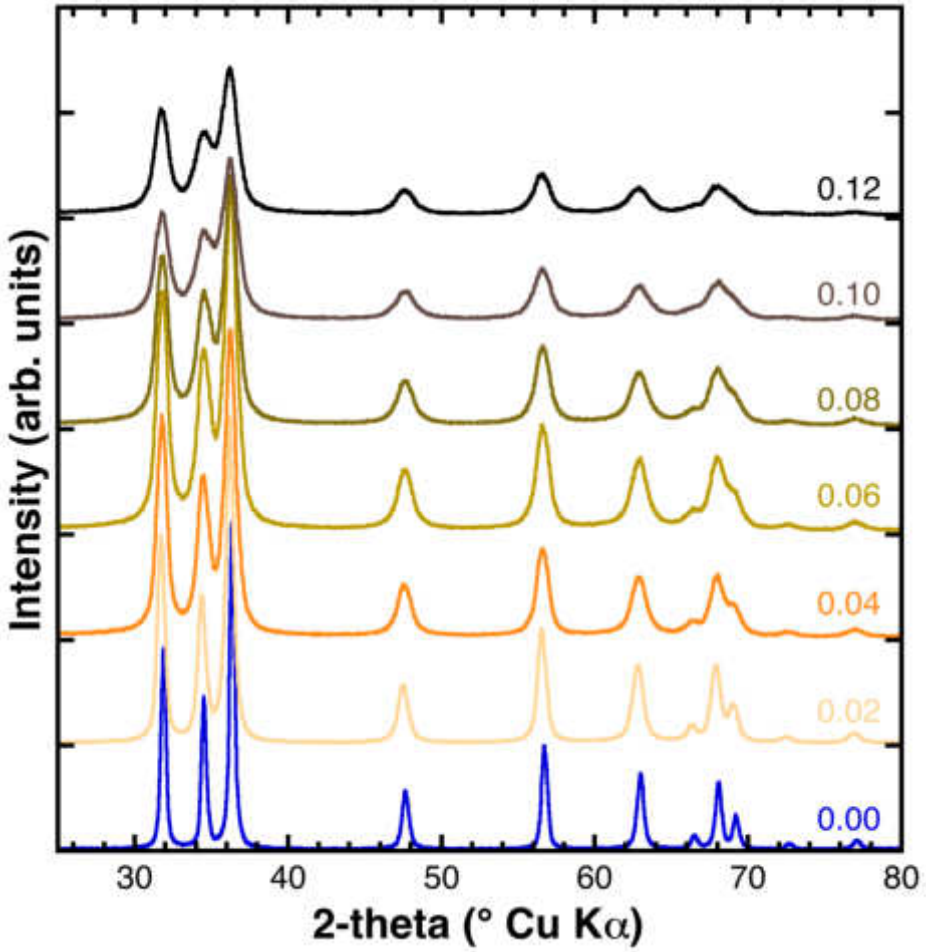

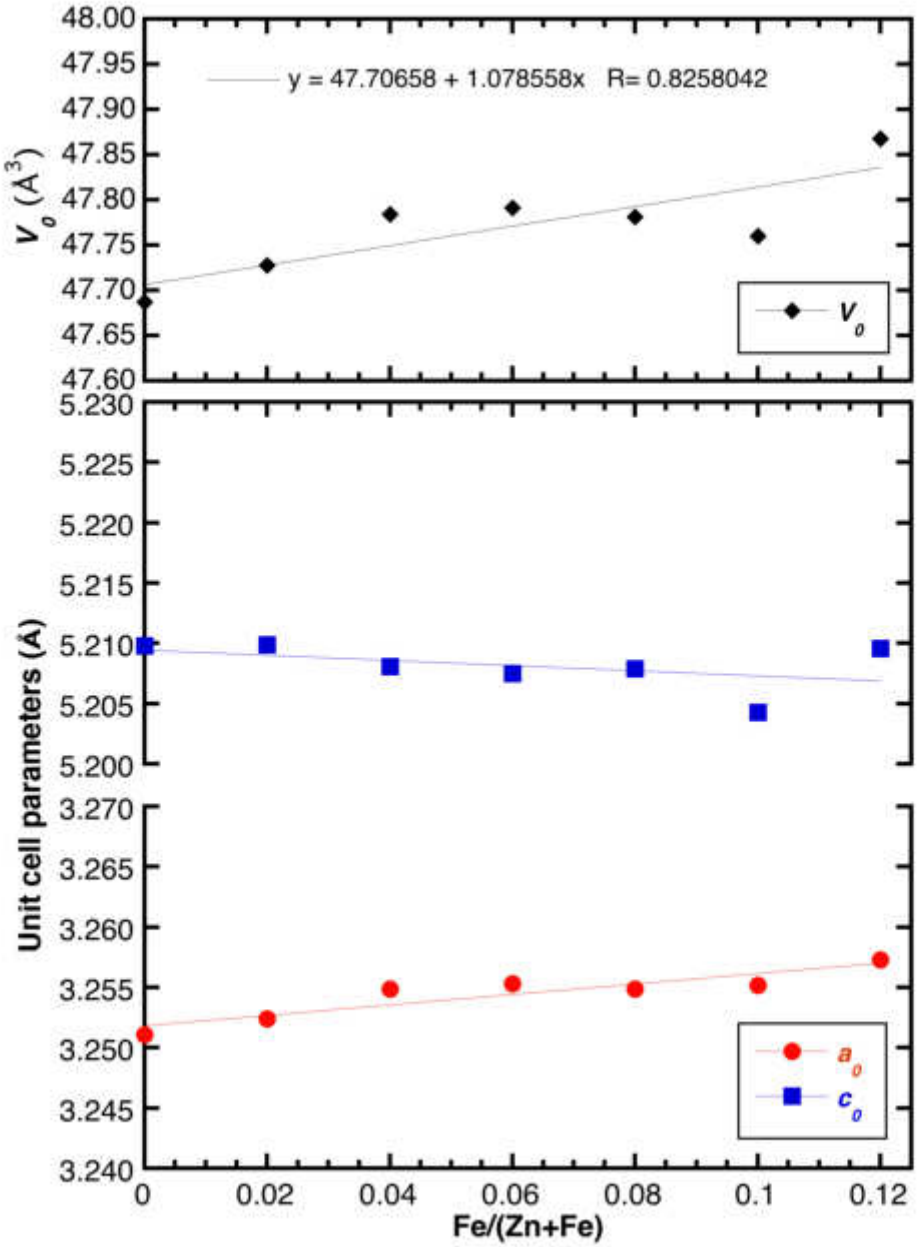
y = 47.70658 + 1.078558x R= 0.8258042
V_o ($Å^3$)
V_o
Unit cell parameters (Å)
a_0
c_0
Fe/(Zn+Fe)

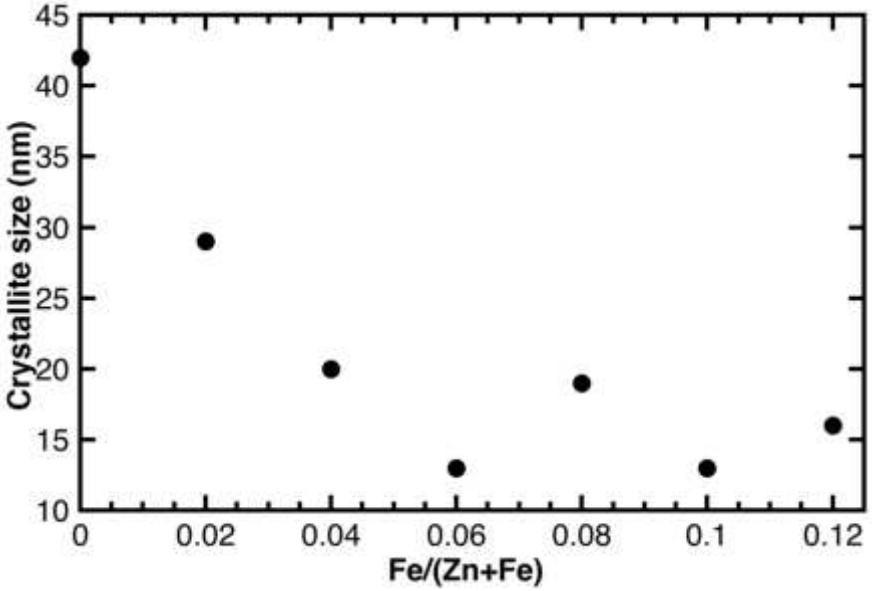
Crystallite size (nm)
Fe/(Zn+Fe)

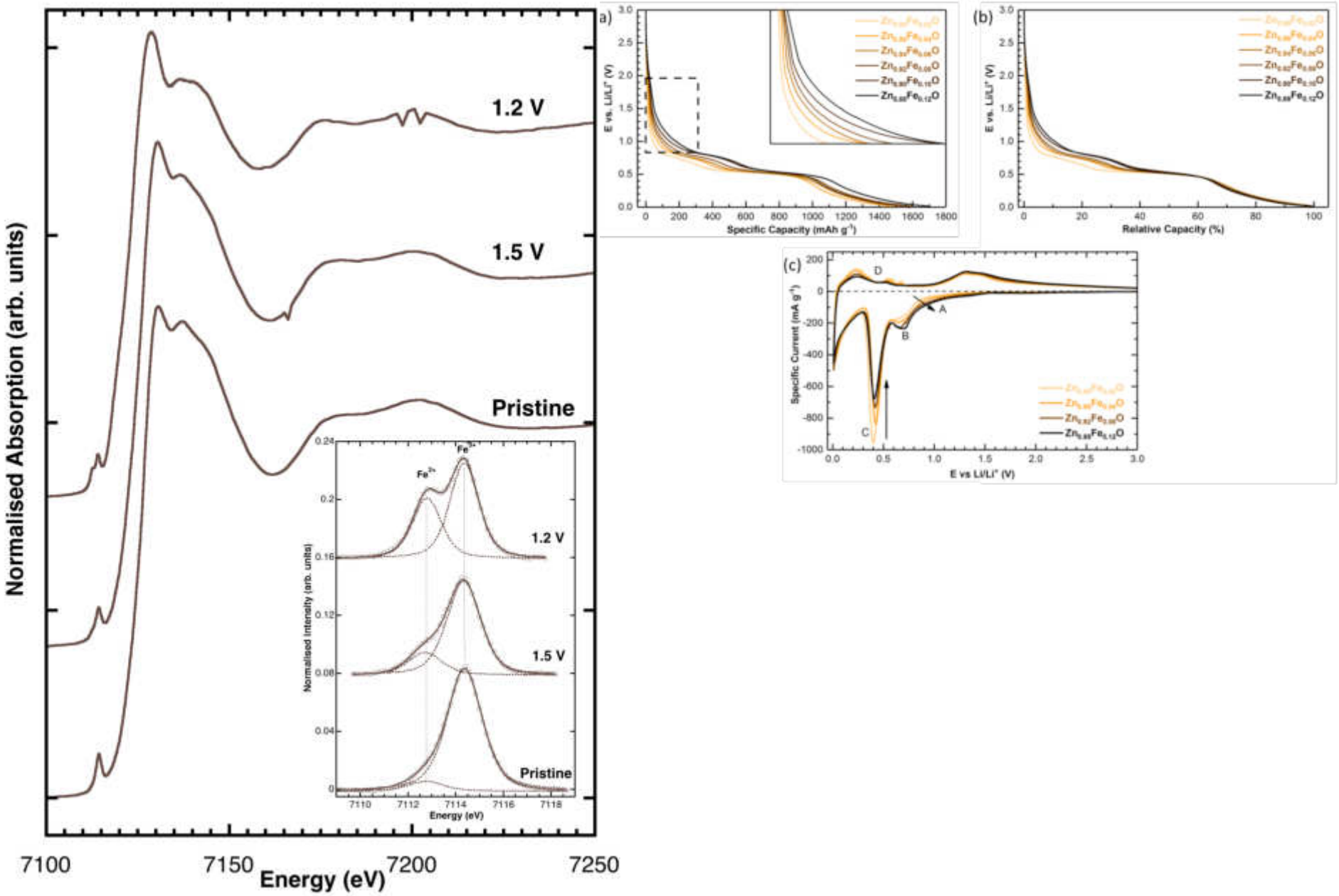
Normalised Absorption (arb. units)
1.2 V
1.5 V
Pristine
7100
7150
7200
7250
Energy (eV)
Normalised Intensity (arb. units)
Fe3+
Fe2+
1.2 V
1.5 V
Pristine
7110
7112
7114
7116
7118
Energy (eV)
a)
E vs. Li/Li+ (V)
Specific Capacity (mAh g-1)
(b)
Relative Capacity (%)
(c)
Specific Current (mA g-1)
E vs Li/Li+ (V)
A
B
C
D

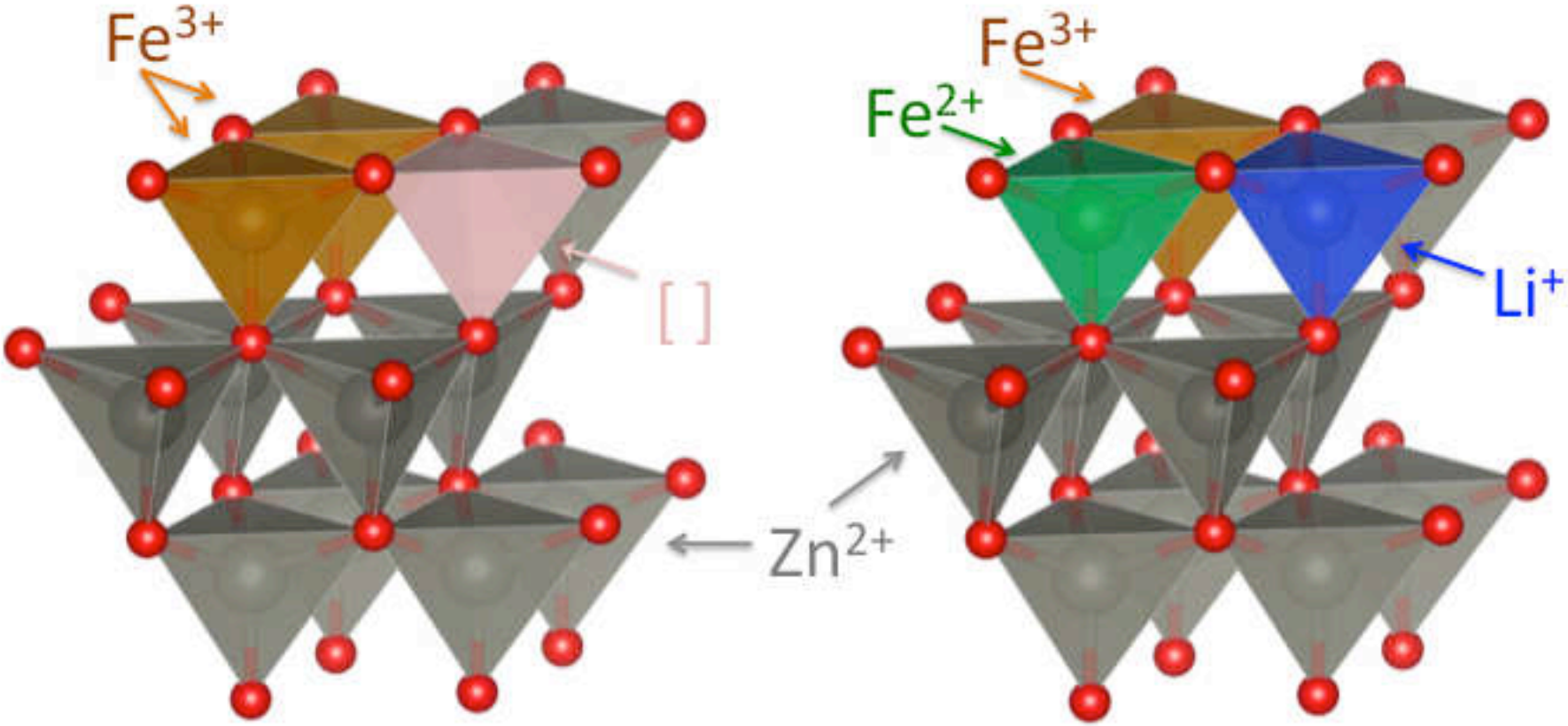

- Fe^{3+} content greatly affects crystallinity introducing ^{Zn}V;
- 1 vacancy compensates 2 Fe sites;
- Possible formation of FeO_4 dimers or oligomers;
- During initial litiation, Li enters vacant sites;
- When vacancies are filled, conversion starts.

Giuli et al., 2018, Materials., 11(1), 49

Fe- Co- and Mn-doped SnO_2 as anode material for Li-ion batteries

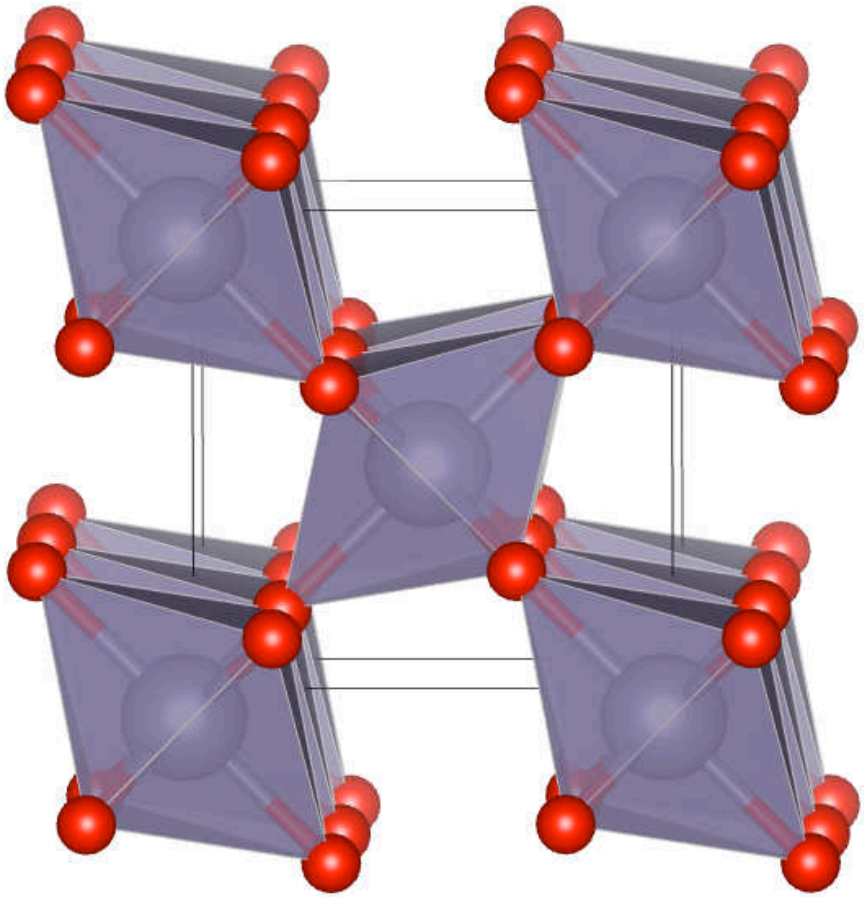

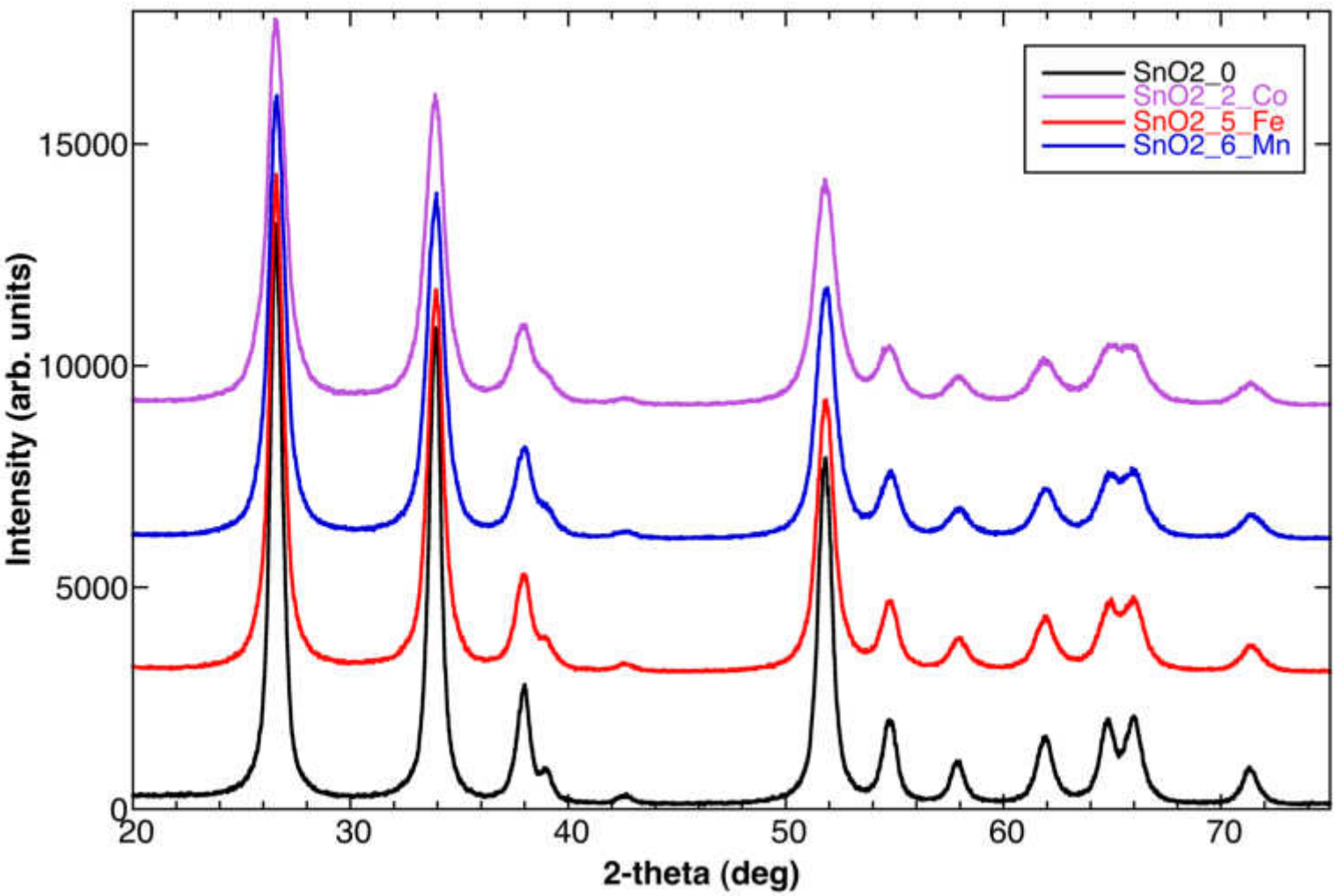
SnO2_0
SnO2_2_Co
SnO2_5_Fe
SnO2_6_Mn
Intensity (arb. units)
0
5000
10000
15000
20
30
40
50
60
70
2-theta (deg)

	SnO_2	$Sn_{0.9}Co_{0.1}O_2$	$Sn_{0.9}Fe_{0.1}O_2$	$Sn_{0.9}Mn_{0.1}O_2$
a_0(Å)	4.7399(1)	4.7403(1)	4.7392(1)	4.7367(1)
c_0 (Å)	3.1870 (1)	3.1856(1)	3.1853(1)	3.1836(1)
V_0 (Å^3)	71.601 (2)	71.582(1)	71.503(1)	71.428(1)
M-O (2x)	2.0279	2.0199	2.0037	2.029
M-O (4x)	2.0716	2.0764	2.0854	2.068
wRp	6.63	6.22	6.83	5.73
Rp	5.27	4.77	5.26	4.43
R_F2	2.47	2.12	3.51	1.85
R_F	1.44	1.14	2.03	1.02
c_0/a_0	0.6724	0.6720	0.6721	0.6721
W.H. intercept[1]	0.0047	0.0124	0.0094	0.0090
W.H. slope[1]	0.0017	0.0018	0.0014	0.0025
Crystallite size (nm)	30	11	15	16

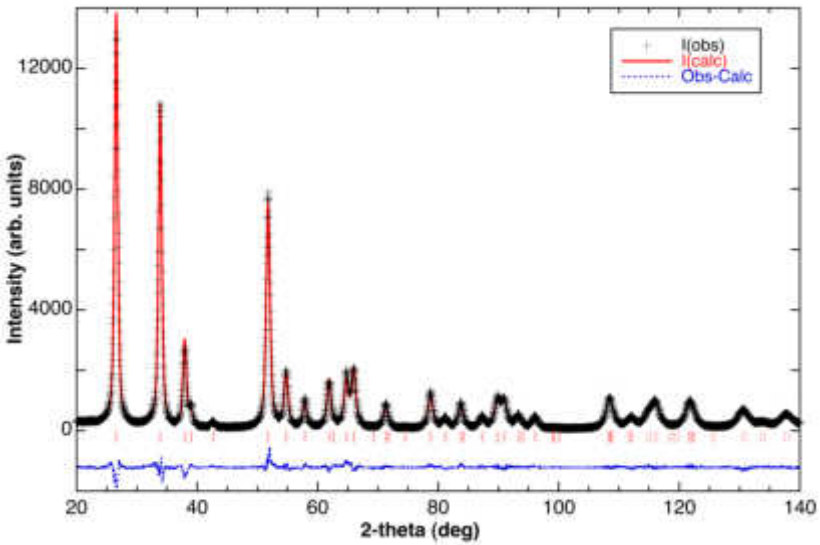

Work in progress

- Varying decreasing rate of crystallite size
  suggest different oxidation states of Co, Fe, Mn
- Consistent with XPS data
- *XAS data acquisition in progress*

➔ Can we generalize the findings for TM-doped ZnO and SnO_2?

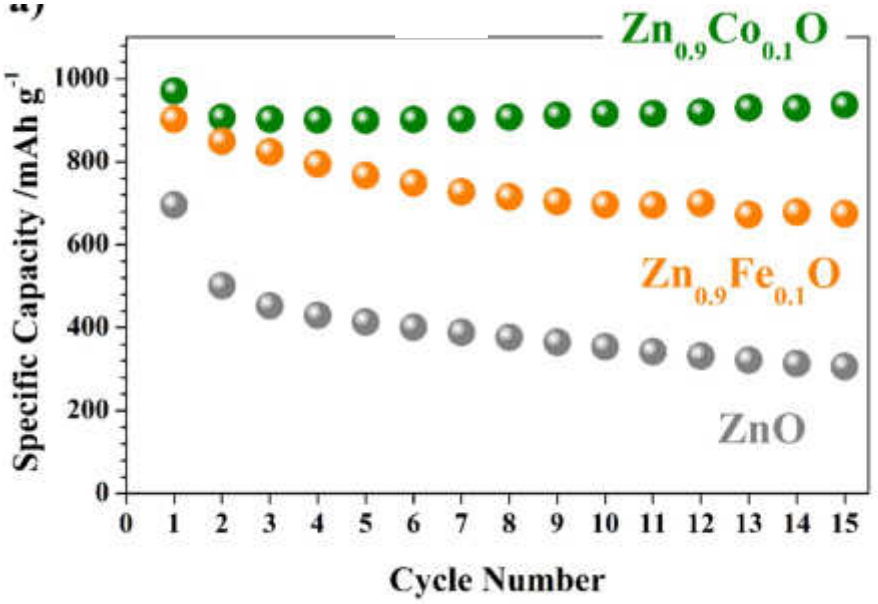

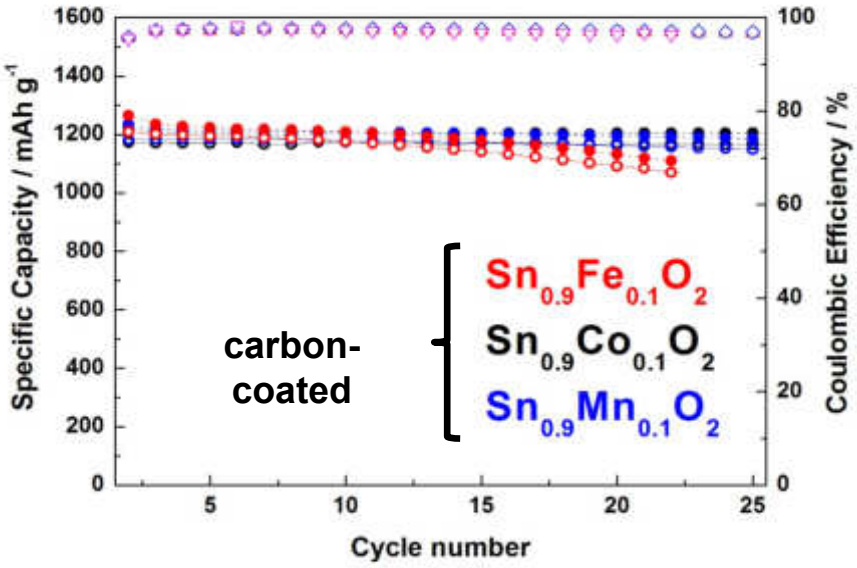

➔ Improved cycling stability by using Co as dopant also in case of ZnO

➔ Higher electronic conductivity *(1.8 vs. 1.2 x10^7 S m^{-1})* as reason for this enhanced cycling?

… though it is relatively low for Mn *(0.07 x10^7 S m^{-1})* …

➔ Besides, the diffusivity appears to play an important role …

… to be further investigated.

Bresser et al., Chem. Mater. 2013 (25) 4977; Bresser et al. Energy Environ. Sci. 2016 (9) 3348.

•The introduction of the *'charge carrier concept'* has enabled the rapid evolution of portable electronic devices in the recent past;

•consequently, opened up a continuously increasing interest in enhancing the existing technologies and realizing new ones;

•New materials have been developed based on the continuously increasing fundamental understanding;

• As such "battery research" is a truly interdisciplinary field, including electrochemistry, physical chemistry, in-/organic chemistry, materials science, physics, and potentially also Mineralogy (in addition to engineering).

- In depth study of crystal chemical behaviour

  Both average/local structure and Oxidation state

- Defect chemistry can profoundly affect physical/chemical properties
- Apparently simple phases (ZnO) can reveal complex behaviour
- Important to combine results from different techniques

Thank you for your attention